Lithium Batteries and Cathode Materials

M. Stanley Whittingham*

Department of Chemistry and Materials Science, State University of New York, Binghamton, New York 13902-6000

Received June 16, 2004

Contents

* To whom correspondence should be addressed. Phone and fax: (607) 777-4623. E-mail: stanwhit@binghamton.edu.

1. Introduction

In the previous paper Ralph Brodd and Martin Winter described the different kinds of batteries and fuel cells. In this paper I will describe lithium batteries in more detail, building an overall foundation for the papers that follow which describe specific components in some depth and usually with an emphasis on the materials behavior. The lithium battery industry is undergoing rapid expansion, now representing the largest segment of the portable battery industry and dominating the computer, cell phone, and camera power source industry. However, the present secondary batteries use expensive components, which are not in sufficient supply to allow the industry to grow at the same rate in the next decade. Moreover, the safety of the system is questionable for the large-scale batteries needed for hybrid electric vehicles (HEV). Another battery need is for a high-power system that can be used for power tools, where only the environmentally hazardous Ni/Cd battery presently meets the requirements.

A battery is a transducer that converts chemical energy into electrical energy and vice versa. It contains an anode, a cathode, and an electrolyte. The anode, in the case of a lithium battery, is the source of lithium ions. The cathode is the sink for the lithium ions and is chosen to optimize a number of parameters, discussed below. The electrolyte provides for the separation of ionic transport and electronic transport, and in a perfect battery the lithium ion transport number will be unity in the electrolyte. The cell potential is determined by the difference between the chemical potential of the lithium in the anode and cathode, $\Delta G = -EF$.

As noted above, the lithium ions flow through the electrolyte whereas the electrons generated from the reaction, $Li = Li^+ + e^-$, go through the external circuit to do work. Thus, the electrode system must allow for the flow of both lithium ions and electrons. That is, it must be both a good ionic conductor and an electronic conductor. As discussed below, many electrochemically active materials are not good electronic conductors, so it is necessary to add an electronically conductive material such as carbon

10.1021/cr020731c CCC: $48.50
Published on Web 09/14/2004

M. Stanley Whittingham was born in Nottingham, England, and received his B.A. and D.Phil. degrees in Chemistry from Oxford University working with Peter Dickens. In 1968 he went to Professor Robert A. Huggins research group in the Materials Science Department at Stanford University as a Postdoctoral Research Associate to study fast-ion transport in solids. In 1972 he joined Exxon Research and Engineering Company to initiate a program in alternative energy production and storage. After 16 years in industry he joined the Binghamton campus of the State University of New York as Professor of Chemistry to initiate an academic program in Materials Chemistry. Presently he is also Professor of Materials Science and Director of the Materials Science Program and Institute for Materials Research. He was awarded the Young Author Award of the Electrochemical Society in 1971, a JSPS Fellowship in the Physics Department of the University of Tokyo in 1993, and the Battery Research Award of the Electrochemical Society in 2002 and was elected a Fellow of the Electrochemical Society in 2004. He was Principal Editor of the journal *Solid State Ionics* for 20 years. His recent work focuses on the synthesis and characterization of novel microporous and nano-oxides and phosphates for possible electrochemical and sensor applications.

black. To physically hold the electrode together, a binder is also added. In these cases the electrochemical reaction can only occur at those points where the active material, the conductive diluent, and electrolyte meet. Thus, most electrodes are complex porous composites.

This review will be mainly concerned with the cathode. The anode, the source of lithium, is normally a graphitic carbon and will be discussed in detail by Rachid Yazami in a future issue. The electrolyte solution commonly comprises a lithium salt dissolved in a mixture of organic solvents, examples include $LiPF_6$ or LiBOB (the BOB is the anion with the boron coordinated by two oxalate groups) in an ethylene carbonate/dimethyl carbonate solvent; Kang Xu discusses electrolytes later in this issue. Although organic polymers containing lithium ions have been studied for several decades as possible electrolytes, their conductivity is still too low, and so they are only used when a liquid is added to give a plasticized state. In a few cases, solid electrolytes have been used for a few specialized applications such as for oil well logging where elevated temperatures are found. Though the ions flow through the electrolyte, the anode and cathode must be physically separated to prevent an electrical short. This is accomplished by using a porous separator material, which allows wetting by the electrolyte and the flow of lithium ions through it. P. Aurora discusses these materials in detail.

For most consumer devices, energy storage is key: operating time is key, so the more the better, as, for example, in cell phones, laptop computers, and MP3 players such as the iPOD. For some larger applications, such as the battery in hybrid electric vehicles (HEV), power is most important as the materials must be able to charge sufficiently fast to take advantage of regenerative braking; otherwise, much of the gas savings are lost. The all-electric consumer electric vehicle is probably dead, at least in the United States, because of its limited range and the user's desire for instant heating and air-conditioning among other high-power consumption devices. However, there is still much interest in Asia, particularly for scooters as well as for all electric vehicles.

The key requirements for a material to be successfully used as a cathode in a rechargeable lithium battery are as follows.

(1) The material contain a readily reducible/oxidizable ion, for example a transition metal.
(2) The material react with lithium in a reversible manner.
  (a) This dictates an intercalation-type reaction in which the host structure essentially does not change as lithium is added.
(3) The material react with lithium with a high free energy of reaction.
  (a) High capacity, preferably at least one lithium per transition metal.
  (b) High voltage, preferably around 4 V (as limited by stability of electrolyte).
  (c) This leads to a high-energy storage.
(4) The material react with lithium very rapidly both on insertion and removal.
  (a) This leads to high power density, which is needed to replace the Ni/Cd battery or for batteries that can be recharged using HEV regenerative braking.
(5) The material be a good electronic conductor, preferably a metal.
  (a) This allows for the easy addition or removal of electrons during the electrochemical reaction.
  (b) This allows for reaction at all contact points between the cathode active material and the electrolyte rather than at ternary contact points between the cathode active material, the electrolyte, and the electronic conductor (such as carbon black).
  (c) This minimizes the need for inactive conductive diluents, which take away from the overall energy density.
(6) The material be stable, i.e., not change structure or otherwise degrade, to overdischarge and overcharge.
(7) The material be low cost.
(8) The material be environmentally benign.

Almost all of the research and commercialization of cathode materials has centered on two classes of materials. The first contains layered compounds with an anion close-packed or almost close-packed lattice in which alternate layers between the anion sheets are occupied by a redox-active transition metal and lithium then inserts itself into the essentially empty remaining layers. This structure is depicted in Figure 1. This group is exemplified by first $LiTiS_2$, followed

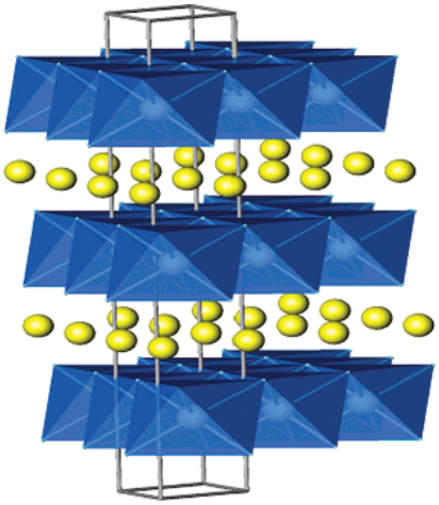

Figure 1. Layered structure of $LiTiS_2$, $LiVSe_2$, $LiCoO_2$, $LiNiO_2$, and $LiNi_yMn_yCo_{1-2y}O_2$, showing the lithium ions between the transition-metal oxide/sulfide sheets. The actual stacking of the metal oxide sheets depends on the transition metal and the anion.

by $LiCoO_2$, $LiNi_{1-y}Co_yO_2$, and today $LiNi_yMn_yCo_{1-2y}O_2$. The spinels may be considered as a special case where the transition-metal cations are ordered in all the layers. The materials in the second group have more open structures, like many of the vanadium oxides, the tunnel compounds of manganese dioxide, and most recently the transition-metal phosphates, such as the olivine $LiFePO_4$. The first group, because of their more compact lattices, will have an inherent advantage in energy stored per unit of volume, but some in the second group, such as $LiFePO_4$, are potentially much lower cost. The following discussion will center predominantly on these two classes of materials.

2. Origins of the Lithium Battery

2.1. Early Concepts

Some of the earliest concepts came from Japan, where Matsuchita developed[1] the $Li/(CF)_n$ battery that was used, for example, in fishing floats. Lithium fluoride and carbon are the final reaction products, but the cell potential of 2.8−3.0 V suggests a different electrochemical reaction. It was proposed that lithium initially intercalates the carbon monofluoride lattice and subsequently the lithium fluoride is formed:[2] $Li + (CF)_n \rightarrow Li_x(CF)_n \rightarrow C + LiF$. Although much work has continued sporadically on the carbon fluorides, by Exxon and others, the major challenge has been to make this reaction reversible even when lower fluoride levels were used. Sanyo, the largest manufacturer today of both lithium rechargeable and nickel metal hydride batteries, developed[3,4] one of the earliest lithium batteries with the Li/MnO_2 system that they initially sold in solar rechargeable calculators.[5] Some early work on ambient systems was also underway in the United States by 1970, for example, by Dey et al.[6] on the lithium reactivity with a range of metals, such as aluminum.

Many primary lithium batteries have been developed for use in the medical field starting with the lithium iodine cell. The majority of the implantable cardiac defribrillators use in the last 20 years have used, as active cathode material, silver vanadium oxide, $Ag_2V_4O_{11}$.[7−9] During discharge the silver is reduced to silver metal, and in addition, more than one lithium per vanadium can be reacted, giving it a capacity over 300 mAh/g. The presence of metallic silver greatly improves the electronic conductivity and thus the rate capability. Future medical devices, such as heart-assist devices, will require rechargeable systems because the capacity of primary cells cannot provide the power needed for active medical devices. The copper analogue also reacts by exuding the metal.

2.2. Molten Salt Systems at Argonne National Laboratory and General Motors

Most of the early work[10−12] on lithium rechargeable batteries used a molten salt as electrolyte and operated at around 450 °C. The earliest cells used molten lithium and molten sulfur as the two electrodes, but the problems with electrode containment proved insurmountable. The anode used in the final versions was the lithium aluminum alloy, LiAl, and iron sulfides, such as FeS and FeS_2, which replaced the molten sulfur of the early designs. Development ceased around 1990 when corrosion, temperature, and other issues overwhelmed the advantages of the system, the sodium sulfur system appeared more promising, and early results on ambient lithium rechargeable systems began to show promise. These low-cost iron sulfides were also considered in the 1970s in ambient temperature cells. Iron pyrite was found[13] to react with an initial constant potential of 1.5 V, allowing it to replace the more expensive Ag−Zn button cells and later making it a drop-in replacement for the Zn/MnO_2 alkaline cell. It is presently marketed by Eveready as a primary high-energy cell. On recharge the structure changes and the subsequent discharge has a two-step profile with an initial discharge of around 2 V.[13]

It is still the dream of battery researchers to develop a cell based on the lithium/sulfur couple which on paper has a simple chemistry, has a much higher energy density than most of the cathode materials to be discussed below, and should be capable of high rates if the sulfur is in solution. Recent work[14] has achieved high capacities at 2 V even at as low temperatures as −40 °C in electrolyte solvents of dioxolane and dimethoxyethane. These cells with their liquid polysufide cathode have generated specific power exceeding 750 W/kg at 25 °C. However, such cells still have significant issues with self-discharge on standing, lithium recharging, and the highly resistive nature of the cathode. Whether all these issues will be overcome is still much debated. A recent concept[15] to protect the lithium anode from the reactive polysulfide medium is to coat it with a single-ion conducting glass.

2.3. Concept of Mixed Conductors

In 1967 Yao and Kummer reported[16] the remarkable electrolytic behavior of the β-alumina class of

materials, $Na_{1+x}Al_{11}O_{17}$, which was proposed as the electrolyte for a battery having a molten sodium anode and a molten sulfur cathode operating around 300 °C. The measurement of the ionic conductivity of these materials required a new approach, as their high ionic conductivity required the use of ionically reversible electrodes and the obvious electrode sodium was too difficult to handle. To overcome this problem, the nonstoichiometric oxide bronzes of tungsten and vanadium were used,[17−19] for example, Na_xWO_3 and $Li_xV_2O_5$; these bronzes have a wide range of composition, are metallic conductors, and thus could readily serve as electrodes reversible to both alkali ions and electrons. Their mixed conductivity also led to the proposed use of the vanadium oxide as electrodes for sodium or lithium batteries: $Li-Li_xV_2O_5$.

2.4. Early Intercalation Concept

Around 1970 two groups began studying the idea of placing electrochemically active species inside an electrically conductive host. At Bell Laboratories, Broadhead et al.[20,21] conceived of intercalating iodine or sulfur between the layers of a dichalcogenide host material such as niobium diselenide. They believed that the dichalcogenide host material itself was electrochemically inert.[22] Such materials showed good cyclability at low depths of discharge. Subsequently, they found that when selenium reacted with $NbSe_2$, it formed the triselenide $NbSe_3$ which exhibited very good electrochemical behavior.[23] At Stanford, Armand et al.[24−26] tried to incorporate oxides such as CrO_3, and subsequently halides, between the layers of graphite. Again, electrochemical activity was found. However, subsequent work showed that in both these cases no intercalation had occurred and that the electrodes were mixtures of the guest and host materials. The large amount of host material required also made this concept infeasible due to the resulting poor energy density. A similar concept,[27] still not tested, was to use as electrodes two known graphite materials C_8K and C_8Br where on discharge the potassium and bromine would react in a suitable solvent and on charge would be intercalated into their respective graphite electrodes.

3. 1972–1980: Birth of the Rechargeable Lithium Battery

3.1. Intercalation in the Layered Dichalcogenides

Around 1970 researchers at Stanford[28] discovered that a range of electron-donating molecules and ions could be intercalated into the layered dichalcogenides, in particular, tantalum disulfide, TaS_2. These guest−host intercalation reactions modified the physical properties and, in particular, were found to enhance the superconducting transition temperature from 0.8 to over 3 K. It was also discovered that such compounds remained superconducting even when the guest molecules were paramagnetic.[29] These studies continued at Exxon, where an investigation of the formation of the hydrated alkali-metal intercalates of tantalum disulfide, which showed the highest superconducting transition temperature, resulted in the discovery of the very high free energy of reaction of the alkali ions with these layered materials. Thus, the stability of the hydrates, $K_x(H_2O)$-TaS_2, could be explained[30] as being due to their salt-like behavior, in contrast to the metallic-like behavior of the corresponding compounds of graphite, C_8K. It was also found that such intercalation reactions could also be accomplished in an electrochemical cell either by electrolyzing dissolved salts or by inserting ions from the anode.[31−33]

Of all the layered dichalcogenides, titanium disulfide was the most appealing for consideration as an energy storage electrode:[34−38] it was the lightest. It was subsequently discovered that it was a semimetal,[39] so no conductive diluent was needed in the cathode structure, and any such addition was found to be detrimental to the electrochemical behavior. It was also found to form a single phase with lithium over the entire composition range of Li_xTiS_2 for $0 \leq x \leq 1$.[40] This lack of phase change enables all the lithium to be removed reversibly, without the need for energy wastage associated with the nucleation of new phases or the sluggish reactions when massive rearrangement of the host must occur as the lithium content is changed. This behavior may be contrasted with that observed in $LiCoO_2$, to be discussed below, where phase changes result in only about one-half of the lithium being readily cycled in to and out of the compound; today the capacity has been improved but is still well below the goal of one lithium per transition-metal ion. Some specifics of the lithium titanium disulfide cell will now be described, as they are typical of what is desired in advanced lithium batteries. Although they will not be discussed here, there was also interest[41−44] in using the disulfides as the cathodes of sodium batteries; such systems are seriously complicated by phase changes as the sodium content changes in Na_xTiS_2 or Na_xTaS_2 due to the sodium favoring trigonal prismatic coordination at intermediate x values and octahedral coordination as x approaches one.

Titanium disulfide has a hexagonal close-packed sulfur lattice with the titanium ions in octahedral sites between alternating sulfur sheets, as shown in Figure 1. The TiS_2 sheets are stacked directly on top of one another, giving the sulfur anion stacking sequence ABAB. For nonstoichiometric sulfide $Ti_{1+y}S_2$ or for TiS_2 prepared at high temperatures, some of the titanium is found in the empty van der Waals layer. These disordered titanium ions prevent the intercalation of large molecular ions and impede the intercalation of even small ions such as lithium by pinning the TiS_2 sheets together,[45] thus reducing their diffusion coefficients. Thus, material with the highest reactivity for lithium should have an ordered structure, which dictates that it be prepared at temperatures below around 600 °C.[46−48] We will see that this is also important for the similarly structured layered oxides, discussed below, and even for tunnel structures such as $LiFePO_4$, where errant Fe ions in the Li sites can reduce reactivity[49,50] and diffusion of lithium.[51]

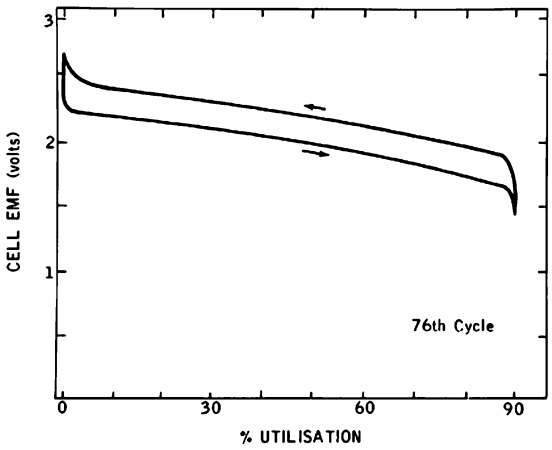

Figure 2. Discharge/charge curve of Li/TiS_2 at 10 mA/cm^2 (reprinted with permission from ref 13, copyright 1978 Elsevier).

A typical insertion/removal galvanostatic cycle for lithium in titanium disulfide is shown in Figure 2, where the current used is 10 mA/cm^2. This curve shows the behavior typical of a single phase all the way from TiS_2 to $LiTiS_2$, so that no energy is expended in nucleating a new phase. However, closer examination of the intercalation potential curve, using the incremental capacity method for the first time, showed localized ordering of the lithium ions.[52] The electrolyte used was 2.5 M lithium perchlorate in dioxolane, which was found to be an exceptional electrolyte for effective lithium plating; this solvent also does not co-intercalate with the lithium into the sulfide. In contrast, when propylene carbonate was used as the solvent, any trace amount of moisture resulted in the co-intercalation of the propylene carbonate with a concomitant large expansion of the lattice.[45] Such co-intercalation of solvent also prevented the use of graphite as an anode for lithium for many years, until appropriate nonintercalating solvents were found,[53,54] initially dioxolane and then a mixture of carbonate solvents. Dioxolane was also found to be an effective electrolyte solvent for cells using niobium triselenide.[55,56] However, the electrolyte of $LiClO_4$ in dioxolane is inherently unsafe.[57] This clean electrolyte system allows these intercalation reactions to be readily followed by in-situ X-ray diffraction[58] and in the optical microscope, which show the microscopic details of the intercalation process.[59]

The ready reversibility of lithium in titanium disulfide has permitted deep cycling for close to 1000 cycles with minimal capacity loss, less than 0.05% per cycle, with excess lithium anodes. Exxon marketed button cells with LiAl anodes[60] and TiS_2 cathodes for watches and other small devices in 1977−1979; the LiAl anode improved the safety of the cells. Some of the largest lithium single cells built to date are those exhibited by Exxon at the Electric Vehicle Show in Chicago in 1977, shown in Figure 3.

Most of the other dichalcogenides are also electrochemically active,[13] and many show a similar single-phase behavior with lithium intercalation. Vanadium diselenide is an exception,[61] showing two-phase behavior as shown in Figure 4. Initially, VSe_2 is in equilibrium with Li_xVSe_2, where $x \approx 0.25$, then Li_xVSe_2 is in equilibrium with $LiVSe_2$, and finally $LiVSe_2$ is in equilibrium with Li_2VSe_2. The initial two-phase behavior may be associated with the unusual *c*/*a* ratio, which is presumably caused by the desire of group VB elements to have trigonal prismatic coordination with sulfur and selenium, but in VSe_2 the vanadium is octahedral (this *c*/*a* is almost that of TP coordination). When lithium is intercalated, the structure becomes typically octahedral with a standard *c*/*a* ratio. The ready reversibility of lithium in VSe_2, even at 10 mA/cm^2, shows that single-phase behavior is not critical to effective use as a battery cathode; however, the phases formed only differ by slight deformations of the octahedra, not wholesale movement of anion sheets as in the conversion of Li_xCoO_2 to CoO_2.

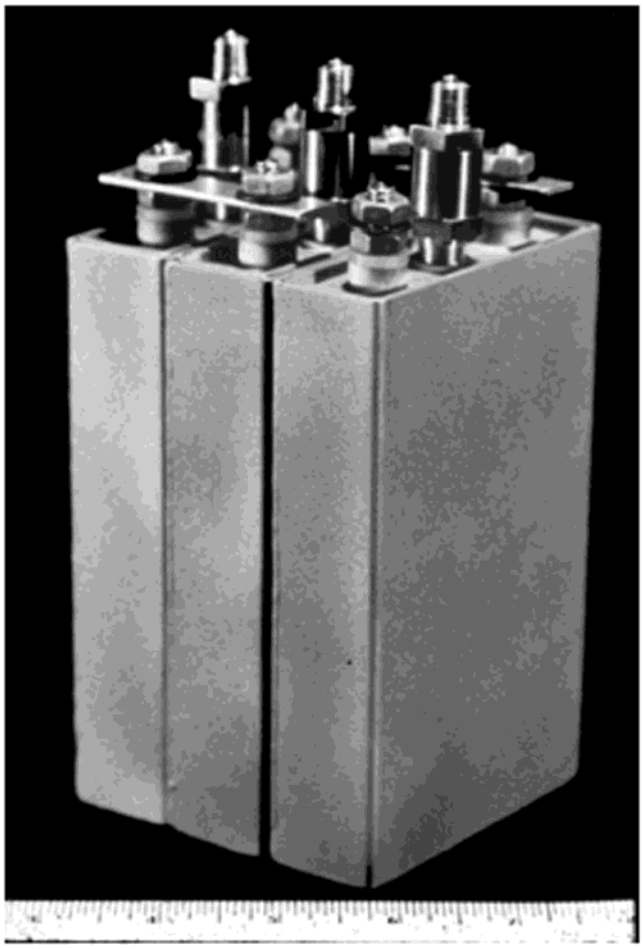

Figure 3. Large cells of $LiTiS_2$ constructed for the Chicago automotive show in 1977; vents were used for the $LiB(CH_3)_4$ salt in dioxolane.

Vanadium diselenide also showed the feasibility of intercalating a second lithium into the lattice. The $LiVSe_2/Li_2VSe_2$ system must be two phase, as the lithium in $LiVSe_2$ is in octahedral coordination whereas in Li_2VSe_2 the lithium must move to tetrahedral coordination and both sites cannot be occupied at the same time. This two-lithium intercalation[61,62] can be accomplished either electrochemically or chemically, for example, by using butyllithium. Other dilithium layered materials such as Li_2NiO_2 have also been formed[63] both electrochemically and chemically

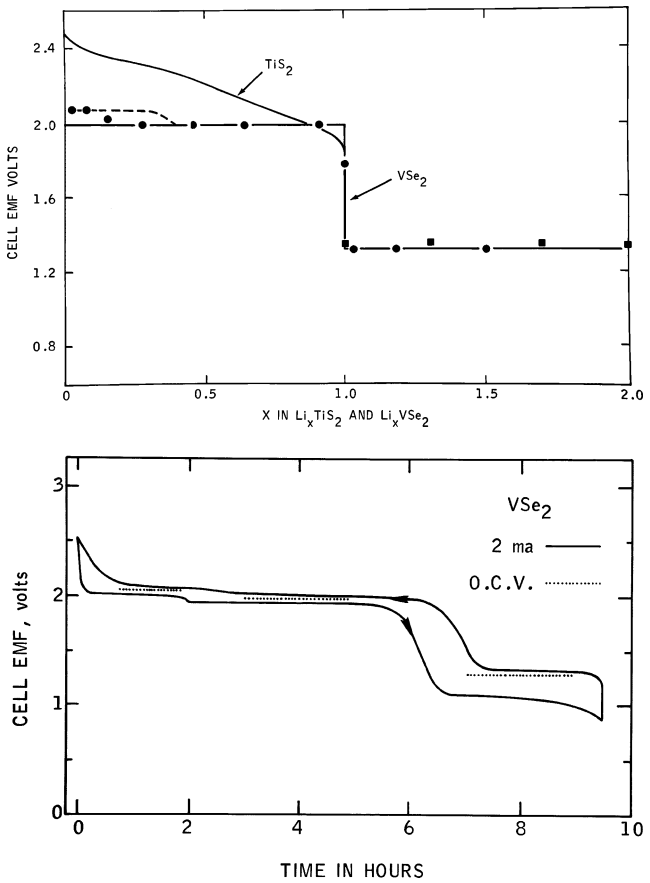

Figure 4. Electrochemical insertion of lithium into vanadium diselenide, showing reaction of two lithium (reprinted with permission from ref 61, copyright 1978 Elsevier):[61] (top) open-circuit potentials, (bottom) behavior on cycling at 2 mA/cm^2.

using lithium benzophenone in tetrahydrofuran; it's structure switches from the 3R−$LiNiO_2$ phase to one identical to those of Li_2TiS_2 and Li_2VSe_2, where the lithium ions sit in all the tetrahedral sites between the NiO_2 sheets forming a 1T structure. In a similar manner, $Li_2Mn_{0.5}Ni_{0.5}O_2$ has also been synthesized in electrochemical cells, and both lithium ions can be cycled when part of the Mn is substituted by titanium.[64]

The group VI layered disulfides were originally not thought to be of much interest because of poor rechargeability. However, Haering et al.[65] showed that in MoS_2, which occurs naturally as molybdenite, if the molybdenum coordination could be changed from trigonal prismatic to octahedral, then the MoS_2 so formed could be effectively used as a cathode. They accomplished this transformation by inserting one lithium per MoS_2 into the lattice and then letting it convert to the new phase. This system formed the foundation of a commercial battery developed by MoliEnergy in British Columbia.[65]

Although the Li/TiS_2 batteries were usually constructed in the charged state with pure lithium or LiAl anodes,[60] they were also built[34] in the discharged state with $LiTiS_2$ cathodes as now used in all $LiCoO_2$ cells. In this scenario the cells must first be charged by the deintercalation of the lithium ions. Whereas $LiVS_2$ and $LiCrS_2$ were well known in the literature, the lithium-free compounds had not been successfully

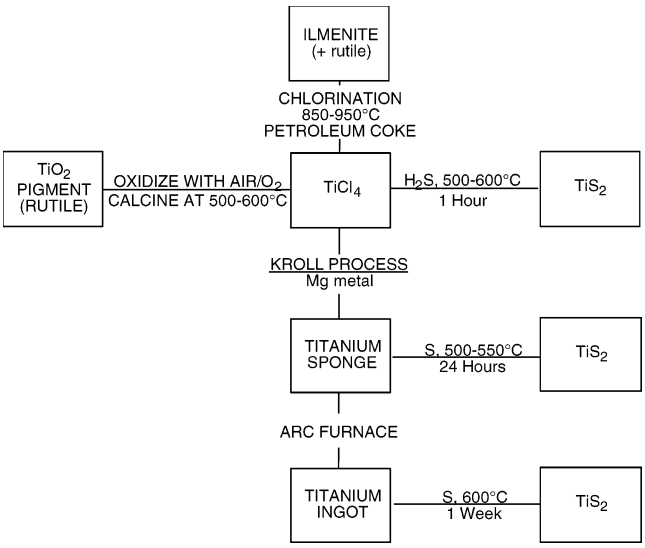

Figure 5. Synthesis approaches for titanium disulfide, after ref 46.

synthesized because the sulfides VS_2 and CrS_2 are thermodynamically unstable at the usual temperatures used for synthesis. Murphy et al.[66,67] showed that these compounds could be formed by the deintercalation of the lithium at ambient temperatures; this work has led to a new route for the synthesis of metastable compounds—the deintercalation of stable phases.

The metastable spinel form of TiS_2, which has cubic close-packing of the sulfide ions, was similarly formed by the deintercalation of copper from $CuTi_2S_4$.[68−70] This cubic structure can also be reversibly intercalated with lithium, although the diffusion coefficient is not as high as in the layered form.

When a battery is being commercialized, the synthesis process used in the laboratory often cannot be used because of the processing costs or cost of the starting materials. As an example, titanium disulfide will be considered where in the laboratory bulk titanium was used to provide electronic-grade titanium disulfide and sponge titanium provided research battery-grade material. The latter could be produced 1 lb at a time in silica tubes, had a surface area of 5 m^2/g, and allowed current densities of 10 mA/cm^2 to be achieved. However, both involved reaction with sulfur, which took from hours for the sponge to days for the bulk metal. Such material would cost more than $100/lb. An inspection of the commercial process, shown in Figure 5, for sponge manufacture revealed that the precursor was titanium tetrachloride, a liquid at room temperature. This tetrachloride is available in tonnage quantities as it is used in the manufacture of titanium dioxide paint pigment. Therefore, a manufacturing process was devised by two European companies that involved the formation of stoichiometric TiS_2 by deposition from the gas-phase reaction of $TiCl_4$ with H_2S. This produced a sulfide with a morphology with many plates growing in three dimensions from a single central point, which shows excellent electrochemical behavior.

The stoichiometry and ordering of the titanium is critical to the electrochemical behavior of TiS_2. Stoi-

chiometric and ordered TiS_2 has been shown to exist[71] if the temperature is kept below 600 °C and to have metallic conductivity.[39] The titanium disorder can be readily measured by attempting to intercalate weakly bonding species such as ammonia or pyridine. In practice, a slight excess of titanium, ≤1%, is beneficial in that it reduces the corrosiveness of the sulfur without significantly impacting the cell potential or the lithium diffusion coefficient. It is preferable to add this extra metal to the initial reaction medium.

3.2. Trichalcogenides and Related Materials

As noted above, Trumbore et al. at Bell Labs discovered the electrochemical behavior of the triselenide of niobium. $NbSe_3$ was found[23,72,73] to react reversibly with three lithium ions to form Li_3NbSe_3 in a single phase. The other trichalcogenides also readily react with lithium but not in such a reversible manner. Thus, in TiS_3, which is best represented as TiS(S−S), the polysulfide group reacts first with two lithium, breaking the S−S bond to form Li_2TiS_3 in a two-phase reaction; this is followed by the reduction of the titanium from Ti^{4+} to Ti^{3+} in a single-phase reaction similar to TiS_2 itself.[40] Only this second step is readily reversible, unlike Li_3NbSe_3, where all three lithium ions are reversible.

A number of other chalcogenide-rich materials have been studied, but although many of them have a high capacity, their rates of reaction or conductivity are low. This can be ameliorated to some extent by admixing them with a high rate high-conductivity material such as TiS_2 or VSe_2.[74,75] At high rates of lithium insertion the latter undergo reaction first, and then when the rate is reduced they are recharged by the other component, making them available for the next high-current pulse. This mixed-cathode approach might reemerge as batteries must meet both high-power and high-energy demands.

In this time period a range of chemical reagents was devised to mimic the electrochemical reaction, either lithium reaction or lithium removal, so as to speed-up the evaluation of new materials and get an idea of ease and depth of reaction. The most common lithiating agent is *n*-butyllithium in hexane, a straw-colored liquid, with clean clear easily identified reaction products such as octane, butane, and butene.[62,76,77] Although highly reactive with a potential of around 1 V versus lithium metal, this reactant gave much purer products than prior methods using naphthalene or liquid ammonia solvent. A series of other chemical reagents with known redox potentials can be used to control the reductive or oxidative intercalation of materials.[78]

3.3. Movement into Oxides

3.3.1. Layered Oxides

Surprisingly the layered oxides with the same structures as the layered dichalcogenides were not studied in that time period. The thought was presumably that oxides toward the right of the periodic table would be of little interest, and it was not considered that lithium could be readily removed from the layered materials such as $LiCoO_2$, which were of more interest for their magnetic properties.

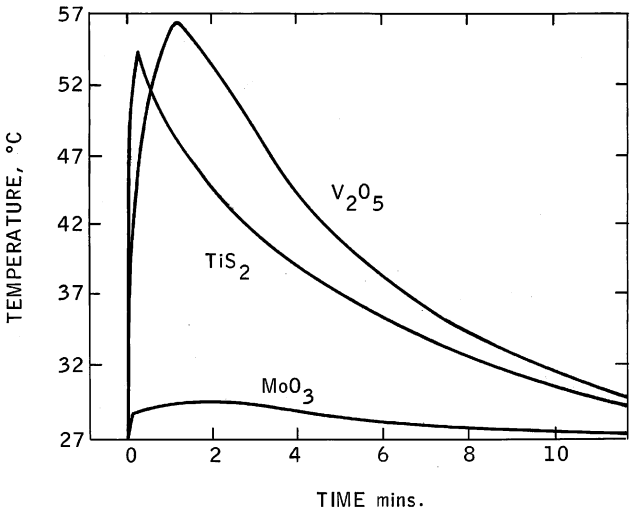

Figure 6. Reaction of *n*-butyllithium with titanium disulfide, vanadium pentoxide, and molybdenum trioxide (reprinted with permission from ref 77, copyright 1977 The Electrochemical Society).

3.3.2. High-Valent Oxides of Vanadium and Molybdenum

Vanadium pentoxide, V_2O_5, and molybdenum trioxide, MoO_3, were two of the earliest studied oxides. Molybdenum oxide reacts readily with around 1.5 lithium/molybdenum,[40,79] but is of little interest because of its low rate of reaction which is readily determined by the rate of temperature rise when the solid is added to the chemical lithiating agent *n*-butyllithium.[77] Figure 6 shows the heat of reaction for three cathode materials, TiS_2, V_2O_5, and MoO_3; the higher the temperature increase, the greater the power capability of the material. A high-power material should be able to boil the hexane solution.

Vanadium pentoxide has been investigated for 30 years;[40,80−84] it has a layered structure with weak vanadium−oxygen bonds between the layers and is now known to react by an intercalation mechanism:[40,85] $x\mathrm{Li} + V_2O_5 = \mathrm{Li}_xV_2O_5$.

The structural behavior on lithium insertion is fairly complex with the initial lithium merely intercalating the structure, first forming the α-phase ($x < 0.01$) and then the ϵ-phase ($0.35 < x < 0.7$), where the layers are more puckered. At $x = 1$, shifting of one layer out of the two leads to the δ-phase. However, if more than one lithium is discharged, then significant permanent structural changes occur, giving the γ-phase, which can be cycled in the range $0 \le x \le 2$. In the α-, ϵ-, and δ-phases the VO_5 square pyramids that make up the structure of V_2O_5 are arranged in rows which have the apexes ordered up, up, down as shown schematically in Figure 7. In contrast, in the highly puckered γ-phase, these are organized up, down, up, down. A rock-salt structure is formed when still more lithium is added; this compound is called the ω-$Li_3V_2O_5$ phase. This ω-phase cycles in a single solid−solution phase with the last lithium coming out at over 4 V, clearly showing the difference between this phase and the initial vanadium pentoxide phase, which has an open-circuit

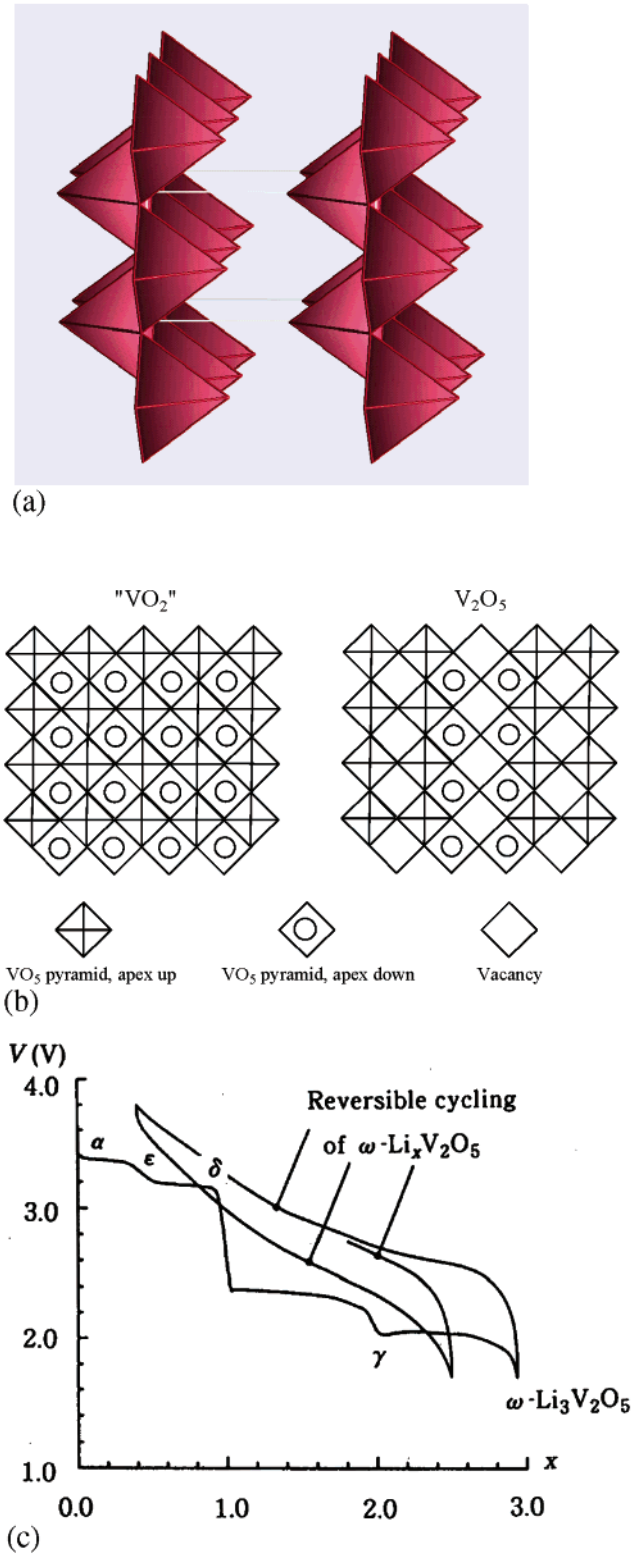

Figure 7. Structure and discharge of vanadium pentoxide: (a) structure of V_2O_5 showing the square pyramids sharing edges of the basal planes; (b) schematic showing basal planes sharing edges and the orientation of the apexes of the pyramids comparing the structure in the perfect lattice of VO_2 compared with the ordered defect lattice of V_2O_5 (reprinted with permission from ref 364, copyright 1996 The Electrochemical Society); and (c) electrochemical lithium intercalation into V_2O_5 showing the evolution of phases with degree of lithium intercalation and the cycling of ω-phase (reprinted with permission from ref 82, copyright 1994 Elsevier).

potential of 3.5 V. This behavior is shown in Figure 7. The ω-material has a tetragonal structure, which on extended cycling becomes a simple rock-salt structure with $a = 4.1$ Å with the formula $Li_{0.6}V_{0.4}O$. Delmas[82] reviewed these structural modifications and attributes the high OCV at low lithium content to the metastability of the defective rock-salt lattice which can contain up to 60% vacancies on the cation sublattice. The single sloping discharge plateau from almost 4 to under 2 V makes it uninteresting for practical applications where the change in potential should preferably be under 0.5 V; moreover, this phase also rapidly loses capacity on cycling.

3.3.3. Mixed-Valent Oxides of Vanadium—V_6O_{13} and LiV_3O_8

Murphy et al.[86] made an extensive study of a number of vanadium oxides and discovered the excellent electrochemical behavior of the partially reduced vanadium oxide, V_6O_{13}, which reacts with up to 1 Li/V. They also recognized that the method of preparation, which determines the V:O ratio, critically controls the capacity for reaction with lithium. The structure consists of alternating double and single sheets of vanadium oxide sheets made up of distorted VO_6 octahedra. A variety of sites are available for lithium intercalation, which if filled sequentially would lead to the various steps seen in the discharge curve. The lattice first expands along the *c*-axis and then along the *b*-axis. Thomas et al.[87−91] made an in-depth study of the complex intercalation process in single crystals of V_6O_{13}. This phase was one of the leading candidates for polymer electrolyte batteries, which require a lower voltage system because of the limited thermodynamic stability of the polymer.

Another vanadium oxide that has received much attention is LiV_3O_8, which has a layer structure composed of octahedral and trigonal bipyramidal ribbons that can be swelled just like other layered compounds and can intercalate lithium.[92,93] Here again, the method of preparation is important to its electrochemical characteristics.[94] West et al.[95] made a systematic study of the impact of synthesis technique on capacity and cycling and showed that amorphous material increased the capacity above 2 V from 3−4 lithium per mole of LiV_3O_8 at low current drains, 6−200 μA/cm^2.

3.3.4. Double-Sheet Structures: Xerogels, δ-Vanadium Oxides, and Nanotubes

There has been much interest in vanadium oxides formed by sol−gel processes.[96−98] These can be formed by acidification of a sodium vanadate solution, for example, by passing it down an acidified ion-exchange column. The resulting orange gel on drying has the formula $H_xV_2O_5 \cdot nH_2O$. About 1.1 mol of water may be removed under vacuum or on mild heating, leading to $H_{0.3}V_2O_5 \cdot 0.5H_2O$, based on its high cation-exchange capability. The interlayer spacing is around 8.8 Å, which swells to 11.5 Å for the more hydrated form with $1.8H_2O$. The protons and water can be readily exchanged for lithium and polar solvents. These vanadium oxide gels can be also

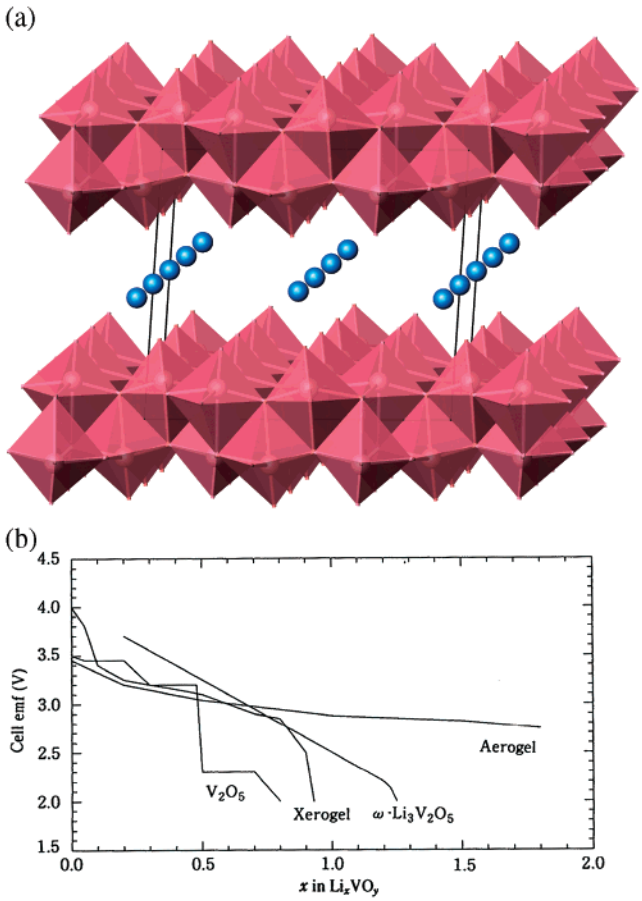

Figure 8. (a) Structure of the two-layer structure found in xerogel, and (b) comparison of the electrochemical behavior of the crystalline,[82] xerogel,[362] ω-phase,[83] and aerogel[100] forms of vanadium pentoxide.

made[99] by the hydrogen peroxide treatment of V_2O_5. These xerogel vanadium pentoxides contain sheets comprised of two vanadium oxide layers, with all the vanadyl bonds on the outside leading to a distorted octahedral coordination around the lithium instead of the square pyramidal coordination found in crystalline V_2O_5. Recently, it was reported[100] that making V_2O_5 through an aerogel process with supercritical drying in CO_2/acetone gives a much more electrochemically active product, $H_yV_2O_5{\cdot}0.4H_2O{\cdot}$carbon; the amount of carbon was 3.9 wt %. The dried material, which had a 12.5 Å lattice spacing, reacts with lithium in a single continuous discharge curve with a midpoint emf of around 3.1 V and a total lithium uptake of 4.1 Li by 2.8 V, thus giving a much higher capacity than crystalline V_2O_5 as shown in Figure 8.

The double layers of vanadium oxide found in the xerogel have been described in a number of other vanadium oxides by Galy[101] and Oka;[102] they also form the double sheets described above for V_6O_{13}. These oxides, in which the vanadium is found in distorted VO_6 octahedra, show particularly attractive electrochemical capacities[103−107] exceeding 200 mAh/g in some cases, as shown in Figure 9. However, at the present time their rate capability appears somewhat limited. More recently vanadium oxide nanotubes have been synthesized, first by Spahr et al.;[108,109] these compounds also contain double sheets of vanadium oxide and again have interesting but complex

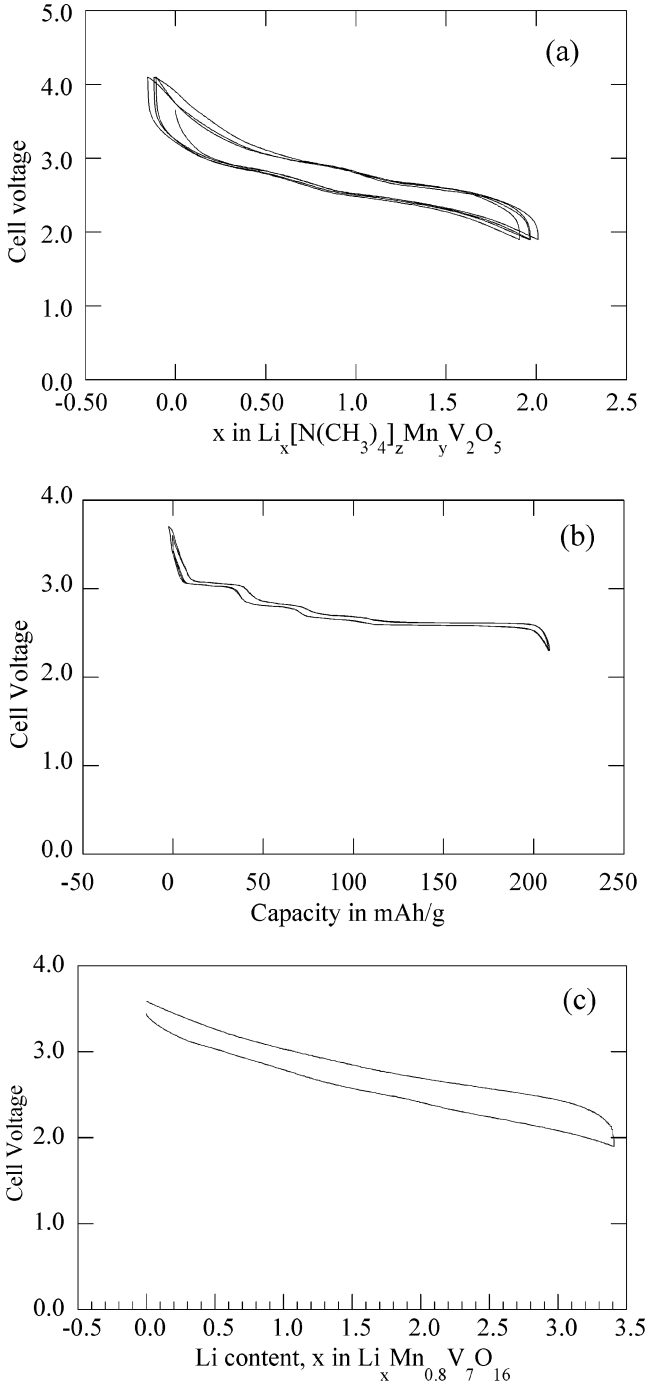

Figure 9. Electrochemical behavior of (a) δ-Mn$_y$V$_2$O$_5$ (reprinted with permission from ref 105, copyright 2000 Elsevier), (b) δ-$NH_4V_4O_{10}$, and (c) Mn vanadium oxide nanotubes.[112]

electrochemical behavior.[110] In some cases the capacity increases on cycling;[111] the electrochemical behavior of the manganese ion-exchanged compound is also shown[112] in Figure 9.

4. 1980–1990: Era of Layered Oxides and First Large Commercialization

4.1. Early Studies of Layered Oxides

Although the heavier alkali-metal compounds of the oxides of manganese, cobalt, chromium, and

others had been extensively studied by a number of groups, in particular, at Bordeaux by Hagenmuller and Delmas[113−119] in the 1970s, there was essentially no in-depth study of the corresponding lithium compounds. This was not dissimilar to the situation in Nantes, where Rouxel et al.[119−122] were researching the layered dichalcogenides at the same time. This can be in part associated with the lack of a good lithiating agent, which was solved with the discovery of the synthetic prowess of *n*-butyllithium and electrochemical synthesis.

In the studies in the 1970s the structures of these layered oxides and chalcogenides were extensively studied. Whereas lithium only occupies octahedral sites in the strictly layered materials when the Li/transition-metal ratio is unity or less, the larger alkali ions often occupy trigonal prismatic sites. Which site is occupied depends on the alkali cation size and their concentration, with some ions such as sodium exhibiting a range of structures. The stacking of the MO_2 slabs in the overall structure depends on the alkali site occupancy. As significant reorganization of the lattice must occur in switching from one structure to another, such changes will impede electrochemical reactions. Thus, it is important to know the phases formed as the alkali concentration changes. In the case of the small lithium ion, one needs only be concerned with the stacking sequence and whether it changes as the lithium concentration changes as the lithium ion normally occupies only the octahedral sites for $x \leq 1$ in Li_xMO_2. For most layered oxides the transition metal also only occupies octahedral sites. There are at least three different stacking sequences of the MO_2 slabs (building blocks) that can form the unit cell; the lithium ions reside between the slabs. These three stacking arrangements are as follows.

(a) Single blocks stacked upon one another, as in, for example, $LiTiS_2$, CoO_2, and TiS_2. This is the CdI_2 structure. This is a hexagonal close-packed lattice. A special case of the single block structure is given by the dilithium compounds, such as Li_2VSe_2, where the lithium resides on all the tetrahedral sites.

(b) Double blocks stacked upon one another, normally formed by ion exchange from a sodium-containing compound.

(c) Triple blocks, each block displaced by one-third in the basal plane, stacked on top of one another. This sequence is very common in the lithiated oxides, such as $LiCoO_2$ (the α-$NaFeO_2$ structure). This is a cubic close-packed lattice.

In addition, at very low lithium contents not every layer between the slabs need be occupied by lithium ions but, for example, just every other layer. This is known as a second-stage compound. The above three stacking arrangements can also be described in terms of the positions of the atoms. Thus, if a slab is described by the designation AcB, where A, B, and C represent the three possible positions of the anions in the hexagonal lattice and a, b, and c represent the cation positions, then the three stacking sequences described above may be represented for the dioxide MO_2 and lithiated $LiMnO_2$ as follows.

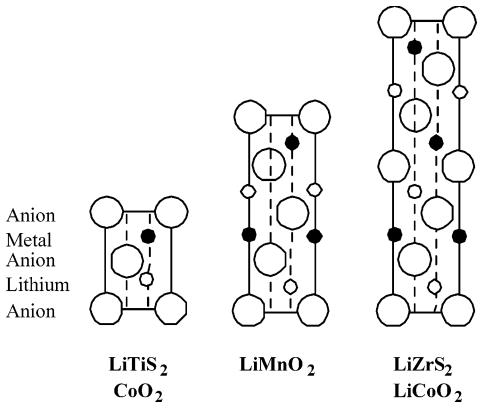

Figure 10. Schematic of stacking of building blocks for one-block, two-block, and three-block structures.

slab stacking	MO_2	$LiMO_2$
single block	..(AcB)(AcB)..	..(AcB)*c*(AcB)..
double block	..(AcBCaB)(AcBCaB)..	..(AcB*a*CaB)*c*(AcB*a*CaB)..
triple block	..(AcBCbABaC)-(AcBCbABaC)..	..(AcB*a*CbA*c*BaC)*b*-(AcB*a*CbA*c*BaC)..

It can thus be seen that long-range atomic motion (slab-sliding) is required to convert one of these structures into another one. These arrangements are shown schematically in Figure 10. It can also be noted that in the single block structures all the cations are stacked directly above each other, while in the triple block structure all the cations are staggered to minimize any ionic interactions. Thus, the former tends to be formed by more covalent lattices and the latter by the more ionic lattices. In addition to these idealized hexagonal lattices, there are a number of instances in which the lattice is distorted and where cations migrate between the slabs and the interslab region. This, often unintended migration, can play a significant role in the reactivity and electrochemical behavior of the material. The special case of the dilithium compounds, Li_2MO_2, where the lithiums are in tetrahedral sites, can be represented by the slab-stacking sequence ..(AcB)-*ba*(AcB)... There is only one realistic stacking sequence because an octahedral site in the transition-metal layer cannot be occupied directly opposite a tetrahedral site. Where some octahedral sites are occupied in the lithium layer, the total lithium content will be less than two and/or the lattice will become distorted or even amorphous.

4.2. Lithium Cobalt Oxide, $LiCoO_2$

Goodenough recognized that $LiCoO_2$ had a structure similar to the layered structures of the dichalcogenides and showed that the lithium could be removed electrochemically, thus making it a viable cathode material.[123] $LiCoO_2$ has the α-$NaFeO_2$ structure with the oxygens in a cubic close-packed arrangement. On complete removal of the lithium, the oxygen layers rearrange themselves to give hexagonal close packing of the oxygen in CoO_2.[124] Between these composition limits several phases are

formed with varying degrees of distortion of the ccp oxygen lattice. The composition $Li_{0.5}CoO_2$ can also be formed in the spinel form,[125] though it appears to be metastable and is not normally formed during the cycling of the Li_xCoO_2 electrode. However, a recent TEM study[126] has identified the spinel phase originating on the surface of heavily cycled $LiCoO_2$ cathodes.

SONY combined the $LiCoO_2$ cathode with a carbon anode to make the first successful Li-ION battery,[127,128] which now dominates the lithium battery market. The carbon anode, which forms the compound LiC_6 on reaction with lithium, makes a much safer battery than if pure lithium is used as there is much less chance of the formation of dendritic lithium, which can lead to cell shorting. The use of graphitic carbon can result in the loss of 100−300 mV in cell potential, which is feasible with the higher potential $LiCoO_2$ cathode but not with the lower potential of the TiS_2 cathode. The commercial cell is built in the discharged state: C-$LiCoO_2$. It thus must be charged before use. The theoretical capacity of the $LiCoO_2$ cell is relatively low at around 130 mAh/g because only around 0.5 Li/Co can be reversibly cycled without causing cell capacity loss due to changes in the $LiCoO_2$ structure. This can be associated with two factors: phase changes that cause low reaction rates and the poor stability of the electrode at low lithium contents. The message here may be that reactive nanosize materials/components may not be viable for commercial batteries because of safety and life considerations.

The diffusion of lithium in $LiCoO_2$ is 5×10^{-9} cm^2/s, which compares with 10^{-8} cm^2/s for $LiTiS_2$.[129] These high diffusivity values are consistent with the ability to cycle these two cathodes at 4[129] and 10 mA/cm^2,[13] respectively. However, the conductivity of Li_xCoO_2 remains a challenge as it is reported[130] to change dramatically with composition, behaving like a metal at $x = 0.6$ and a typical semiconductor at $x = 1.1$ (the typical lithium-rich material used in commercial cells), changing by 2[131] (for the $x = 1.1$ compound) to 4[130] (for the $x = 1.0$ compound) orders of magnitude at ambient temperatures and up to 6 orders of magnitude at lower temperatures.[131]

The energy density of commercial cells has almost doubled since their introduction in 1991; since 1999 the volumetric energy density has increased from 250 to over 400 Wh/l.[132] Details of the original commercial cells have been reviewed by Nishi,[133] where key aspects are discussed concerning the need for large particle size, 15−20 μm, to increase safety and the intentional incorporation of lithium carbonate into the cathode to provide a safety valve. The lithium carbonate decomposes, releasing carbon dioxide when the charging exceeds 4.8 V, which breaks electrical flow in the cell. These lithium cobalt oxides also contain excess lithium and can be best represented by the formula $Li_{1+x}Co_{1-x}O_2$.

In 1999 Cho et al. reported[134−138] in a pioneering series of papers that the capacity could be improved by coating a metal oxide or phosphate on the surface of the $LiCoO_2$ particles. They found that the capacity could be increased to 170 mAh/g when cycled between 2.75 and 4.4 V without capacity fade over 70 cycles. Other researchers[139−141] quickly confirmed the positive results of surface coatings. The mechanism of protection is related to minimizing the reactivity of Co^{4+} on charge with the acidic HF in the electrolyte coming from the interaction of moisture with the electrolyte salt $LiPF_6$.[142] Removing the source of the HF should eliminate the capacity loss as found[143,144] for the spinel $LiMn_2O_4$, where switching to the LiBOB salt essentially eliminated manganese dissolution and capacity loss. This was also the case for $LiCoO_2$,[145] where replacing the $LiPF_6$ salt by LiBOB or by completely drying the $LiCoO_2$ by heating to over 550 °C, improved the capacity retention at 180 mAh/g at a 4.5 V cutoff. Above this 4.5 V level, the three-block cubic close-packed Li_xCoO_2 converts to the 1T one-block hexagonal close-packed structure of CoO_2; this requires substantial movement of the oxygen layers in going from ABCA to ABA stacking sequence which will eventually significantly disrupt/disorder the structure. Thus, one cannot expect capacities for $LiCoO_2$ much above 180 mAh/g to be attainable over hundreds of cycles. A more recent study[146] suggests that CoO_2 has a monoclinically distorted $CdCl_2$ structure, whereas NiO_2 has a monoclinically distorted CdI_2 structure, but little detail is given and no mention is made of the nickel content or distribution.

Although the $LiCoO_2$ cathode dominates the rechargeable lithium battery market, there is a limited availability of cobalt, which causes it to have a high price. This price limits it use to small cells, such as those used in computers, cell phones, and cameras. An alternative cathode will be needed for large-scale applications, as envisioned in HEV or for load leveling. The $LiCoO_2$ patent[147] covered more than this one cathode, describing all layered transition-metal oxides with the α-$NaFeO_2$ structure where the transition metal is vanadium through nickel. In addition, combinations of the transition metals were described, such as $LiCo_{1-y}Ni_yO_2$. In addition, another patent[148] covers the electrodeintercalation process for forming the alkali-metal compounds A_xMO_2 with the α-$NaFeO_2$ structure where A is Li, Na, or K and $x < 1$.

4.3. Lithium Nickel Oxide, $LiNiO_2$

Lithium nickel oxide, $LiNiO_2$, is isostructural with lithium cobalt oxide but has not been pursued in the pure state as a battery cathode for a variety of reasons, even though nickel is more readily available than cobalt. First, it is not clear that stoichiometric $LiNiO_2$ exists. Most reports suggest excess nickel as in $Li_{1-y}Ni_{1+y}O_2$; thus, nickel is always found in the lithium layer, which pins the NiO_2 layers together, thereby reducing the lithium diffusion coefficient and the power capability of the electrode. Second, compounds with low lithium contents appear to be unstable due to the high effective equilibrium oxygen partial pressure, so that such cells are inherently unstable and therefore dangerous in contact with organic solvents. A second lithium can be inserted either chemically or electrochemically, as in $Li_{1.8}Ni_{1+y}O_2$, which is a mixture as expected of "$LiNiO_2$" and "Li_2NiO_2".[63]

We will discuss in section 5.2.1 of this review the modification of this material by replacing a part of the nickel by other elements such as cobalt and aluminum. The former assists in ordering the structure, that is keeping the nickel in the nickel layer, and the latter, being redox inactive, prevents the complete removal of all the lithium, thus additionally stabilizing the structure and preventing any phase changes that might occur at very low or zero lithium content. Unlike cobalt and nickel, manganese does not form a stable $LiMnO_2$ phase with the $LiCoO_2$ structure, with the spinel structure being the stable phase at the composition $Li_{0.5}MnO_2$. As there are a myriad of structures[149] with the 1:2 Mn:O ratio, other structures may be stable at different lithium contents.

5. 1990–Present: Second-Generation Lithium Batteries

5.1. Spinels

The spinel cathode $LiMn_2O_4$, originally proposed by Thackeray et al.,[150] has been extensively developed by the Bellcore labs,[151−153] and has recently been reviewed by Thackeray[154] with the key structural aspects by Yonemura et al.[155] The anion lattice again contains cubic close-packed oxygen ions and is closely related to the α-$NaFeO_2$ layer structure, differing only in the distribution of the cations among the available octahedral and tetrahedral sites. The discharge proceeds in predominantly two steps, one around 4 V and the other around 3 V as shown in Figure 11. Usually only the 4 V plateau is used, so that the cell is constructed in the discharged state and must be charged before use just as for $LiCoO_2$.

charging: $LiMn_2O_4 \rightarrow Mn_2O_4 + Li$ (inserted into anode host, such as graphitic carbon)

It has been reported[153,156] that the value of the cubic lattice parameter, which is directly related to the average oxidation state of the manganese, is critical to obtain effective cycling. The lattice parameter should preferably be 8.23Å or less, and such values are associated with lithium-rich materials, $Li_{1+x}Mn_{2-x}O_4$, where the average manganese oxidation state is 3.58 or higher; this value minimizes dissolution of manganese and also the impact of the

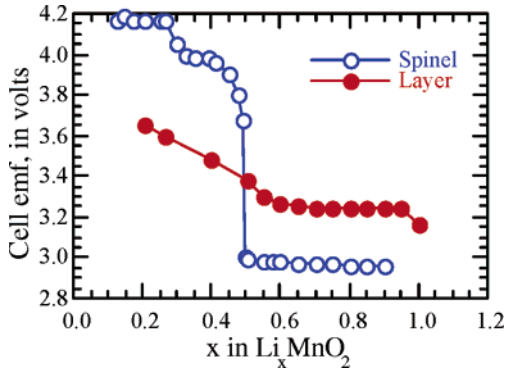

Figure 11. Potential profile of $LiMnO_2$ and spinel $LiMn_2O_4$ (data from Bruce and Whittingham).

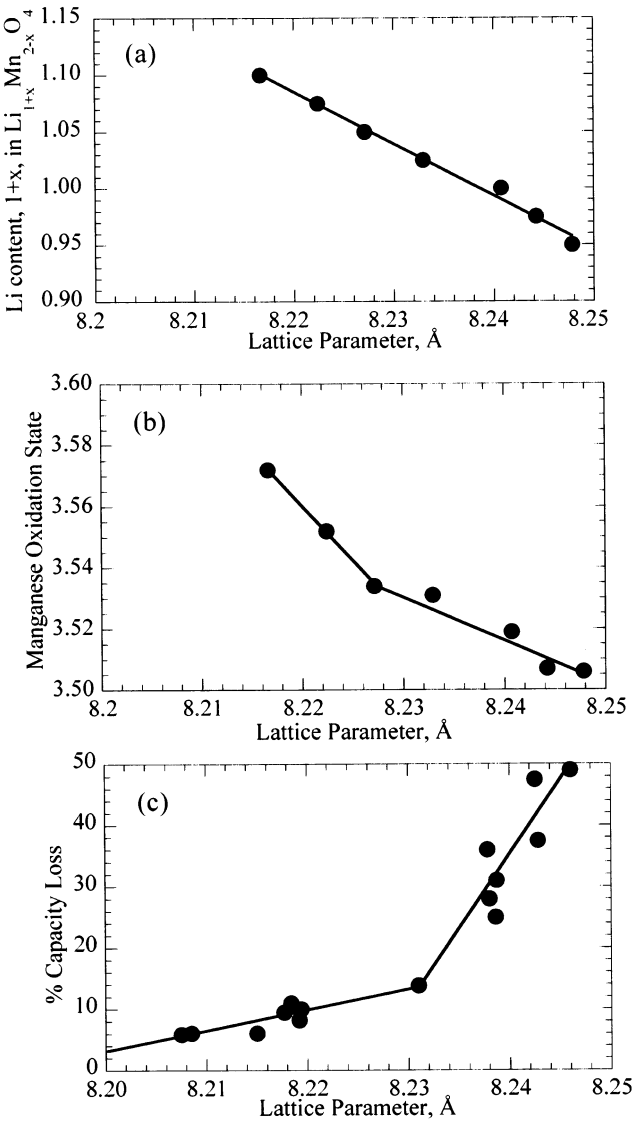

Figure 12. Correlation of the lattice parameter of the spinel $Li_{1+x}Mn_{2-x}O_4$ with (a) the lithium content, (b) manganese oxidation state, and (c) capacity loss of the cell over the first 120 cycles, after ref 157.

Jahn−Teller distortion associated with the Mn^{3+} ion. The variation in lattice parameter, a_o, with chemical composition in $Li_{1+x}Mn_{2-x}O_2$ is shown in Figure 12a (after ref 157); its variation is given by $a_o = 8.4560 - 0.21746x$.

The lattice parameter may also be used as an indirect measurement of the manganese oxidation state, shown in Figure 12b. Figure 12c, in addition, shows clearly the impact of lattice parameter on the percent capacity loss over the first 120 cycles. The retention of cycling capacity at elevated temperatures can be helped by the simultaneous doping with aluminum and fluoride ions, as in $Li_{1+x}Mn_{1-x-y}Al_yO_{4-z}F_z$, where y and z are around 0.2.[157] Moreover, if the potential on the surface of the spinel is kept above that for the formation of the $Li_2Mn_2O_4$ phase, then the formation of Mn^{2+} by the disproportionation of surface Mn^{3+} ions is minimized: $2Mn^{3+} = Mn^{2+} + Mn^{4+}$. It is the divalent manganese ions that are soluble in the acidic electrolyte, and so every attempt must be made to minimize their formation. Once dissolved into the electrolyte, the manganese ions can

diffuse across to the anode and be reduced there to manganese metal, thereby using up the lithium and reducing the electrochemical capacity of the cell.

This spinel is presently the center of much interest as the cathode of a high-power lithium battery for hybrid electric vehicles, even though under high drain rates its capacity is only around 80 mA/g. This material has been plagued by self-discharge when left under full charge, particularly at elevated temperatures; however, this problem may have been solved by switching from the fluoride-containing $LiPF_6$ salt, which in the presence of traces of moisture can generate HF, to salts such as LiBOB.[143,144] The spinel used is in a stabilized form in which a part of the manganese has been substituted as in $Li_{1.06}Mn_{1.95}Al_{0.05}O_4$, and there have been several hundred studies on the impact of this substitution.[157−159] These studies will not be discussed here. An alternate solution pioneered by the Korean school is to coat the surface of the spinel particles with materials such as zirconium dioxide or $AlPO_4$, which are believed to act as getters for any HF.

One spinel, $Li_4Ti_5O_{12}$, is under serious consideration as an anode in high-power cells as its charging potential (lithium insertion) is around 1.55 V,[160−162] so there is no danger of lithium metal deposition as might occur on graphitic carbon at high rates. Rates as high as 12C have been claimed (total reaction in 60/12 = 5 min), both with nano- and microstructured materials at 60 °C.[163] This electrode is being considered in combination with a high-rate cathode such as a mixed layered oxide or with the spinel $LiMn_2O_4$ to give a lower cost and safe 2.5 V cell. It has also been coupled with the olivine $LiFePO_4$ (see later in this paper) and cycles well at a potential of 1.8 V with no capacity loss over a 100 cycles.[164] If coupled with a high-voltage spinel, then the cell potential might attain 3.5−4 V.[165]

5.2. Other Layered Oxides

5.2.1. Mixed Nickel–Cobalt Dioxide, $LiNi_{1-y}Co_yO_2$

Many different elements can be substituted into the α-$NaFeO_2$-type structure, and they impact the layeredness of the structure, its stability on lithium removal, and the retention of capacity on cycling. In a series of papers the Delmas group[166−169] and Zhecheva et al.[170] determined the structural details and physical properties of the $LiNi_{1-y}Co_yO_2$ system and showed that there is an increased ordering as the cobalt concentration increases; they found that the $c/3a$ ratio increases monotonically from 1.643 to 1.652 as y increases from 0 to 0.4 and that there is no nickel content on the lithium sites for $y \geq 0.3$. Thus, cobalt suppresses the migration of nickel to the lithium site in the mixed Li nickel/cobalt compounds and one would expect and finds the same behavior in the Li nickel/manganese/cobalt oxides. Cobalt is also reported to facilitate the oxidation of iron atoms in the structure.[171] Other ions, such as iron, do not have the same positive effect as cobalt; thus, in the compound $LiNi_{1-y}Fe_yO_2$ the capacity is reduced with increasing iron content and the iron has no positive effects on the layeredness of the structure.[172] Thus, for $y = 0.10$, 0.20, and 0.30 the amount of 3d metal in the lithium layer is 6.1%, 8.4%, and 7.4%, respectively, for samples formed at 750 °C. Although a $LiFeO_2$ compound would be ideal for a low-cost battery, it has been reported[173] that the lithium cannot be deintercalated within the normal potential ranges used in lithium batteries; this is explained[174] by the lack of compression of the FeO_6 octahedra which makes the reduction of one electron from Fe^{3+} very difficult.

An issue with all these layered oxides is their electronic conductivity, which is not uniformly high across the lithium composition range, or nickel substitution. Thus, cobalt substitution in $LiNiO_2$, as in $LiNi_{0.8}Co_{0.2}O_2$, reduces the conductivity.[169] In addition, as lithium is removed from the phase $Li_xNi_{0.1}Co_{0.9}O_2$[168] or from Li_xCoO_2[130] the conductivity was found to increase dramatically by some 6 orders of magnitude to around 1 S/cm from $x = 1$ to 0.6. These dramatic changes demand that a conductive diluent be added to the cathode-active material, which reduces both the energy storage and the power capabilities.

Studies have shown that the cobalt-substituted nickel oxides are more stable and thus are less likely to lose oxygen than the pure nickel oxide. The addition of a little of a redox-inactive element such as magnesium reduces the capacity fading on cycling,[175] as in $LiNi_{1-y}Mg_yO_2$;[176] this inert element prevents the complete removal of all the lithium and thus minimizes possibly structural collapse and reaching such a high level of oxygen partial pressure−NiO_2 itself is thermodynamically unstable at 25 °C, as the equilibrium oxygen partial pressure exceeds 1 atm.

Substituted nickel oxides, such as $LiNi_{1-y-z}Co_yAl_zO_2$, are prime candidates for the cathode of advanced lithium batteries for use in large-scale systems as required for hybrid electric vehicles. On charging these mixed oxides the nickel is oxidized first to Ni^{4+} then the cobalt to Co^{4+}.[177] SAFT has constructed cells with these substituted nickel oxides that have been cycled 1000 times at 80% depth of discharge with an energy density of 120−130 Wh/kg.[178]

5.2.2. Lithium Manganese Dioxide, $LiMnO_2$

Much interest has been placed on the layered $LiMnO_2$ compound for its prospects of providing not only a low-cost but also an environmentally benign cathode material.[179−181] However, it is not thermodynamically stable at elevated temperature and thus cannot be synthesized by the same methods as used for materials like $NaMnO_2$. Instead, other approaches must be used. One approach is to ion exchange the sodium compound, giving $LiMnO_2$, which was accomplished independently by Bruce[181] and Delmas;[182] starting with different layered structures maintains the stacking order of the parent manganese oxide, thus allowing study of the impact of stacking sequence on electrochemical performance. An alternative preparative approach is to synthesize the structure at low temperatures, as, for example, by hydrothermal synthesis/decomposition of alkali

permanganates,[180,183−185] which in the case of lithium results in the composition $Li_{0.5}MnO_2 \cdot nH_2O$. Mild warming causes the loss of water to give the desired layered Li_xMnO_2; overheating to 150 °C results in the formation of the spinel $LiMn_2O_4$. Birnessite-type phases have also been made by acid treatment of manganese oxides.[186−189]

However, Li_xMnO_2 easily converts to the thermodynamically stable spinel structure upon cycling lithium in and out but apparently not on acid delithiation;[190] this conversion requires no oxygen diffusion as both structures have ccp oxygen lattices. This ccp lattice has oxygen layers in the sequence AcB|*a*CbA|*c*BaC|*b*A, i.e., there are three building blocks—MnO_2 blocks (upper case is oxygen, lower case is manganese, italic lower case is lithium). Two approaches to stabilize the layered $LiMnO_2$ have been taken. In the geometric stabilization approach, non-ccp structures are proposed such as tunnel structures,[191−195] two-block (see Figure 10) or other non CCP close-packed structures,[196] or "pillars" are placed between the layers to provide the stabilization. We reported on compounds $KMnO_2$ [180,184] and $(VO)_y$-MnO_2,[197,198] which are examples of such pillared structures. The former is stable to spinel formation at low current densities, and the latter shows excellent stability but poor rate capability. The groups of Dahn and Doeff among others have pursued non-ccp structures by looking at tunnel structures such as $Li_{0.44}MnO_2$[191,193,194] and also by ion-exchanging layered sodium manganese oxide compounds with non-ccp stacking of the oxygen sheets;[199−205] these sheets cannot readily reorganize after ion exchange to give ccp stacking. This results in, for example, the two-block rather than the three-block structures such as O3, which is that of ccp $LiMnO_2$. Such compounds have also been studied with partial substitution of the manganese by, for example, Co.[205] This ion-exchange process also results in much faulting in the stacking of the layers, which impedes the layers from reordering into the thermodynamically stable O3 phase. However, these phases intercalate lithium over a rather wide range of potential and in some cases over two potential steps.[201]

In the electronic stabilization approach the goal is to make the electronic properties of Mn to be more cobalt-like by substitution of the Mn with more electron rich elements such as Ni.[196] The successful substitution of Mn by Co[190,206,207] and Ni[208−214] has been reported. The first studies on $LiNi_{1-y}Mn_yO_2$, for $0 < y \leq 0.5$, indicated low capacities and poor reversibility.[212] However, Spahr et al. later demonstrated a high capacity and reversibility for $LiNi_{0.5}Mn_{0.5}O_2$[213] with a discharge curve typical of that of $LiNiO_2$. More recently, the compounds $LiNi_{1-y-z}Mn_yCo_zO_2$ have been extensively investigated in the last 3 years and found to have properties that qualify them as possible candidates for the replacement of $LiCoO_2$.[198,215−237] In addition to their high lithiation capacities and reversibility, these compounds show higher thermal stabilities compared to the Co-free compounds. These compounds are discussed in the next sections. The layered-to-spinel phase transition in Li_xMnO_2 has also been considered theoretically[238] and found to go in a two-step process; in the first step a fraction of the lithium and manganese ions move rapidly into tetrahedral sites, and in the second stage these order into the spinel arrangement of cations.

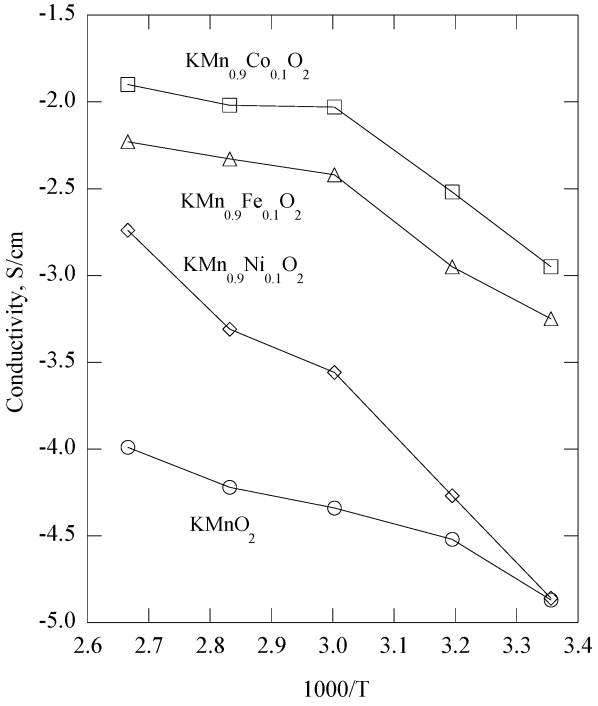

Figure 13. Electronic conductivity of pillared $KMnO_2$ with 10% Co, Ni, and Fe substitution of the Mn.

5.2.3. Mixed Manganese–Cobalt Dioxide, $LiMn_{1-y}Co_yO_2$

Bruce et al.[206,239,240] investigated the synthesis and electrochemical behavior of cobalt-substituted $LiMn_{1-y}Co_yO_2$. They synthesized this material from the sodium analogue by ion exchange and achieved values of y up to 0.5. These substituted materials have the α-$NaFeO_2$ structure. These materials, just like the unsubstituted $LiMnO_2$, convert to the spinel structure on cycling even at the low cycling rate of 0.1 mA/cm^2; for $y = 0.1$, this begins to occur on the first cycle and is not apparent until the thirtieth cycle for $y = 0.3$. However, they cycle over the 3 V spinel plateau very well. The conversion to spinel is expected to occur very rapidly at elevated temperatures.

The partial substitution of the manganese ions by cobalt, iron, or nickel was found to significantly increase the electronic conductivity of the manganese oxide, which in the pure state as in $LiMnO_2$ or $KMnO_2$ is around 10^{-5} S/cm, too low to allow rapid reaction without addition of a conductive diluent. To obtain sufficiently dense material for conductivity measurement, the potassium analogues were synthesized at elevated temperatures with 10% of the manganese substituted. The data,[241] shown in Figure 13, clearly show the advantage of adding cobalt, which enhanced the conductivity by almost 2 orders of magnitude. Nickel had the least effect, and we will discuss the impact of joint additions of cobalt and nickel as in $LiNi_{0.4}Mn_{0.4}Co_{0.2}O_2$.[219]

These cobalt-substituted materials can also be prepared hydrothermally, and their cycling behavior

is much improved over the cobalt-free compounds.[242] Conversion to spinel is observed on the first charge cycle at rates of 1 mA/cm^2, even when larger cations such as potassium are incorporated into the structure as pillaring agents. The layered-to-spinel phase transition in Li_xMnO_2 has subsequently been explained through modeling.[238]

Work on these cobalt-substituted α-$NaFeO_2$ structure materials, where manganese is the redox-active ion, has essentially ceased because of the inability to maintain the structure relative to conversion to the spinel structure under realistic cycling conditions. Doping elements other than cobalt have also been investigated, but substitution by nickel leads to a system where the manganese becomes the structure stabilizer and nickel the electrochemically active ion. These compounds are thus best described as substituted nickel oxides in which the manganese remains in the tetravalent state and the nickel is redox active between the +2 and +4 oxidation states; the manganese helps in reducing the cost and stabilizing the lattice. Cobalt, as will be discussed below, plays a critical role in controlling the ordering of the 3d ions in the structure.

5.2.4. Mixed Nickel–Manganese Dioxide, $LiNi_{1-y}Mn_yO_2$—Multielectron Redox Systems

The groups of Ammundsen and Davidson announced results on the Li−Mn−Cr−O_2 system[243,244] at the 2000 Lithium Battery meeting in Como. They found[245−250] that these mixed-metal compounds had the $NaFeO_2$ structure and cycled well when a substantial part of the transition metals were substituted by lithium as in Li_3CrMnO_5 or described in the layered form as $Li[Li_{0.2}Mn_{0.4}Cr_{0.4}]O_2$. The discharge curve showed the typical behavior of a single phase rather than the two-phase, two-step behavior of the spinel. The manganese has the 4+ oxidation state, and all the lithium can be removed giving Cr(VI). What was surprising was the high mobility of the chromium, which during the redox process must move from an octahedral to a tetrahedral site; increasing the temperature from 20 to 55 °C increased the cell capacity from around 125 to 165 mAh/g, consistent with having to move the highly charged chromium ion as well as the lithium ion. Capacities as high as 220 and 200 mAh/g were obtained at low rates, 3[248] and 10 mA/g,[247] respectively, from 2.5 to 4.5 V. The lithium ions in the transition-metal layer were found clustered around the manganese ions as in Li_2MnO_3, and the system can be considered as a solid solution of Li_2MnO_3 and $LiCrO_2$. Although of little commercial interest, because of the toxicity of Cr(VI), this pioneering research provoked much thinking about other multielectron redox reactions which are discussed below. The corresponding solution between Li_2MnO_3 and $LiCoO_2$ did not show similar behavior, with the capacity decreasing with increasing manganese content when cycled between 3.0 and 4.2 or 4.3 V.[207,251]

The $LiNi_{1-y}Mn_yO_2$ phase system was studied by the Dahn group[212] in 1992. They reported a solid solution for $y \leq 0.5$ but a deterioration of the electrochemical behavior with increasing manganese content. Spahr et al.[213] repeated the work, also showing a maximum solubility of 0.5 Mn. They however found optimum electrochemical behavior for the composition $LiNi_{0.5}Mn_{0.5}O_2$. They reported XPS and magnetic data that are consistent with the present interpretation of Ni^{2+} and Mn^{4+} ions rather than Ni^{3+} and Mn^{3+} and showed electrochemical cycling curves very reminiscent of $LiNiO_2$. This compound, which we will call the 550 material (0.5 Ni, 0.5 Mn, 0.0 Co) was rediscovered by Ohzuku[214] in 2001, who reported very good electrochemical data, and this was reconfirmed almost immediately by the Dahn group.[252] These papers ignited a substantial amount of work on this composition and on the cobalt-substituted compounds, in particular those with the formula $LiNi_yMn_yCo_{1-2y}O_2$, where $0.5 \leq y \leq 0.33$, which can be considered as a solid solution of $LiNi_{0.5}Mn_{0.5}O_2$ and $LiCoO_2$.

Manganese shows no significant layer stabilization capability as up to 10% nickel is found on the lithium sites, 9.3%[253] for a sample formed at 1000 °C, and 11.2% for a sample formed at 900 °C;[254] this nickel is expected to reduce the rate capability of the electrode. The phase $LiNi_{0.5}Mn_{0.5}O_2$ has the expected hexagonal lattice with $a = 2.894$ Å and $c = 14.277$Å,[213] $a = 2.892$ Å and $c = 14.301$ Å,[214] $a = 2.891$ Å and $c = 14.297$ Å,[253] $a = 2.888$ Å and $c = 14.269$ Å,[254] $a = 2.887$ Å and $c = 14.262$ Å,[255] $a = 2.895$ Å and $c = 14.311$ Å,[256] and mean $c/3a = 1.647$. There is some disagreement about the structure formed on lithium removal. Venkatraman et al. reported[254] a single phase for $0 \leq Li \leq 1$ with continuously varying lattice parameters; the data reported for $Li_{0.2}Ni_{0.5}Mn_{0.5}O_2$ is consistent with single-phase behavior. However, Yang et al.[256] reported that on delithiation a second hexagonal phase with $a = 2.839$ Å, $c = 14.428$ Å was formed; this is in contrast to the pure $LiNiO_2$, where a third hexagonal phase is also found. Arachi et al. reported[253] the formation of a monoclinic phase for $Li_{0.5}Ni_{0.5}Mn_{0.5}O_2$with $a = 4.924$ Å, $b = 2.852$ Å, $c = 5.0875$ Å, $\beta = 108.81°$. Yang et al.[256] also reported that excess lithium could be intercalated with a slight expansion of the hexagonal cell to $a = 2.908$ Å and $c = 14.368$ Å; this is possibly the phase $Li_2Ni_{0.5}Mn_{0.5}O_2$ and if so raises the question of which site the nickel in the lithium layer occupies if the lithium takes up the tetrahedral sites. One would not expect the rhombohedral structure reported but rather a single block structure with c around 4.8 Å if the lithiums are in the tetrahedral sites; the lithium ions in tetrahedral sites would be much too close to the transition-metal ions in the transition-metal layer. There is no data reported on the stability of this phase, which might be expected to be metastable like Li_2NiO_2, which converts[63] at 400 °C to the orthorhombic form of Li_2NiO_2.[257]

Spahr et al. reported[213] in 1998 a capacity of 150 mAh/g falling to 125 mAh/g after 25 cycles and to 75 mAh/g after 50 cycles for a 550 sample prepared at 700 °C; they also showed that the capacity and capacity retention increased as the synthesis temperature was increased from 450 to 700 °C, which we now know to be too low a temperature for optimum electrochemical behavior. Ohzuku et al.[214]

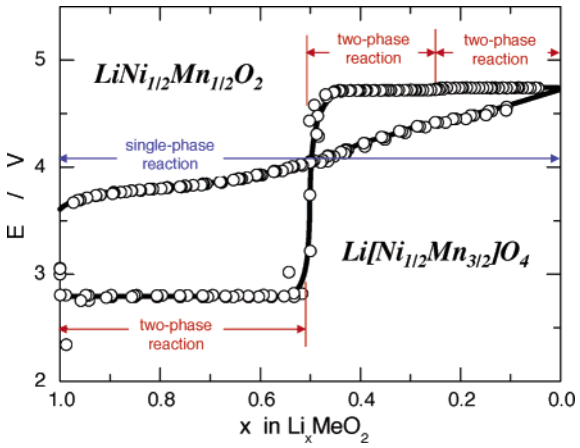

Figure 14. Lithium cell potentials of the two lithium nickel manganese dioxides with layered and spinel structures.[260]

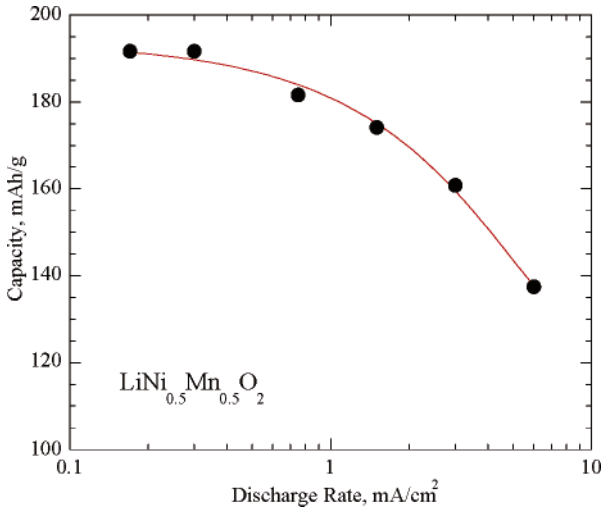

Figure 15. Ragone plot for $LiNi_{0.5}Mn_{0.5}O_2$ showing the capacity of the cathode as a function of the discharge current density (data from ref 258).

prepared the 550 material at 1000 °C and reported a constant capacity of 150 mAh/g at 0.1 mA/cm^2 for 30 cycles using top-up charging at 4.3 V. The cell potential[214,258,259] varies from around 4.6 to 3.6 V as shown in Figure 14;[260] it shows a single phase for all x values in $Li_xNi_{0.5}Mn_{0.5}O_2$. The composition $LiNi_{0.25}Mn_{0.75}O_4$, which has the spinel rather than the layered structure, shows the typical two-phase, two-step spinel discharge potential and is very similar to that of $LiMnO_2$ shown in Figure 11 except for the higher potentials in this case. The 550 material, synthesized at 900 °C and quenched to room temperature, also showed a capacity exceeding 150 mAh/g for over 50 cycles in thin film configuration.[252] Material cycled[261] with a 4.4 V top-up constant potential charge after a constant current charge to 4.4 V showed an initial capacity exceeding 170 mAh/g but decayed over 20 cycles to less than 150 mAh/g, whereas a sample charged to just 4.2 V only had a capacity of 130 mAh/g but maintained this capacity much better; increasing the temperature to 50 °C increased the fade rate except where the maximum charge potential was limited to 4.2 V. The 550 composition showed a lithium diffusion coefficient of around 3×10^{-10} cm^2/s for most of the lithium composition range. A contradictory report[255] shows good cycling stability at 0.1 mA/cm^2 (10 mA/g) even when charged to 4.6 V, with the capacity increasing from 150 to 190 mAh/g as the charging cutoff potential is raised from 4.3 to 4.6 V. A material formed at 1000 °C showed a lower capacity of around 120 mAh/g at 0.1 mA/cm^2; the capacity was increased to about 140 mAh/g by addition of 5% cobalt, aluminum, or titanium.[262] This suggests that the synthesis temperature of 1000 °C may be too high, leading possibly to excess nickel in the lithium layer. This 550 compound can intercalate a second lithium, particularly when some titanium is added, $yLiNi_{0.5}Mn_{0.5}O_2{\cdot}(1-y)Li_2TiO_3$, which results from reduction of Mn(IV) to Mn(II);[64] no structural data was given for this new phase. Lu et al.[252] showed that the capacity could be increased from around 160 to 200 mAh/g at 30 °C by substituting a part of the transition metals by lithium, $Li[Ni_{1/3}Mn_{5/9}Li_{1/9}]O_2$. There is one report[263] of conductive carbon coatings raising the capacity, but even then the capacity was lower than those reported above. The rate capability has been determined in another study,[258] where the capacity approaches 200 mAh/g at 0.17 mA/cm^2, falling off to 130 mAh/g at 6 mA/cm^2; all cells were charged at 0.17 mA/cm^2 and then held at 4.5 V for 19 h; cathode loading was around 15 mg/cm^2. These data are shown in Figure 15 as a Ragone plot and strongly suggest that pulse discharge rates in excess of 10 mA/cm^2 should be achievable. Rate data will also be needed on charging if such cells are to be considered for HEV applications.

The electrochemically active element in this compound is nickel, which cycles between the +2 and +4 valence states, while the manganese remains as +4 throughout independent of the lithium content. First-principal quantum mechanical calculations[264] as well as structural measurements confirm this redox assignment. As the manganese is always 4+, there is no concern with the Jahn−Teller distortion associated with the Mn^{3+} ion. Consistent with this model it should be possible to replace the manganese by an element such as titanium; Kang et al.[265] synthesized the compound $Li_{0.9}Ni_{0.45}Ti_{0.55}O_2$ with the α-$NaFeO_2$ structure by ion exchange of the sodium analogue, as high temperatures lead to complete cation disorder and a rock-salt structure. About one-half of the lithium could be removed in an electrochemical cell, with only about one-half of that being re-intercalated on discharge; this is believed to be due to cation, probably titanium, migration into the lithium layer. Clearly, the manganese ion plays a key stabilizing influence on the α-$NaFeO_2$ structure.

Little is known about the electrical conductivity of the 550 material. One measurement shows a conductivity of 6×10^{-5} S/cm at 25 °C[219] for the fully lithiated $LiNi_{0.5}Mn_{0.5}O_2$. The magnetic susceptibility exhibits Curie−Weiss behavior at elevated temperatures.[262]

The precise details of the structure of $Li_xNi_{0.5}Mn_{0.5}O_2$ are complex, with a superstructure being observed in the X-ray diffraction pattern.[252,266] Long-range order has been detected by transmission electron microscopy,[267] and the domain size of this

ordering increases with the lithium content from 1 to 2 nm in the 550 compound to complete ordering in Li_2MnO_3. As noted above, there is apparently always 8−10% nickel in the lithium layer and a corresponding amount of lithium in the transition-metal layer. Grey et al.,[268] using NMR studies, have shown that the lithium in the transition-metal layer is surrounded by six manganese ions, as in Li_2MnO_3. Ceder and Grey thus propose,[269] supported by experiments and calculations, that the composition of the transition-metal layer requires 0.5/6 lithium (~8%); the manganese ions in turn are surrounded by nickel ions on the hexagonal lattice, leading to a $2\sqrt{3} \times 2\sqrt{3}$ superlattice. On charging, the lithium is initially removed from the lithium layer, but when two adjacent lithium sites become vacant in that layer, then the lithium ion in the transition-metal layer can drop down from its octahedral site into the vacant tetrahedral site. This is consistent with the NMR observation of the reversible removal of the lithium ion from the transition-metal layer on charging the material. This tetrahedral lithium is only removed at the highest potential, i.e., only after all the octahedral lithium is removed. This model is consistent with the presence of the tetrahedral lithium in $Li_{0.5}Ni_{0.5}Ni_{0.5}O_2$ proposed by Kobayashi et al.[270,271]

In conclusion, the 550 material has the following cathode characteristics.

(1) It has a capacity of around 180 mAh/g for at least 50 cycles under mild cycling conditions.
  (a) Overcharging increases capacity fade, but a protective coating might help.
  (b) The synthesis temperature should be in excess of 700 °C and less than 1000 °C, probably optimally around 900 °C.
(2) There are always nickel ions in the lithium layer, up to 10%, which will restrict the rate capability and compromise the energy density.
  (a) Cobalt additions can reduce the level of nickel in the lithium layer, as in $LiNi_{1-y}Co_yO_2$.
  (b) The lithium in the transition-metal layer may be a necessary structural component.
(3) The structure of the lithium poor phase is unclear.
(4) Nickel is the electrochemically active ion.
(5) The electronic conductivity needs increasing.

5.2.5. Mixed Nickel–Manganese–Cobalt Dioxide, $LiNi_{1-y-z}Mn_yCo_zO_2$

Consideration of the above leads logically to a mixing of the three transition metals, and the reports of such compounds were first published in 1999 by Liu et al.[272] and in 2000 by Yoshio et al.,[228] and the latter hypothesized that the addition of cobalt to $LiMn_{1-y}Ni_yO_2$ would stabilize the structure in a strictly two-dimensional fashion. They found that the transition-metal content in the lithium layer fell from 7.2% for $LiMn_{0.2}Ni_{0.8}O_2$ to 2.4% for $LiMn_{0.2}Ni_{0.5}Co_{0.3}O_2$ and that the lithium insertion capacities exceeded 150 mAh/g for the cobalt-substituted compounds. Ohzuku et al.,[215] studying the symmetric compound $LiNi_{0.33}Mn_{0.33}Co_{0.33}O_2$, synthesized at 1000 °C, also found a capacity of around 150 mAh/g cycling between 2.5 and 4.2 V at 0.17 mA/cm^2 at 30 °C; raising the charge cutoff potential to 5.0 V increased the capacity to over 220 mAh/g, but capacity fade was evident. This compound will be referred to as the 333 material.

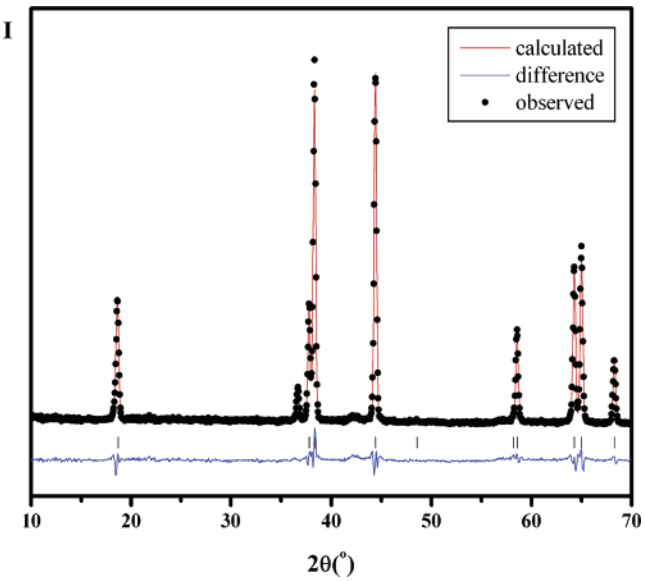

Figure 16. Neutron powder diffraction pattern of a layered substituted nickelate, $LiNi_{0.4}Mn_{0.4}Co_{0.2}O_2$.

The synthesis of these $LiNi_{1-y-z}Mn_yCo_zO_2$ compounds is typically accomplished using a modified mixed-hydroxide approach by reacting $Ni_{1-y-z}Mn_yCo_z(OH)_2$ with a lithium salt in air or oxygen as described in Liu's first synthesis[272] at 750 °C, which is now known to be below the optimum temperature of 800−900 °C.[219] These conditions result in a single phase with the layered O3 structure. A typical diffraction pattern, as given in Figure 16, conforms to the $R\bar{3}m$ symmetry of the α-$NaFeO_2$ structure. The structure consists of a cubic close-packed arrangement of the oxide ions. The transition-metal ions in the structure occupy alternating layers in octahedral sites. The structure and properties of the precursor hydroxide compound have been studied;[273] it has the CdI_2 structure like TiS_2 but with some turbostratic disorder and on heating can convert to a spinel phase.

The cell parameters[219,228,233,236] of this tri-transition-metal compound are slightly dependent on the transition metals as shown in Figure 17. Both the in-plane *a* parameter and the interlayer spacing *c* increases with the Ni content and decreases with the Co content for constant Mn content.[219,228] For compositions $LiNi_yMn_yCo_{1-2y}O_2$, the *a* and *c* parameters obey Vegard's law, decreasing linearly with increasing cobalt content.[233] For constant nickel content, the *a* parameter is directly proportional to [Mn] and inversely proportional to [Co], which is indicative of a larger Mn ion compared to the Co ion. This observation is contrary to the suggestion[236] that Mn does not have any effect on the parameters.

The ratio $c/3a$ of the lattice constants is a direct measure of the deviation of the lattice from a perfect cubic close-packed lattice, which is it measures the layeredness of the lattice. An ideal ccp lattice has a $c/3a$ ratio of 1.633, whereas a pure layered lattice with no transition metal in the lithium layer has a

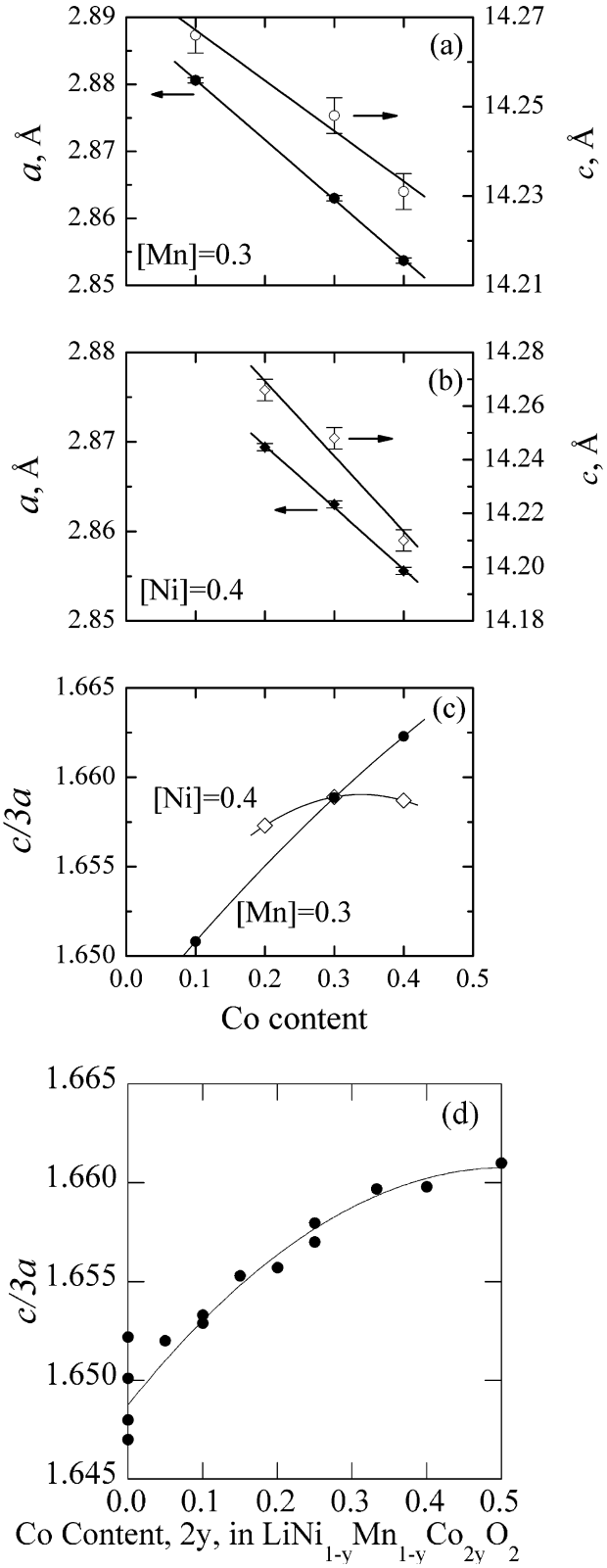

Figure 17. Cell parameters and $c/3a$ ratio of layered $LiNi_yMn_zCo_{1-y-z}O_2$, and $c/3a$ ratio of the symmetric $LiNi_{1-y}Mn_{1-y}Co_{2y}O_2$. (Parts a−c are reproduced with permission from ref 219, copyright 2004 The Royal Society of Chemistry.)

$c/3a$ ratio of 1.672 for TiS_2 and when intercalated increases to 1.793 for $LiTiS_2$.[45] The unusually low value for CoO_2 of 1.52[124] increases to 1.664 for $LiCoO_2$. ZrS_2 also has an anomalously low value of 1.592, which increases to 1.734 in $LiZrS_2$. The closer the value is to 1.633, the greater the transition-metal content in the lithium layer; thus, $LiNiO_2$ has a $c/3a$ ratio of 1.639,[213] almost the same as in the spinel $LiNi_2O_4$,[274] and that for $LiNi_{0.5}Mn_{0.5}O_2$ is 1.644−1.649 depending on the investigator;[213,252,270] addition of a second lithium as in Li_2NiO_2[63] and $Li_2Ni_{0.5}Mn_{0.5}O_2$[256] changes the c/a ratio very little, 1.648 and 1.647, respectively. Figure 17 shows that this ratio becomes much larger as soon as any cobalt is added to the structure, indicating that cobalt confers layer-like behavior to the lattice. Whereas the plot for [Mn] = 0.3 shows a closer approach to the cubic ideal value of 1.633, as the Co content decreases (that is as the Ni content increases), that for [Ni] = 0.4 shows little change. Thus, the $c/3a$ ratio is strongly determined by the nickel concentration, with the cobalt presence lessening the amount of nickel in the lithium layer. Figure 17d shows that the $c/3a$ ratio increases continuously with the cobalt content when [Ni] = [Mn]. An analysis of the published data[213,270] on $LiNi_{1-y}Mn_yO_2$ indicates essentially no change of the $c/3a$ ratio of 1.644 ± 0.005 with manganese content for $0.1 \leq y \leq 0.5$. The mean of all the data for the composition $LiNi_{0.33}Mn_{0.33}Co_{0.33}O_2$ is 1.657, which is more layered than the mean 1.647 for the cobalt-free $LiNi_{0.5}Mn_{0.5}O_2$. For the 333 composition, the $c/3a$ ratio decreases with increase of formation temperature from 900 to 1100 °C according to the equation $c/3a = 1.680 - 2.35 \times 10^{-5}\ T$, indicating an increasing nickel content in the lithium layer with increasing temperature.

Rietveld refinement was used[276] to determine the distribution of the transition-metal ions in the layered structure between the 3b and 3a sites; in a fully ordered layered structure, these sites should be fully occupied by transition metal and lithium, respectively. The average scattering factor of the transition-metal ions in the metal layer, 3b sites, was taken to be equal to that of Co, whereas that in the lithium layer occupying the interlayer site, 3a, was taken to be equal to that of Ni. Figure 16 shows the neutron diffraction pattern of the 442 material, and Rietveld comparison with the X-ray powder diffraction clearly showed that the transition metal in the lithium layer is nickel, not cobalt or manganese. A similar conclusion[234] was reached in a recent neutron study on the 333 composition. Figure 18 shows the occupancy on the Li site (3a site) as a function of overall composition and synthesis temperature. The data clearly indicates that the transition-metal disorder is suppressed by increasing cobalt content but not to the same degree as in $LiNi_{1-y}Co_yO_2$, where nickel disorder is only observed for $y \leq 0.3$, and increased by increasing the nickel content. However, the synthesis temperature has as profound an effect as composition, as also indicated in Figure 18 for the composition $LiNi_{0.4}Mn_{0.4}Co_{0.2}O_2$, where the sample prepared at 1000 °C then rapidly cooled to ambient temperatures has almost 10% Ni occupancy in the lithium layer. Kim et al. also reported[234] a high Ni content of 5.9% on the Li site for samples of the 333 composition prepared at 950 °C. Only at 800 °C does the nickel disorder drop to zero with increasing cobalt content. At 900 °C even with more cobalt than nickel

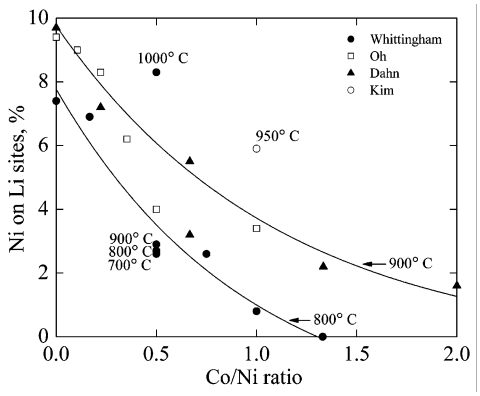

Figure 18. Lattice disorder, percent of lithium sites occupied by nickel ions in $LiNi_yMn_zCo_{1-y-z}O_2$. Materials synthesized at 800 °C for Whittingham[219] and 900 °C for Oh,[278] Dahn,[216,236] and Kim[234] unless otherwise stated.

in the material there is still considerable nickel disorder, almost 2% more Ni in the lithium layer at 900 °C than at 800 °C for all compositions. Clearly high temperature increases the disorder of the nickel ions just as earlier observed for TiS_2; this effect may be reduced by a slow cooling of the sample in an oxidizing environment or a hold at 800 °C or slightly lower if the original synthesis is carried out at higher temperatures. This will allow the partial reordering of the ions.[235]

Although these materials show good electrochemical behavior, their electronic conductivity is still low for a high-rate cathode, and a means needs to be found to increase the conductivity without the addition of excessive amounts of a conductor such as carbon black, which will reduce the volumetric energy storage capacity. There has also been a report[237] of the low packing density of powders which will also severely reduce the volumetric energy density. The conductivity of $LiNi_{0.5}Mn_{0.5}O_2$ was 6.2×10^{-5} S/cm; this increased on cobalt addition to 1.4×10^{-4} S/cm for $LiNi_{0.4}Mn_{0.4}Co_{0.2}O_2$ at 21 °C and 6.8×10^{-4} S/cm at 100 °C.[219] The value of the cobalt-free compound is similar to that observed previously[241] for $KMnO_2$ and $LiMnO_2$, but in that case 2−10% Co substitution led to a 100-fold increase in the conductivity to around 10^{-3} S/cm. This rather low effect of cobalt substitution is not totally unexpected as cobalt substitution in $LiNiO_2$, as in $LiNi_{0.8}Co_{0.2}O_2$, reduces the conductivity.[169] Sun et al.[233] reported conductivity values of $2-5 \times 10^{-4}$ S/cm essentially independent of composition for cobalt contents up to 0.5, which suggests that changes in the electrochemical behavior with composition is not a function of changes in conductivity. However, they found[233] that increasing the cobalt content increased the rate capability, which might be associated with the lack of pinning Ni^{2+} ions in the lithium layers, which would reduce the diffusivity of the lithium.

There have been a number of studies of the physical and bonding behavior of these mixed transition-metal oxides, which conclude that in the fully lithiated compounds the cobalt is trivalent, the nickel predominantly divalent, and the manganese tetravalent. Thus, the electrochemically active species is predominantly nickel with the cobalt playing an

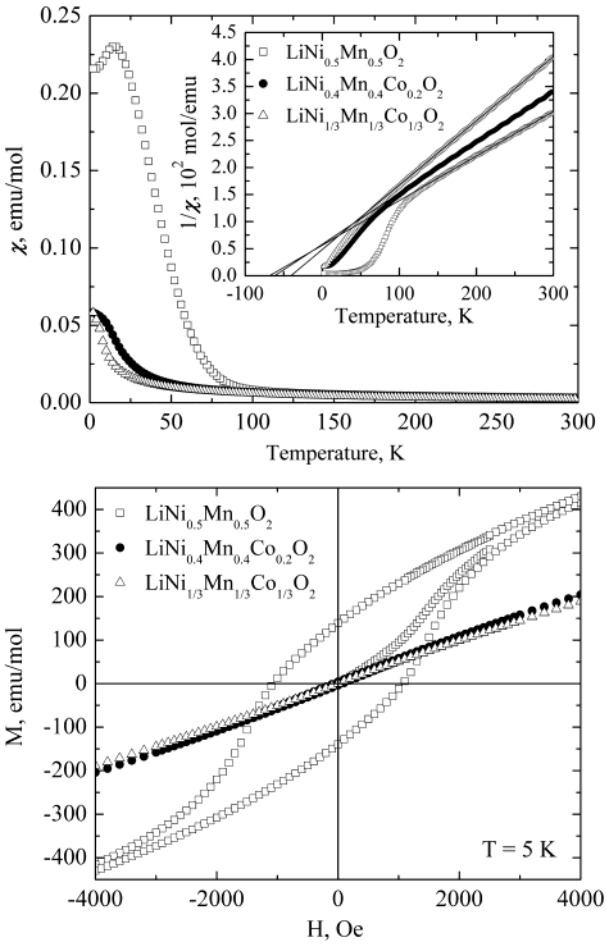

Figure 19. Magnetic behavior of $LiNi_{0.5}Mn_{0.5}O_2$, $LiNi_{0.4}Mn_{0.4}Co_{0.2}O_2$, and $LiNi_{0.33}Mn_{0.33}Co_{0.33}O_2$: (a) susceptibility and (b) field effect (after Ma et al.).[276]

active redox role only in the later stages of lithium removal. The manganese is merely a spectator ion but a critical one as at a minimum it reduces the cost of the cathode. Studies of the magnetic behavior of the compounds gives information about the location of the nickel ions, but studies of the magnetic moment from Curie−Weiss behavior do not give much key information as the combination $Ni^{3+} + Mn^{3+} + Co^{3+}$ gives an almost identical moment to the combination $Ni^{2+} + Mn^{4+} + Co^{3+}$.[219] However, the presence of nickel ions in the lithium layer results in a hysteresis loop in the magnetic moment both for the mixed material $Li(NiMnCo)O_2$ and in $LiNi_{1-y}Al_yO_2$.[275] The magnetic behavior of several of these phases is shown in Figure 19 and shows that at the higher temperatures they obey the Curie−Weiss law; as the addition of cobalt increases from 0.0 to 0.2 to 0.33, the hysteresis loop decreases, indicating a reduction in the Ni^{2+} content in the lithium layer.[276]

XPS studies have been made on a number of compositions of these transition-metal oxides, and all indicate predominantly divalent nickel. Thus, for the 442 compound the Co spectrum is clearly Co^{3+}, and the Mn spectrum can be assigned to 80% Mn^{4+} with 20% Mn^{3+}. The Ni spectrum is characterized by an intense and complicated satellite structure and consistent with 80% Ni^{2+} and 20 Ni^{3+}. Studies on $LiNi_{0.33}Mn_{0.33}Co_{0.33}O_2$,[224] $LiNi_{0.5}Mn_{0.5}O_2$,[277] and

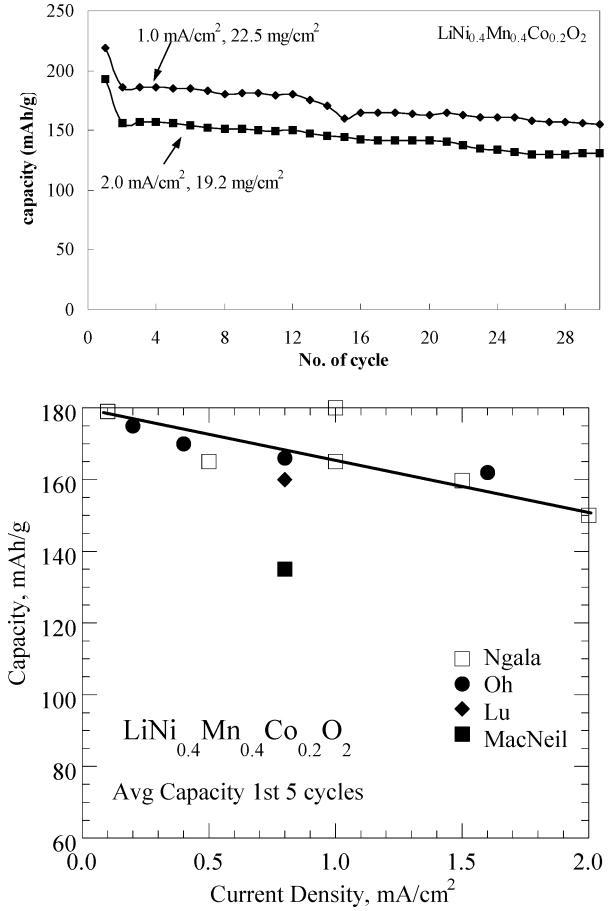

Figure 20. Electrochemical behavior of $LiNi_{0.4}Mn_{0.4}Co_{0.2}O_2$: (a) capacity as a function of a cycle at 1 and 2 mA/cm^2 (reproduced with permission from ref 219, copyright 2004 The Royal Society of Chemistry) and (b) capacity as a function of discharge rate, average capacity of first five cycles. Cutoff on charge, 4.3 V at 22 °C Ngala,[219] 4.4 V at 30 °C Oh,[278] 4.4 V at 30 °C Lu,[216] and 4.2 V at 30 °C MacNeil.[236]

$LiNi_yCo_{1-2y}Mn_yO_2$,[216] with y = 1/4 and 3/8, also suggested 2+ and 4+ as the predominant oxidation states for nickel and manganese, respectively, which then designates the nickel as the key electrochemically active species.

The electrochemical behavior of a number of different compositions over a range of current densities have been studied, and two of these studies identified[198,219,220,278] the 442 material as having the highest capacity and maintaining its capacity on cycling. Pure $Li_{1-y}Ni_{1+y}O_2$ had the lowest capacity. The electrochemical behavior of a sample of the 442 composition,[220] synthesized at 900 °C, at 22 °C is shown in Figure 20, for current densities of 1 and 2 mA/cm^2 within the potential window 2.5−4.3 V; these are equivalent to rates of 44 and 104 mA/g. All the samples had an initial potential around 3.8 V. The temperature of synthesis was found to be important with the optimum capacity and capacity retention being found at 800−900 °C, with a much lower capacity being found for samples prepared at 1000 °C.[220] The rate capability of the 442 composition is also shown in Figure 20 and shows the excellent reproducibility between the different research groups. Oh et al.[278] found a constant capacity for 442 of 175 mAh/g at 0.2 mA/cm^2 (20 mA/g or C/8) for 30 cycles within the potential window of 2.8−4.4 V; this capacity dropped slightly to 170, 165, and 162 mAh/g as the current density increased to 40, 80, and 160 mA/g (1.6 mA/cm^2 or C rate). The Dahn group has found similar good cycling ability for the close composition $LiNi_{0.375}Mn_{0.375}Co_{0.25}O_2$, where one sample[216] with 5.5% Ni on the lithium sites showed at 30 °C a capacity of 160 mAh/g dropping to 140 mAh/g after 50 cycles at a rate of 40 mA/g; raising the temperature to 55 °C increased the capacity to 170 mAh/g, and it dropped only to 160 mAh/g after 50 cycles. A second sample[236] which had only 3.2% Ni on the Li site had a lower capacity of 135−130 mAh/g over 50 cycles at 30 mA/g due to only being charged to 4.2 V; increasing the charging to 4.4 V increases the capacity by 20−30 mAh/g. This shows the critical effect of charging potential. As noted for the $LiCoO_2$ cathode above, without doubt an appropriate coating would allow the charging potential and hence the capacity to be increased. It is not clear yet how critical the nickel level in the lithium layer is as most studies have been made on compounds with 2−5% nickel levels with no obvious difference in behavior. This is an area that merits further evaluation and understanding.

There have been the largest number of studies on the 333 composition, which have been made by a number of synthetic techniques over a wide range of temperatures. Most of these studies show similar behavior with the capacity increasing with increasing charging potential. Increase of synthesis temperature from 800 to 900 °C increases the initial capacity from 173 to 190 mAh/g and the capacity after 16 cycles to 180 from 160 at the 0.3C rate in the potential window 3.0−4.5 V.[226] Ohzuku similarly reported[215,231] capacities of 150 mAh/g for a 4.2 V cutoff and 200 mAh/g for 4.6 and 5.0 V charging; others have reported[224,225] similar increases in capacity on increasing the charging potential, but in some cases there is marked capacity fade.[234] Spray drying the powder has been reported[279] to increase the capacity, 195 mAh/g at 0.2 mA/cm^2 (20 mA/g) within the potential window of 3−4.5 V. Replacing one-half of the cobalt ions by iron in the 333 composition with the goal of increasing the cell capacity below 4.5 V resulted in a higher cell polarization, lower capacity, and increased capacity fade.[280]

The structural changes accompanying the removal of Li from a number of these materials have been investigated. In the case of $LiNi_{0.4}Mn_{0.4}Co_{0.2}O_2$, the change in cell volume is less than 2%, much less than the 5% reported for $Li_xNi_{0.75}Co_{0.25}O_2$[281] and Li_xTiS_2,[40] making this compound much less liable to mechanically fracture on cycling. The 333 compound also shows a volume change of less than 2% as the lithium is removed.[234] This small change of volume is associated with compensating changes in the a and c parameters. When the c parameter increases, the a parameter contracts and vice versa. These results are shown in Figure 21 for the 442 compound,[276] where the X-ray pattern was forced to fit the simple hexagonal lattice of the $LiMO_2$. In reality the situation is probably more complex when x is less than around 0.3, and a more in-depth interpretation is

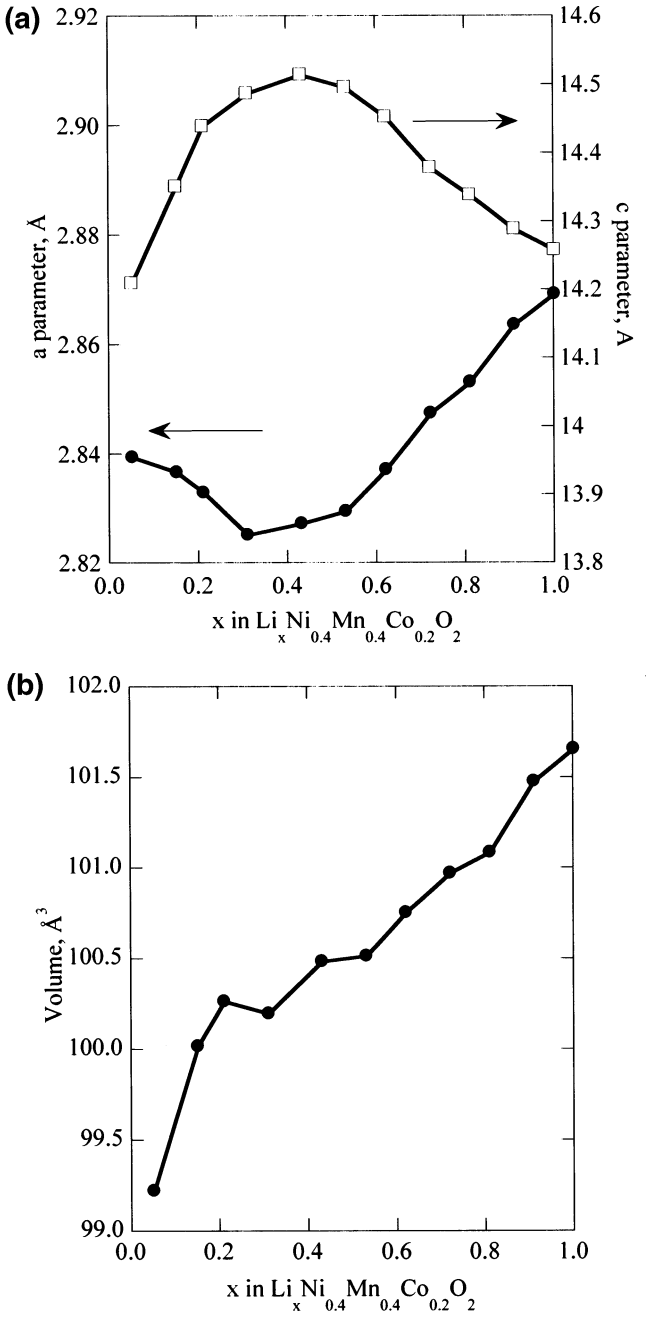

Figure 21. Lattice parameters of $Li_xNi_{0.4}Mn_{0.4}Co_{0.2}O_2$: (a) *a* and *c* in Å and (b) volume in Å^3 (after Ma et al.).[276]

underway. At the lowest lithium content $Li_{0.05}Ni_{0.4}Mn_{0.4}Co_{0.2}O_2$ there is a trace amount of the one-block structure (1T) of TiS_2 or CoO_2, in contrast to $LiCoO_2$ itself where large amounts of this structure would be seen. Thus, it appears that the 2−3% Ni on the Li sites is impeding the structural reorganization; this might be very advantageous for capacity retention on deep cycling of the material and speaks toward leaving some nickel disorder in the structure. This is consistent with an earlier study[282] on the NiO_2 phases, which found that the 1T phase is formed for $Ni_{1.02}O_2$ but not for nickel contents above 1.07, suggesting that the NiO_2 slabs are pinned by the extra nickel and thus cannot slide to form the 1T form. That study also found that the 1T phase slowly and irreversibly transformed at high potentials into a rhombohedral phase due to the migration of additional nickel ions into the interslab region. Thus, every effort should be made to prevent formation of the 1T structure in nickel-rich compounds to avoid capacity fade on deep charging. In the case of MnO_2 itself, the manganese ions migrate at high potentials to form a spinel-like phase[242] and do not migrate back when lithium is re-intercalated.

Inspecting Figure 21 shows that as the electron density on the oxygen ions decreases, their effective size also decreases, leading to the smaller *a* parameter (oxygen diameter). Reducing the lithium content causes the *c* parameter to increase, presumably as the electrostatic attractive forces between the negative layers and the positive lithium ions decrease. Although a cursory study of the X-ray diffraction patterns suggests a continuous change in the structure as the lithium is removed, more in-depth studies suggest otherwise. Thus, one report[217] proposes that four hexagonal phases are formed as the lithium is removed from the 333 compound, and another[229] suggests that a monoclinic phase is formed. Clearly additional studies are required ideally on single crystals if they can be synthesized, much as was accomplished with V_6O_{13}.

Are these cathodes ready and able to replace the stabilized $LiCoO_2$ used in most Li-Ion batteries today? A recent joint academic/industrial study[283] suggests that the 333 compound is at least equal to or superior to the $LiCoO_2$ cathode. In a prismatic cell configuration, it showed a constant capacity of 600 mAh over 30 cycles at C rate. The cell can also be charged to a higher potential cutoff without the capacity loss associated with CoO_2 structure changes (O3 to 1T—ccp to hcp) in $LiCoO_2$, which results in a 10−20 mAh/g higher storage capability. An issue with all these layered oxides is their inherent thermodynamic instability upon lithium removal. Although MnO_2 is stable in air at room temperature, neither CoO_2 or NiO_2 is, both having effective oxygen partial pressures in excess of 1 atm. The stable oxidation states of Mn, Co, and Ni in their simple binary oxides are 4, 2, and 2, respectively; on heating to over 500 °C, Mn_2O_3 becomes the stable oxide followed by Mn_3O_4 at still higher temperatures. Thus, their kinetic stability can create problems if there is any thermal excursion in the cell. For the four oxides $Li_xNi_{1.02}O_2$, $Li_xNi_{0.89}Al_{0.16}O_2$, $Li_xNi_{0.70}Co_{0.15}O_2$, and $Li_xNi_{0.90}Mn_{0.10}O_2$, a structural transformation first to a spinel phase and then to a rock-salt phase was found[284,285] for lithium *x* values of 0.5 or less. The second transformation is accompanied by a loss of oxygen, and the first may be depending on the composition but usually when *x* is less than 0.5; the latter oxygen release occurs at lower temperature as the lithium content decreases and as low as 190 °C for $Li_{0.3}Ni_{1.02}O_2$. The stability is improved on aluminum or cobalt substitution. The compound $Li_{0.1}NiO_2$ is reported[286] to lose weight at 200 °C forming a rock-salt structure. The substitution of manganese for nickel appears to move the transition to the spinel to higher temperatures; thus, $Li_{0.5}Ni_{0.5}Mn_{0.5}O_2$ even after 3 days at 200 °C is still layered,[287] but a spinel phase is formed above 400 °C and is stable to much higher temperatures for the 1:1 Ni:Mn lithium-free

compound, eventually giving a mixture of spinel and nickel oxide in air and NiO + Mn_3O_4 in nitrogen.[288] The compounds $Li_{0.5}Ni_{0.4}Mn_{0.4}Co_{0.2}O_2$ and $Li_{0.5}Ni_{0.33}Mn_{0.33}Co_{0.33}O_2$ both begin to lose weight above 300 °C with major weight loss, 7−8%, only above 450 °C,[276] which corresponds to reduction of Co(III) to Co(II) and any Ni(IV) to (Ni(II); the manganese remains Mn(IV), and the structure begins to change to spinel by 350 °C, and the spinel phase is still present at 600 °C.

In conclusion the solid solutions of the 550 material and $LiCoO_2$ have the following cathode characteristics.

(1) They have a capacity of around 170 mAh/g for at least 50 cycles under mild cycling conditions to 4.4 V and over 150 mAh/g at 2 mA/cm^2.
  (a) A higher charge potential cutoff increases capacity.
  (b) The synthesis temperature should be in excess of 700 °C and less than 1000 °C, probably optimally around 900 °C.
(2) The cobalt reduces the number of nickel ions in the lithium layer.
  (a) The final heating temperature needs to be no higher than 800 °C.
    (i) The ratio of Co/Ni needs to be greater than 1 to eliminate all Ni in the lithium layer.
  (b) For a final anneal temperature of 900 °C, there will always be nickel ions in the lithium layer.
  (c) A certain level of nickel ions will deter the formation of the one-block structure at low lithium concentrations.
    (i) Minimization of formation of the one-block structure on charging will help maintain capacity on cycling.
    (ii) There is a need for a determination of the acceptable or desirable level of nickel in the lithium layer, as it may well not be zero.
(3) There is probably not a single phase for all lithium values from 0 to 1 in $Li_x(NiMnCo)O_2$.
  (a) The structure needs determining at low x values.
    (i) The 442 compound only forms small amounts of the one-block structure by $x = 0.05$.
(4) Nickel is the electrochemically active ion at low potentials.
  (a) Cobalt is only active at the higher potentials.
(5) The electronic conductivity needs increasing.
(6) The optimum composition is still to be determined for energy storage, power capability, lifetime, and cost considerations.

5.2.6. Lithium-Rich Mixed-Metal Dioxides, $Li_{1+x}M_{1-x}O_2$

As discussed earlier in the case of the chromium[243,244] and cobalt[251] systems, excess lithium can be incorporated into the layered structure through a solid solution of Li_2MnO_3 and LMO_2, where M = Cr or Co. The transition-metal cation can also be nickel or manganese including mixtures such as $LiNi_{1-y}Co_yO_2$ as pointed out by Yoshio,[228] Thackeray,[289,290] and Dahn,[252] and the Li_2MnO_3 can be replaced by related materials such as Li_2TiO_3 and Li_2ZrO_3. Li_2MnO_3 can be represented in the normal layered notation as $Li[Li_{1/3}Mn_{2/3}]O_2$. These solid solutions can thus be represented as $LiM_{1-y}[Li_{1/3}Mn_{2/3}]_yO_2$, where M can be, for example, Cr, Mn, Fe, Co, Ni, or mixtures thereof. Addition of extra lithium will tend to push the manganese away from trivalent to tetravalent, thus minimizing the impact of any Jahn−Teller distortion coming from Mn^{3+}.

Of particular curiosity is the end-member Li_2MnO_3 which has been shown[291,292] to exhibit unexpected electrochemical activity on charging as the manganese is already in the 4+ oxidation state. This "overcharging" can be associated with two phenomena, removal of lithium with the concomitant loss of oxygen giving a defective oxygen lattice and the removal of lithium by decomposition of the electrolyte giving protons which can ion exchange for the lithium. Which mechanism predominates depends on the temperature and chemical composition of the oxide lattice.[293] In both cases the manganese oxidation state remains unchanged. When significant amounts of hydrogen are ion exchanged, the MO_2 slabs slide to give prismatic coordination between the layers as this, combined with a contraction in the interlayer spacing of around 0.3 Å, leads to optimum hydrogen bonding.[292] These protons are lost as water on heating the oxide to around 150 °C.[292] Acid leaching of Li_2MnO_3 also results in the removal of lithium, and here again both mechanisms of Li_2O removal[294,295] and proton exchange[296] are believed to be operative. Acid leaching of the lithium stoichiometric compounds, such as $LiNi_{0.4}Mn_{0.4}Co_{0.2}O_2$, also results in removal of lithium and a small amount of proton exchange.[276]

The ease of oxygen removal from the close-packed lattice when lithium rich had been demonstrated[297] by its ready reduction by ammonia gas at 200 °C in the case of the spinel $Li[Li_{1/3}Mn_{5/3}]O_4$. It was also shown[297] that this oxygen could be removed by electrochemically charging above around 4.3 V; the material then showed the 4 V discharge behavior typical of a spinel. These reduced materials can best be represented as $Li[Li_{1/3}Mn_{5/3}]O_{4-\delta}$.

Dahn et al. studied[252] the solid solution Li_2MnO_3−$LiNiO_2$, which can be written as $Li[Ni_yLi_{(1/3-2y/3)}Mn_{(2/3-y/3)}]O_2 = yLiNiO_2 + (1-y)Li[Li_{1/3}Mn_{2/3}]O_2$. The a and c hexagonal lattice parameters increased linearly with the nickel content, y, from 0.08 to 0.5 with the $c/3a$ ratio decreasing linearly, showing that the layeredness decreased with increasing nickel content as expected. Cells of these materials showed an irreversible charging plateau around 4.5 V, which is believed to be due to loss of oxygen as described above. Before the plateau all the nickel is oxidized to Ni^{4+}. After this "overcharging" the electrodes were found to cycle well at 30 °C between 2.0 and 4.6 V with the capacity increasing inversely with the value of y: 160, 180, and 200 mAh/g, respectively, for $y =$ 1/2, 5/12, and 1/3 (this trend has been confirmed[298]).

The first has no excess lithium and the lowest capacity, showing the advantage of excess lithium. The capacity of the $y = 1/3$ material increased to 220 mAh/g when the cycling temperature was increased to 55 °C. However, this high charging level results in a lower thermal stability of the material.[252] The addition of excess lithium to the 550 composition, $Li_{1+x}(Ni_{0.5}Mn_{0.5})_{1-x}O_2$ was reported[299] to increase the stability of the material. The system Li_2MnO_3−$LiNiO_2$−$LiMnO_2$ has been studied,[300] and it shows complete solubility along the Li_2MnO_3−$LiNiO_2$ line; the electrochemical capacity was found to fall rapidly as the nickel content decreased when the charging potential was limited to 4.3 V.

Thackeray et al.[301] showed that Li_2TiO_3 forms a solid solution with $LiNi_{0.5}Mn_{0.5}O_2$ and that the titanium helped allow the intercalation of a second lithium into the structure.[64] The advantages of adding Li_2MnO_3 to the layered cathode material have even been reported for manganese-rich materials, which would be unstable otherwise relative to spinel formation. Thus, $Li[Li_{0.2}Ni_{0.2}Mn_{0.6}]O_2$ showed a steady-state capacity of around 200 mAh/g between 2.0 and 4.6 V at 0.1 mA/cm^2, after gaining capacity for the first 10 cycles.[302] The behavior and stability of this material at higher rates was not reported. Addition of some cobalt to these manganese-rich compounds was reported to help retain the capacity at higher discharge rates.[222] Magnesium has also been proposed as a stabilizing agent for manganese-rich materials.[303]

Thus, there is one more parameter, the lithium excess content, to be considered in addition to the nickel, cobalt, and manganese ratios in designing the optimum composition for the ideal cathode. Each of these elements has its own role to play, whether it is stabilizing the lattice (the manganese), being the electrochemically active member (the nickel), ordering the transition metals and perhaps increasing the rate capability and the conductivity (the cobalt), or increasing the capacity (the lithium). Whether other elements will play a critical role is yet to be determined, but some elements such as titanium have been found to decrease the rate capability and migrate to the lithium layer.

5.3. Iron Compounds Including Oxides and Phosphates

A number of researchers,[173,304,305] particularly in Japan, have been pursuing the oxides of iron as potential cathode materials for lithium cells. However, materials of the type $LiFeO_2$ have shown little ability for lithium removal. A number of other iron compounds have been studied over the years, including FeOCl,[306] $FePS_3$,[307] $KFeS_2$,[308] and FeS_2,[13] but none showed much reversibility. Although metal phosphates have been studied for more than 20 years since the discovery of fast ion transport in NASICON, it is only recently that they have been considered as cathodes[309−312] or anodes[312−314] of lithium batteries.

5.3.1. Olivine Phase

Emphasis changed radically in 1997 with the discovery of the electrochemical properties of the olivine phase, in particular $LiFePO_4$, by Padhi et al.[309] This is the first cathode material with potentially low cost and plentiful elements and also environmentally benign that could have a major impact in electrochemical energy storage. For $LiFePO_4$, the discharge potential is about 3.4 V vs lithium and no obvious capacity fading was observed even after several hundred cycles. Its capacity approaches 170 Ah/kg, higher than that obtained by $LiCoO_2$ and comparable to stabilized $LiNiO_2$, and moreover, it is very stable during discharge/recharge. Since its discovery, many research groups have tried to improve the performance of this material.[49,50,198,315−326]

$LiFePO_4$ can be synthesized by high-temperature reactions,[309] under hydrothermal conditions,[50] or by sol−gel methods.[327] Although the olivine phase can be very easily synthesized hydrothermally within just a few minutes and its X-ray pattern looks good, it gives poor electrochemical properties; a close examination of the structure showed that there are about 7% iron atoms in the lithium site, and this is reflected in the lattice parameters of $a = 10.381$ Å, $b = 6.013$ Å, and $c = 4.716$ Å compared with those for ordered $LiFePO_4$ of $a = 10.333$ Å, $b = 6.011$ Å, and $c = 4.696$ Å.[198] These iron atoms essentially block diffusion of the lithium ions, as the diffusion is fast only along the tunnel and not between them;[51] thus, it will be critical in the use of this material to ensure ordering of the lithium and iron atoms. Firing the hydrothermal material to 700 °C resolved the disorder. Recent studies suggest that the hydrothermal approach can be improved by modifying the synthesis conditions, for example, by adding a reducing agent such as ascorbic acid[328] to prevent surface ferric films; the hydrothermal method can also produce material with excellent electrochemical behavior even without a carbon coating,[329] as is necessary in most instances as discussed below.

As this material has a very low conductivity at room temperature, it could achieve the theoretical capacity only at a very low current density[315] or at elevated temperatures,[317] as suggested by Padhi[309] due to the low lithium diffusion at the interface. Ravet et al.[318] showed that a carbon coating significantly improves the electrochemical performance of this material; sucrose was proposed[319] as one carbon precursor, and it was used on the initial hydrothermal samples.[50] Many other studies have been made on finding means to improve the electronic conductivity of the $LiFePO_4$ particles.[49,198,320,321,323−326] Very pure $LiFePO_4$ samples are reported to have an electronic conductivity of 10^{-9} S/cm,[324] whereas samples made from reagent-grade carbon-containing materials have a conductivity of around 10^{-5}−10^{-6} S/cm.[198] Huang et al.[320] proposed coating the material with carbon-gel during the synthesis step and found capacities approaching 100% at very low cathode loadings, 5 mg/cm^2, and rather high carbon contents, 20%. They obtained 800 cycles at around 120 mAh/g at high rates. Masquelier proposed[321] extensive milling of the material with carbon and then found high capacities at elevated temperatures. A 2002 paper by Chang et al.[324] showed excellent electrochemical behavior when the $LiFePO_4$ was "doped" with parts

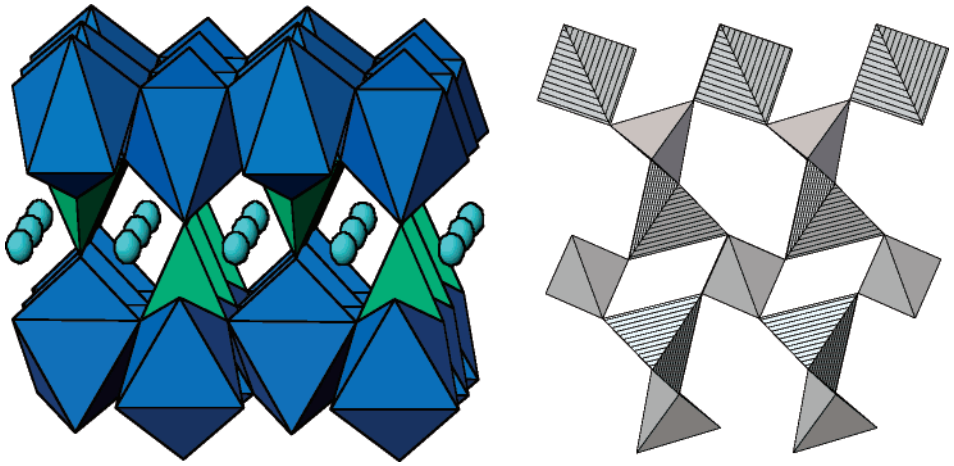

Figure 22. Structures of orthorhombic $LiFePO_4$ and trigonal quartz-like $FePO_4$.

per million of elements such as niobium, which increased the conductivity by 8 orders of magnitude. This paper caused a surge of interest in this compound and in an understanding of what causes the conductivity changes; a recent paper by Nazar et al.[325] has shown that the conductivity increase is related to the formation of a highly conductive iron phosphide, Fe_2P, surface film; this film is formed at high temperature, particularly in the presence of a reducing agent such as carbon.

The olivine structure is shown in Figure 22, and on lithium removal the phase $FePO_4$ is formed; $LiFePO_4$ and $FePO_4$ have essentially the same structure. This $FePO_4$ is isostructural with heterosite, $Fe_{0.65}Mn_{0.35}PO_4$. This is a two-phase system with $LiFePO_4$ being in equilibrium with $FePO_4$ as shown in the cycling plot in Figure 23a.[198] This figure shows that 100% capacity of the lithium is cyclable at 1 mA/cm^2 at 60 °C even at electrode loadings of 80 mg/cm^2; at room temperature, around 70% can be cycled at 1 mA/cm^2 and 100% at 0.1 mA/cm^2. Even at 10 mA/cm^2, almost 70% of the capacity is obtained at low loadings, as shown in Figure 23b.

Critical to the use of $LiFePO_4$ is its reactivity and thermal stability and that of its charged product, $FePO_4$. Thomas reported[317] that there were no thermal excursions observed in cells or in a DSC experiment in the range 25−85 °C. However, the olivine structure is inherently unstable because of the edge sharing between octahedra and tetrahedra, and under pressure it converts to the spinel phase as observed in the earth's mantle. Recently, the transformation of orthorhombic $LiFePO_4$ to an olivine-like $LiFePO_4$ with the lithium in tetrahedral sites has been reported;[330] this form is electrochemically inactive. In addition, more than two crystalline forms of $FePO_4$ are known: the orthorhombic form isostructural with $LiFePO_4$ where the iron is found in FeO_6 octahedra and the trigonal form in which the iron is found in FeO_4 tetrahedra. These are shown in Figure 22. The orthorhombic structure has been discussed extensively.[309] The trigonal form is composed of FeO_4 and PO_4 tetrahedra, each FeO_4 tetrahedron shares its four corners with four PO_4 tetrahedra and vice versa, giving a quartz-like structure. The all-tetrahedral form is electrochemically unreactive as Fe(II) is not stable in tetrahedral configuration, and moreover, surface glassy films tend to form at high temperatures.[49] Thus, care must be taken to ensure that it is not formed during the synthesis of $LiFePO_4$

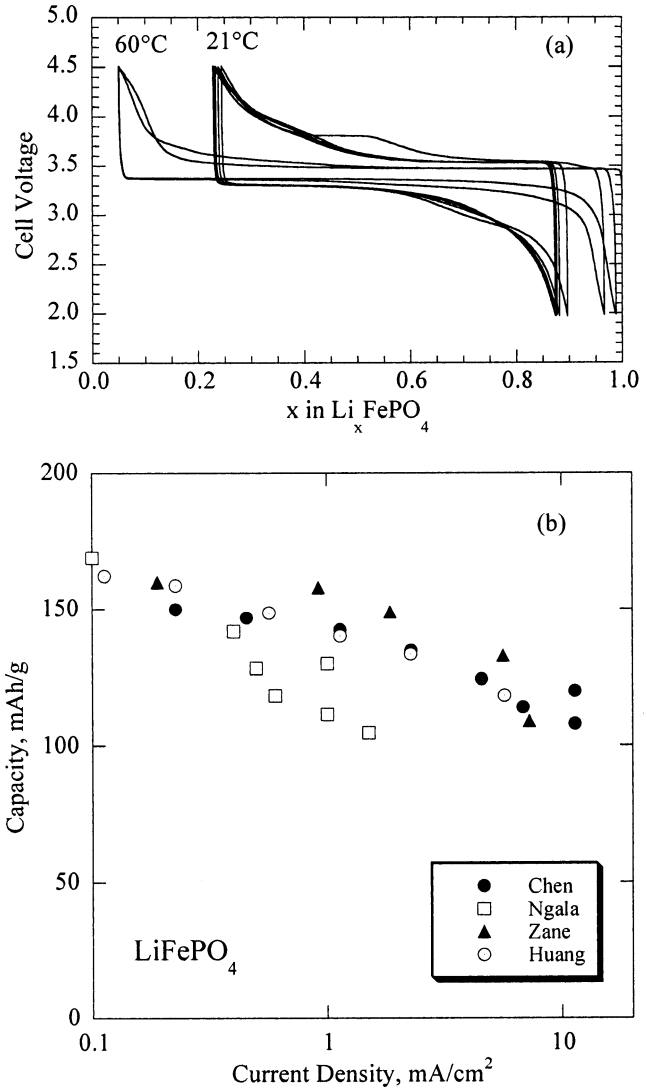

Figure 23. Electrochemical behavior of $LiFePO_4$: (a) cycling at 1 mA/cm^2 at 21 and 60 °C (reprinted with permission from ref 198, copyright 2003 Elsevier) and (b) Ragone plot for $LiFePO_4$ from four groups, Chen[332] (8 mg/cm^2 loading and about 10 wt % carbon), Ngala[219] (20−80 mg/cm^2 and 10% carbon), Zane[363] (10 mg/cm^2 and 20% carbon), and Huang[320] (5 mg/cm^2 and 20% carbon).

Table 1. Chemical Reactivity of Iron Phosphates[49]

compound	synthesis method	BuLi reactivity (mol/Fe)
$LiFePO_4$	high temperature	1.85
LiFePO4	hydrothermal	0.29
$FePO_4$	orthorhombic	3.25
$FePO_4$	trigonal (700 °C-tetrahedral iron)	2.90
$FePO_4 \cdot 2H_2O$	amorphous phase	7.20
$LiFePO_4(OH)$	hydrothermal	3.24

or its precursors. At low temperatures, when lithium ions are absent, amorphous $FePO_4 \cdot 2H_2O$ can be formed (see below); although it is electrochemically active, dehydration at high temperatures leads to the tetrahedral form of $FePO_4$, which is electrochemically inactive.[331]

It is essential to understand the long-term stability of electrode materials to ensure the extended life of any battery. Thus, it is important to better understand the reactivity of both the $LiFePO_4$ and the $FePO_4$ orthorhombic phases. For example, what happens when $LiFePO_4$ is over discharged or does the orthorhombic $FePO_4$ slowly switch to the quartz form over time? When iron phosphates are reacted with an excess of *n*-butyllithium it was reported[49] that all but one reacted with sufficient butyllithium to form lithium phosphate and iron as shown in Table 1. Thus, it appears that these phosphate lattices are destroyed at low lithium potentials; *n*-butyllithium is about 1 V versus pure lithium. An electrochemical study[49] where the $LiFePO_4$ cathode was subjected to a discharge down to 1.0 V at 0.4 mA/cm^2 confirmed that lithium reacts with destruction of the $LiFePO_4$ lattice and considerable loss of capacity. After five cycles the capacity had dropped by 80%. Thus, lithium iron phosphate cells will require overdischarge protection in commercial applications. On the other hand, no evidence has been found for the conversion of the metastable orthorhombic $FePO_4$ phase to the quartz-like trigonal phase under normal electrochemical conditions. Moreover, unlike the layered oxides described earlier, there is no tendency to lose oxygen on lithium removal from the lattice.

The low density of $LiFePO_4$ results in a low volumetric density, and so it is critical that the minimum volume of carbon and organic binder be used in the electrode. Taking the density of $LiFePO_4$, Teflon, and carbon black as 3.6, 2.2, and 1.8 g/cm^2, respectively, then an electrode containing 10 wt % carbon and 5 wt % Teflon will have a volumetric energy density 25% less than the theoretical value. This assumes that all the particles pack equally efficiently, which is unlikely to be the case with the poor packing associated with carbon, particularly with decomposed sugar. A tap density study suggested that this carbon packs poorly, so the volumetric density penalty may be very significant.[332] A number of carbons have been studied to determine how much carbon is needed for optimum electrochemical behavior. For carbon black little difference was observed for carbon loadings from 6 to 15 wt %, except that the polarization observed was slightly higher at 6 wt %; the method of carbon addition, whether carbon black, carbon gel, sugar, or aqueous gelatin,[333] did not appear to be important. However, the temperature of firing the reaction mixture appears to be much more important as that determines the amount of graphitic compound on the $LiFePO_4$ surface; sp^2 carbon was found to be much more effective than sp^3 carbon.[334] The particle size is almost certainly controlled by the carbon in the reaction mixture, even when only coming from carbon in the reagent materials, leading to the positive behavior of several samples.[324] The temperature of preparation was found to be important, with that prepared at 675 °C showing the best behavior in one study.[335]

Much of the above discussion has centered on the iron phase of the $LiMPO_4$ olivine structure, but the transition metal may also be manganese, nickel, and cobalt. The naturally occurring form contains both iron and manganese. None of these other forms has yet showed superior electrochemically behavior to the iron compound, even though they have higher discharge potentials.[336] The mixed Fe−Mn compound discharges in two distinct steps, which can be associated, respectively, with the iron and manganese redox reactions. Several research groups have studied the cycling behavior of the pure $LiMnPO_4$ compound.[337,338] The results are controversial: Yamada et al.[337] related the inability to extract lithium from $LiMnPO_4$ electrochemically to the thermodynamic instability of olivine-type $MnPO_4$ due to the Jahn−Teller effect of Mn^{3+}; Li et al.[338] reported a reversible capacity of about 140 mAh/g for the reaction between $LiMnPO_4$ and $MnPO_4$. Recently, Delacourt et al.[339] studied the $LiMnPO_4$ formed by direct precipitation and obtained a reversible capacity of 70 mAh/g after carbon coating by ball milling the materials with carbon black. This suggests that $MnPO_4$ is thermodynamically stable. Song et al.[340] studied $LiMnPO_4$, formed from the thermal decomposition of $LiMnPO_4(OH)$, and found the Mn^{3+}/Mn^{2+} transformation at about 4.1 V with a high polarization and low capacity; heating with carbon black did not result in any dramatic enhancement of the capacity. Ceder et al.,[341] using an advanced theoretical treatment, have calculated the open-circuit voltages and the band gap in these phosphates, and found that as expected they are very high. The open-circuit voltages are 3.5 V for $LiFePO_4$, 4.1 V for $LiMnPO_4$, 4.8 V for $LiCoPO_4$, and 5.1 V for $LiNiPO_4$, thus explaining the lack of electrochemical activity for $LiNiPO_4$ within the normal cycling potential range. The very high calculated band gaps of 3.7 and 3.8 eV for $LiFePO_4$ and $LiMnPO_4$ are consistent with their color and diffuse reflectance spectra and suggest that band-gap differences do not explain the different electrochemical behavior; the electronic conductivity is likely due to a polaron mechanism.[342] Some other recent theoretical calculations[343,344] suggesting that these materials are semi-metals are inconsistent with their white color and are almost certainly in error due to problems with the theory used.

5.3.2. Other Iron Phosphate Phases

Several other iron phosphate structures have been described. The phase $Li_3Fe_2(PO_4)_3$ has been stud-

ied,[50,311,312] and it discharges below 3 V and carries more phosphate deadweight than $LiFePO_4$, so has been of less interest since the discovery of $LiFePO_4$. Three groups[345−347] have studied the electrochemical behavior of the hydrated and anhydrous phase $FePO_4{\cdot}nH_2O$ and found essentially identical results. Amorphous and crystalline $FePO_4{\cdot}nH_2O$ were prepared hydrothermally and then heat-treated over a range of temperatures. The material obtained from the amorphous dihydrate shows more than double the capacity of the material obtained from the crystalline dihydrate, 0.75 vs 0.3 Li/$FePO_4$, respectively. This might be associated with the amorphous nature of the former relative to the more crystalline structure of the latter; also, the latter has iron in an essentially tetrahedral environment. The capacity of the former is similar to that reported by Prosini et al.[348] for a biphasic mixture of phosphate and iron oxide. Both the amorphous and crystalline materials show behavior more typical of a single-phase reaction, Li_xFePO_4, as opposed to the two-phase behavior of the $LiFePO_4-FePO_4$ system. The discharge curves of amorphous $FePO_4$ obtained at different temperatures at 0.2 mA/cm^2, between 4 and 2 V, are shown in Figure 24 as are also the cycling curves and the rate capability of the amorphous $FePO_4$ sample heated at 350 °C at different current densities, $I_c = I_d$.

Another class of iron phosphates is that related to the minerals Giniite and Lipscombite. The structure in this case consists of rods containing face-sharing FeO_6 octahedra, stacked orthogonally to one another, giving nonintersecting tunnels through which lithium ions can diffuse. The discharge potentials in this case are sloping and lower than those of the $LiFePO_4$/$FePO_4$ system.[349,350]

5.3.3. Vanadium Phosphate Phases

A number of vanadium phosphates have also been studied as potential cathodes, including those of general formula $Li_3V_2(PO_4)_3$[351−356] and $VOPO_4$.[357] $Li_3V_2(PO_4)_3$ exists in two forms: the thermodynamically stable monoclinic form and a rhombohedral form that can be formed by ion exchange from the stable sodium analogue with the NASICON structure. Two lithium ions can be removed from the rhombohedral form at 3.77 V, and only 1.3 can be reinserted.[353] The monoclinic form is of more interest as a cathode as all three lithium ions can be readily removed and reversibly intercalated at high rate.[351,352] However, the electrochemistry of this cathode is complex, showing a series of steps on charging but a solid solution on lithium insertion from 0 to 2 lithium followed by two-phase behavior.[355] This cathode is being commercialized by Valence Technology.

The ϵ-$VOPO_4$ compound has particularly interesting properties,[358] with an approximately 4 V flat discharge potential some 0.5 V higher than $LiFePO_4$ and with higher electronic conductivity, leading to the possibility of attaining higher power systems than for $LiFePO_4$ but at the expense of higher cost. The ϵ-$VOPO_4$ can be synthesized by removal of the hydrogen atoms from $VPO_4{\cdot}2H_2O(=H_2VOPO_4)$ either thermally[359] or by electrochemical deintercalation.[340]

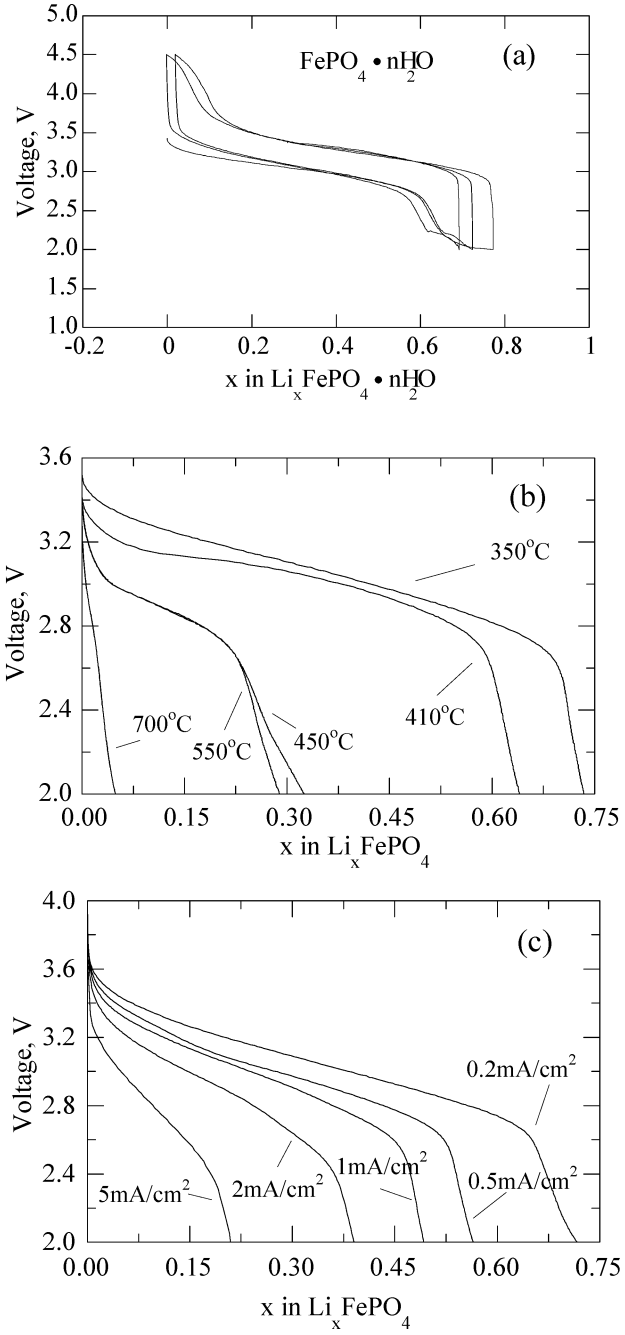

Figure 24. Electrochemical behavior of $FePO_4{\cdot}nH_2O$ formed by the thermal decomposition of $FePO_4{\cdot}nH_2O$: (a) discharge of $FePO_4$ as a function of annealing temperature, (b) cycling of $FePO_4$ annealed at 350 °C, and (c) rate capability of $FePO_4$ annealed at 350 °C (reprinted with permission from refs 49 and 345, copyright 2002 Elsevier).

In the latter, after the H_2VOPO_4 is electrochemically oxidized in a $LiPF_6$/EC-DMC solution to give ϵ-$VOPO_4$, the ϵ-$VOPO_4$ can be reduced by reversing the current flow to give first $LiVOPO_4$ and then Li_2VOPO_4, as shown in Figure 25a.[340] As expected from the ease of these reactions, the structures of all four compounds are closely related, as shown in Figure 25b;[360] the building block for all these structures, which consists of VO_6 octahedra and PO_4 tetrahedra, is shown at the lower right.

If a still higher redox potential is desired, then heating ϵ-$VOPO_4$ with LiF and carbon black at 550

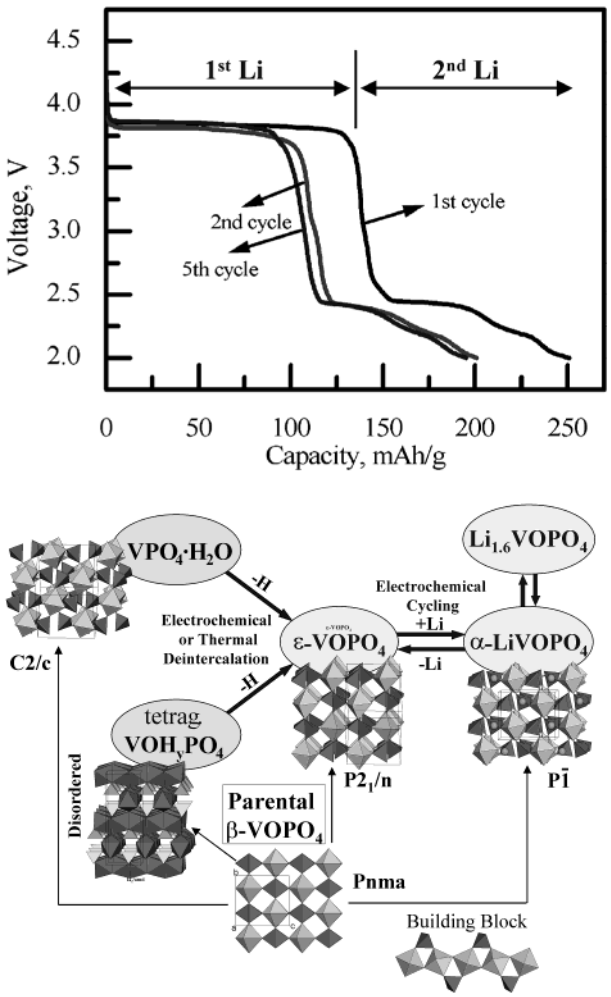

Figure 25. (top) Electrochemical intercalation of lithium into ϵ-$VOPO_4$,[340] and (bottom) relationship between the various structures in the $VOPO_4$ system; the building block for all these structures is shown at the lower right.

°C for 15 min and then rapidly cooling to room temperature leads to the formation of $LiVPO_4F$.[361] This compound is isostructural with $LiMPO_4(OH)$ (M = Fe, Mn). It has a potential of 4.2 V and a capacity of 0.55 Li per formula unit or 156 mAh/g.[340]

6. Conclusions and What Does the Future Hold

Lithium batteries have made substantial and significant gains in the last 30 years from becoming a curiosity to becoming the dominant rechargeable battery for consumer portable applications. However, the next market opportunities will be much tougher to conquer as they mostly demand higher power capabilities at lower costs and often in larger systems with enhanced safety. The prime markets are the high-power segment presently dominated by the environmentally unfriendly Ni/Cd battery and the HEV segment presently occupied by the Ni/metal hydride battery. The layered oxides will, without doubt, continue their ongoing improvement with mixed transition metals slowly displacing the pure cobalt system; they appear to offer enhanced safety with enhanced capacity at a lower cost and are drop-in technology. The lithium iron phosphate cathode offers the first potentially low-cost cathode, but this will only be achieved if the costs of the other cell components are also reduced. These include the electrolyte, a lower cost anode with added safety features including the use of natural graphite, and probably the use of thicker cathodes to reduce the cost of electrode support materials, separators, etc. It can be anticipated that totally new materials with unexpected properties will be discovered, so that the goal of at least one lithium cycling per transition metal at a rate of 10 mA/cm^2 can be achieved with pulse charging and discharging at still higher rates.

7. Abbreviations and Specialized Terms

anode	electropositive electrode
cathode	electronegative electrode
C rate	measure of the time for cell discharge in reciprocal hours, time of discharge = 1/*C* in hours
HEV	hybrid electric vehicle
LiBOB	lithium bis(oxalato)borate $LiB(C_2O_4)_2$
$LiPF_6$	lithium hexafluorophosphate, $LiPF_6$
NASICON	sodium superionic conductor
Ragone plot	a plot of the electrochemical cell capacity as a function of the magnitude of the discharge or charge current
Vegard's Law	for a solid solution the lattice parameter varies linearly with composition

8. Acknowledgments

This work was supported by the US Department of Energy, Office of FreedomCAR and Vehicle Technologies, through the BATT program at Lawrence Berkeley National Laboratory and by the National Science Foundation through grant DMR0313963. I thank Drs. Marca Doeff, Kang Xu, and Michael Thackeray for many constructive suggestions for improving the first draft of this manuscript. I also thank Professor T. Ohzuku for providing Figure 14 and Miaomiao Ma, Natasha Chernova and Peter Zavalij for help and much data.

9. References

(1) Watanabe, N.; Fukuba, M. U.S. Patent 3,536,532, 1970.
(2) Whittingham, M. S. *J. Electrochem. Soc.* **1975**, *122*, 526.
(3) Ikeda, H.; Saito, T.; Tamaru, H. *Denki Kagaku* **1977**, *45*, 314.
(4) Ikeda, H.; Uena, S.; Saito, T.; Nakaido, S.; Tamaru, H. *Denki Kagaku* **1977**, *45*, 391.
(5) Sanyo, Lithium Battery Calculator, Model CS-8176L.
(6) Dey, A. N. *J. Electrochem. Soc.* **1971**, *118*, 1547.
(7) Liang, C. C.; Bolster, M. E.; Murphy, R. M. U.S. Patents 4,310,609 and 4,391,729, 1982.
(8) Takeuchi, E. S.; Thiebolt, W. C. *J. Electrochem. Soc.* **1988**, *135*, 2691.
(9) Crespi, A.; Schmidt, C.; Norton, J.; Chen, K.; Skarstad, P. *J. Electrochem. Soc.* **2001**, A30.
(10) Vissers, D. R.; Tomczuk, Z.; Steunenberg, R. K. *J. Electrochem. Soc.* **1974**, *121*, 665.
(11) Gay, E. C.; Vissers, D. R.; Martino, F. J.; Anderson, K. E. *J. Electrochem. Soc.* **1976**, *123*, 1591.
(12) Kaun, T. D.; Nelson, P. A.; Redey, L.; Vissers, D. R.; Henriksen, G. L. *Electrochim. Acta* **1993**, *38*, 1269.
(13) Whittingham, M. S. *Prog. Solid State Chem.* **1978**, *12*, 41.
(14) Mikhaylik, Y. V.; Akridge, J. R. *J. Electrochem. Soc.* **2003**, *150*, A306.
(15) Visco, S. J. (PolyPlus-Battery) U.S. Patent 6,214,061, 2004.
(16) Yao, Y. Y.; Kummer, J. T. *J. Inorg. Nucl. Chem.* **1967**, *29*, 2453.
(17) Whittingham, M. S.; Huggins, R. A. *J. Chem. Phys.* **1971**, *54*, 414.
(18) Whittingham, M. S.; Huggins, R. A. *NBS Spec. Pub.* **1972**, *364*, 139.
(19) Whittingham, M. S. In *Fast Ion Transport in Solids*; van Gool, W., Ed.; North-Holland: Amsterdam, 1973.

(20) Trumbore, F. A.; Broadhead, J.; Putvinski, T. M. *Electrochem. Soc. Abstr.* **1973**, *1973−2*, 61.
(21) Broadhead, J.; Trumbore, F. A. *Electrochem. Soc. Abstr.* **1973**, *1977−1*, 178/179.
(22) Broadhead, J. U.S. Patent 3,791,867, 1973.
(23) Murphy, D. W.; Trumbore, F. A. *J. Electrochem. Soc.* **1976**, *123*, 960.
(24) Armand, M. B. In *Fast Ion Transport in Solids*; van Gool, W., Ed.; North-Holland: Amsterdam, 1973.
(25) Armand, M. B.; Touzan, P. *Mater. Sci. Eng.* **1977**, *31*, 319.
(26) Armand, M. B. U.S. Patent 4,041,220, 1977.
(27) Whittingham, M. S. *Layered Compounds*; Asilomar: Monterey, CA, 1972.
(28) Gamble, F. R.; Osiecki, J. H.; Cais, M.; Pishardy, R.; Disalvo, F. J.; Geballe, T. H. *Science* **1971**, *174*, 493.
(29) Gamble, F. R.; Thompson, A. H. *Solid State Commun.* **1978**, *27*, 379.
(30) Whittingham, M. S. *Mater. Res. Bull.* **1974**, *9*, 1681.
(31) Whittingham, M. S. *J. Chem. Soc., Chem. Commun.* **1974**, 328.
(32) Whittingham, M. S. U.S. Patent 4040017 and U.K. Patent 1468244, 1973.
(33) SubbaRao, G. V.; Tsang, J. C. *Mater. Res. Bull.* **1974**, *9*, 921.
(34) Whittingham, M. S. U.S. Patent 4009052 and U.K. Patent 1468416, 1973.
(35) Whittingham, M. S. *Science* **1976**, *192*, 1126.
(36) Whittingham, M. S. *Chemtech* **1979**, *9*, 766.
(37) Whittingham, M. S.; Chianelli, R. R. *J. Chem. Educ.* **1980**, *57*, 569.
(38) Holleck, G. L.; Driscoll, J. P. *Electrochim. Acta* **1977**, *22*, 647.
(39) Thompson, A. H. *Phys. Rev. Lett.* **1975**, *35*, 1786.
(40) Whittingham, M. S. *J. Electrochem. Soc.* **1976**, *123*, 315.
(41) Steele, B. C. H. In *Fast Ion Transport in Solids*; van Gool, W., Ed.; North-Holland: Amsterdam, 1973.
(42) Basu, S.; Worrell, W. In *Fast Ion Transport in Solids*; Vashishta, P., Mundy, J. N., Shenoy, G. K., Eds.; Elsevier-North-Holland: New York, 1979.
(43) Newman, G. H.; Klemann, L. P. *J. Electrochem. Soc.* **1980**, *127*, 2097.
(44) Winn, D. A.; Shemilt, J. M.; Steele, B. C. H. *Mater. Res. Bull.* **1976**, *11*, 559.
(45) Whittingham, M. S.; Gamble, F. R. *Mater. Res. Bull.* **1975**, *10*, 363.
(46) Whittingham, M. S.; Panella, J. A. *Mater. Res. Bull.* **1981**, *16*, 37.
(47) Whittingham, M. S. U.S. Patent 4,007,055, 1975.
(48) Whittingham, M. S. U.S. Patent 4,084,046, 1975.
(49) Yang, S.; Song, Y.; Zavalij, P. Y.; Whittingham, M. S. *Electrochem. Commun.* **2002**, *4*, 239.
(50) Yang, S.; Zavalij, P. Y.; Whittingham, M. S. *Electrochem. Commun.* **2001**, *3*, 505.
(51) Morgan, D.; VanderVen, A.; Ceder, G. *Electrochem. Solid State Lett.* **2004**, *7*, A30.
(52) Thompson, A. H. *Phys. Rev. Lett.* **1978**, *40*, 489.
(53) Yazami, R.; Touzain, P. *J. Power Sources* **1983**, *9*, 365.
(54) Basu, S. U.S. Patent 4,423,125, 1982.
(55) Whittingham, M. S.; Newman, G. H. *J. Electrochem. Soc.* **1981**, *128*, 706.
(56) Whittingham, M. S.; Newman, G. H. U.S. Patent 4,086,403, 1976.
(57) Newman, G. H.; Francis, R. W.; Gaines, L. H.; Rao, B. M. L. *J. Electrochem. Soc.* **1980**, *127*, 2025.
(58) Chianelli, R. R.; Scanlon, J. C.; Rao, B. M. L. *J. Electrochem. Soc.* **1978**, *125*, 409.
(59) Chianelli, R. R. *J. Cryst. Growth* **1976**, *34*, 239.
(60) Rao, B. M. L.; Francis, R. W.; Christopher, H. A. *J. Electrochem. Soc.* **1977**, *124*, 1490.
(61) Whittingham, M. S. *Mater. Res. Bull.* **1978**, *13*, 959.
(62) Murphy, D. W.; DiSalvo, F. J.; Hull, G. W.; Waszczak, J. V. *Inorg. Chem.* **1976**, *15*, 17.
(63) Dahn, J. R.; Sacken, U. v.; Michal, C. A. *Solid State Ionics* **1990**, *44*, 87.
(64) Johnson, C. S.; Kim, J.-S.; Kropf, A. J.; Kahaian, A. J.; Vaughey, J. T.; Thackeray, M. M. *Electrochem. Commun.* **2002**, *4*, 492.
(65) Haering, R. R.; Stiles, J. A. R.; Brandt, K. U.S. Patent 4,224,390, 1980.
(66) Murphy, D. W.; Carides, J. N.; DiSalvo, F. J.; Cros, C.; Waszczak, J. V. *Mater. Res. Bull.* **1977**, *12*, 825.
(67) Murphy, D. W.; Cros, C.; DiSalvo, F. J.; Waszczak, J. V. *Inorg. Chem.* **1977**.
(68) Schöllhorn, R.; Payer, A. *Angew. Chem., Int. Ed. Engl.* **1985**, *24*, 67.
(69) Sinha, S.; Murphy, D. W. *Solid State Ionics* **1986**, *20*, 81.
(70) Goodenough, J. B.; Manthiram, A.; Wnetrzewski, B. *J. Power Sources* **1993**, *43−44*, 269.
(71) Thompson, A. H.; Gamble, F. R.; Symon, C. R. *Mater. Res. Bull.* **1975**, *10*, 915.
(72) Trumbore, F. *J. Power Sources* **1989**, *26*, 65.
(73) Murphy, D. J.; Trumbore, F. A. *J. Cryst. Growth* **1977**, *39*, 185.
(74) Whittingham, M. S.; Jacobson, A. J. U.S. Patent 4,233,375, 1979.
(75) Whittingham, M. S.; Jacobson, A. J. *J. Electrochem. Soc.* **1981**, *128*, 485.
(76) Dines, M. B. *Mater. Res. Bull.* **1975**, *10*, 287.
(77) Whittingham, M. S.; Dines, M. B. *J. Electrochem. Soc.* **1977**, *124*, 1387.
(78) Murphy, D. W.; Christian, P. A. *Science* **1979**, *205*, 651.
(79) Dampier, F. W. *J. Electrochem. Soc.* **1974**, *121*, 656.
(80) Walk, C. R.; Gore, J. S. *J. Electrochem. Soc.* **1975**, *122*, 68C.
(81) Walk, C. R.; Margalit, N. *J. Power Sources* **1997**, *68*, 723.
(82) Delmas, C.; Cognac-Auradou, H.; Cocciantelli, J. M.; Ménétrier, M.; Doumerc, J. P. *Solid State Ionics* **1994**, *69*, 257.
(83) Delmas, C.; Cognac-Auradou, H.; Coociatelli, J. M.; Ménétrier, M.; Doumerc, J. P. *Solid State Ionics* **1994**, *69*, 257.
(84) Dickens, P. G.; French, S. J.; Hight, A. T.; Pye, M. F. *Mater. Res. Bull.* **1979**, *14*, 1295.
(85) Whittingham, M. S. *Electrochem. Soc. Abstr.* **1975**, *1975−1*, 40.
(86) Murphy, D. W.; Christian, P. A.; Disalvo, F. J.; Carides, J. N. *J. Electrochem. Soc.* **1979**, *126*, 497.
(87) Bergström, Ö.; Gustafsson, T.; Thomas, J. Abstracts of the XVII International Union of Crystallography Congress, Seattle, WA; International Union of Crystallography (http://www.iucr.ac.uk/): Cambridge, U.K., 1996.
(88) Bergström, Ö.; Gustafsson, T.; Thomas, J. O. *Acta Crystallogr.* **1997**, *C53*, 528.
(89) Bergström, Ö.; Gustafsson, T.; Thomas, J. O. *Acta Crystallogr.* **1998**, *C54*, 1204.
(90) Howing, J.; Gustafsson, T.; Thomas, J. O. *Acta Crystallogr.* **2003**, *B59*, 747.
(91) Bjork, H.; Lidin, S.; Gustafsson, T.; Thomas, J. O. *Acta Crystallogr.* **2001**, *B57*, 759.
(92) Besenhard, J. O.; Schöllhorn, R. *J. Power Sources* **1976**, *1*, 267.
(93) Schöllhorn, R.; Klein-Reesink, F.; Reimold, R. *J. Chem. Soc., Chem. Commun.* **1979**, 398.
(94) Nassau, K.; Murphy, D. W. *J. Non-Cryst. Solids* **1981**, *44*, 297.
(95) West, K.; Zachau-Christiansen, B.; Skaarup, S.; Saidi, Y.; Barker, J.; Olsen, I. I.; Pynenburg, R.; Koksbang, R. *J. Electrochem. Soc.* **1996**, *143*, 820.
(96) Livage, J. *Mater. Res. Bull.* **1991**, *26*, 1173.
(97) Livage, J. *Chem. Mater.* **1991**, *3*, 578.
(98) Livage, J.; Baffier, N.; Pereira-Ramos, J. P.; Davidson, P. *Mater. Res. Soc. Proc.* **1995**, *369*, 179.
(99) Chandrappa, G. T.; Steunou, N.; Livage, J. *Nature* **2002**, *416*, 702.
(100) Le, D. B.; Passerini, S.; Guo, J.; Ressler, J.; Owens, B. B.; Smyrl, W. H. *J. Electrochem. Soc.* **1996**, *143*, 2099.
(101) Galy, J. *J. Solid State Chem.* **1992**, *100*, 229.
(102) Oka, Y.; Yao, T.; Yamamoto, N. *J. Solid State Chem.* **1997**, *132*, 323.
(103) Zhang, F.; Zavalij, P. Y.; Whittingham, M. S. *Mater. Res. Bull.* **1997**, *32*, 701.
(104) Zhang, F.; Zavalij, P. Y.; Whittingham, M. S. *Mater. Res. Soc. Proc.* **1998**, *496*, 367.
(105) Zhang, F.; Whittingham, M. S. *Electrochem. Commun.* **2000**, *2*, 69.
(106) Torardi, C. C.; Miao, C. R.; Lewittes, M. E.; Li, Z. *Electrochem. Soc. Proc.* **2000**, *2000−21*, 68.
(107) Torardi, C. C.; Miao, C. R.; Lewittes, M. E.; Li, Z. *J. Solid State Chem.* **2002**, *163*, 93.
(108) Spahr, M. E.; Stoschitzki-Bitterli, P.; Nesper, R.; Müller, M.; Krumeich, F.; Nissen, H. U. *Angew. Chem., Int. Ed. Engl.* **1998**, *37*, 1263.
(109) Spahr, M. E.; Stoschitzki-Bitterli, P.; Nesper, R.; Haas, O.; Novak, P. *J. Electrochem. Soc.* **1999**, *146*, 2780.
(110) Edström, K.; Gustafsson, T.; Nordliner, S. *Electrochem. Solid State Lett.* **2001**, *4*, A129.
(111) Nordlinder, S.; Edström, K.; Gustafsson, T. *Electrochem. Solid-State Lett.* **2001**, *4*, A129.
(112) Dobley, A.; Ngala, K.; Yang, S.; Zavalij, P. Y.; Whittingham, M. S. *Chem. Mater.* **2001**, *13*, 4382.
(113) Delmas, C.; Devalette, M.; Fouassier, C.; Hagenmuller, P. *Mater. Res. Bull.* **1975**, *10*, 393.
(114) Delmas, C.; Fouassier, C.; Hagenmuller, P. *J. Solid State Chem.* **1975**, *13*, 165.
(115) Delmas, C.; Fouassier, C.; Réau, J.-M.; Hagenmuller, P. *Mater. Res. Bull.* **1976**, *11*, 1081.
(116) Delmas, C.; Fouassier, C. *Z. Anorg. Allg. Chem.* **1976**, *420*, 184.
(117) Delmas, C.; Fouassier, C.; Hagenmuller, P. *Physica* **1980**, *99B*, 81.
(118) Delmas, C.; Braconnier, J.-J.; Fouassier, C.; Hagenmuller, P. *Solid State Ionics* **1981**, *3/4*, 165.
(119) LeBlanc, A.; Danot, M.; Trichet, L.; Rouxel, J. *Mater. Res. Bull.* **1974**, *9*, 191.
(120) Rouxel, J.; Danot, M.; Bichon, J. *Bull. Soc. Chim. Fr.* **1971**, 3930.
(121) Danot, M.; Blanc, A. L.; Rouxel, J. *Bull. Soc. Chim. Fr.* **1969**, 2670.
(122) Danot, M.; Rouxel, J. *C. R. Acad. Sci. Paris* **1973**, *C276*, 1283.
(123) Mitzushima, K.; Jones, P. C.; Wiseman, P. J.; Goodenough, J. B. *Mater. Res. Bull.* **1980**, *15*, 783.

(124) Amatucci, G. G.; Tarascon, J. M.; Klein, L. C. *J. Electrochem. Soc.* **1996**, *143*, 1114.
(125) Rossen, E.; Reimers, J. N.; Dahn, J. R. *Solid State Ionics* **1993**, *62*, 53.
(126) Gabrisch, H.; Yazimi, R.; Fultz, B. *J. Electrochem. Soc.* **2004**, *151*, A891.
(127) Nagaura, T.; Tozawa, K. *Prog. Batteries Solar Cells* **1990**, *9*, 209.
(128) Ozawa, K. *Solid State Ionics* **1994**, *69*, 212.
(129) Goodenough, J. B.; Mizuchima, K. U.S. Patent 4,302,518, 1981.
(130) Imanishi, N.; Fujiyoshi, M.; Takeda, Y.; Yamamoto, O.; Tabuchi, M. *Solid State Ionics* **1999**, *118*, 121.
(131) Levasseur, S.; Menetrier, M.; Suard, E.; Delmas, C. *Solid State Ionics* **2000**, *128*, 11.
(132) Yonezu, I.; Tarui, H.; Yoshimura, S.; Fujitani, S.; Nohma, T. Abstracts of the International Meeting On Lithium Batteries; Electrochemical Society: Pennington, NJ, 2004; Vol. 12, abstract 58.
(133) Nishi, Y. In *Lithium Ion Batteries*; Wakihara, M., Yamamoto, O., Eds.; Kodansha: Tokyo, 1998.
(134) Cho, J.; Kim, G. *Electrochem. Solid State Lett.* **1999**, *2*, 253.
(135) Cho, J.; Kim, C.; Yoo, S. I. *Electrochem. Solid State Lett.* **2000**, *3*, 362.
(136) Cho, J.; Kim, Y. J.; Park, B. *Chem. Mater.* **2000**, *12*, 3788.
(137) Cho, J.; Kim, Y. J.; Park, B. *J. Electrochem. Soc.* **2001**, *148*, A1110.
(138) Cho, J.; Kim, Y. J.; Kim, J. T.; Park, B. *Angew. Chem., Int. Ed.* **2001**, *40*, 3367.
(139) Wang, Z.; Wu, C.; Liu, L.; Chen, L.; Huang, X. *Solid State Ionics* **2002**, *148*, 335.
(140) Wang, Z.; Wu, C.; Liu, L.; Wu, F.; Chen, L.; Huang, X. *J. Electrochem. Soc.* **2002**, *149*, A466.
(141) Liu, L.; Wang, Z.; Li, H.; Chen, L.; Huang, X. *Solid State Ionics* **2002**, *152*, 341.
(142) Cho, J.; Park, B. *Lithium Battery Discussion Electrode Materials*, Bordeaux, 2003; Abstract 1.
(143) Liu, J.; Xu, K.; Jow, T. R.; Amine, K. *Electrochem. Soc. Abstr.* **2002**, *2002−2*, 135.
(144) Amine, K.; Liu, J.; Kang, S.; Belharouak, I.; Hyung, Y.; Vissers, D.; Henriksen, G. *J. Power Sources* **2004**, *129*, 14.
(145) Chen, Z.; Dahn, J. R. *Electrochim. Acta* **2004**, *49*, 1079.
(146) Seguin, L.; Amatucci, G.; Anne, M.; Chabre, Y.; Strobel, P.; Tarascon, J. M.; Vaughan, G. *J. Power Sources* **1999**, *81−82*, 604.
(147) Goodenough, J. B.; Mizuchima, K. U.S. Patent 4,302,518, 1980.
(148) Goodenough, J. B.; Mizushima, K. U.S. Patent 4,357,215, 1981.
(149) Whittingham, M. S.; Zavalij, P. Y. *Solid State Ionics* **2000**, *131*, 109.
(150) Thackeray, M. M.; David, W. I. F.; Bruce, P. G.; Goodenough, J. B. *Mater. Res. Bull.* **1983**, *18*, 461.
(151) Tarascon, J.-M.; Guyomard, D. *Solid State Ionics* **1994**, *69*, 222.
(152) Tarascon, J. M.; McKinnon, W. R.; Coowar, F.; Bowmer, T. N.; Amatucci, G.; Guyomard, D. *J. Electrochem. Soc.* **1994**, *141*, 1421.
(153) Tarascon, J. M.; Wang, E.; Shokoohi, F. K.; McKinnon, W. R.; Colson, S. *J. Electrochem. Soc.* **1991**, *138*, 2859.
(154) Thackeray, M. M. *Prog. Solid State Chem* **1997**, *25*, 1.
(155) Yonemura, M.; Yamada, A.; Kobayashi, H.; Tabuchi, M.; Kamiyama, T.; Kawamoto, Y.; Kanno, R. *J. Mater. Chem.* **2004**, *14*, 1948.
(156) Tarascon, J. M. U.S. Patent 5,135,732, 1992.
(157) Amatucci, G. G.; Pereira, N.; Zheng, T.; Tarascon, J.-M. *J. Electrochem. Soc.* **2001**, *148*, A171.
(158) Amatucci, G. G.; Pereira, N.; Zheng, T.; Plitz, I.; Tarascon, J.-M. *J. Power Sources* **1999**, *81−82*, 39.
(159) Shin, Y.; Manthiram, A. *J. Electrochem. Soc.* **2004**, *151*, A204.
(160) Ferg, E.; Gummow, R. J.; Kock, A. D.; Thackeray, M. M. *J. Electrochem. Soc.* **1994**, *141*, L147.
(161) Ohzuku, T.; Ueda, A.; Yamamoto, N. *J. Electrochem. Soc.* **1995**, *142*, 1431.
(162) Zaghib, K.; Simoneau, M.; Armand, M.; Gauthier, M. *J. Power Sources* **1999**, *81−82*, 300.
(163) Tessier, C.; Fachetti, O.; Siret, C.; Castaing, F.; Jordy, C.; Boeuve, J. P.; Biensan, P. *Lithium Battery Discussion Electrode Materials*, Bordeaux, 2003, Abstract 29.
(164) Franger, S.; Bourbon, C.; LeCras, F. *J. Electrochem. Soc.* **2004**, *151*, A1024.
(165) Panero, S.; Satolli, D.; Salamon, M.; Scrosati, B. *Electrochem. Commun.* **2000**, *2*, 810.
(166) Rougier, A.; Saadouane, I.; Gravereau, P.; Willmann, P.; Delmas, C. *Solid State Ionics* **1996**, *90*, 83.
(167) Saardoune, I.; Delmas, C. *J. Solid State Chem.* **1998**, *136*, 8.
(168) Saadoune, I.; Menetrier, M.; Delmas, C. *J. Mater. Chem.* **1997**, *7*, 2505.
(169) Saadoune, I.; Delmas, C. *J. Mater. Chem.* **1996**, *6*, 193.
(170) Zhecheva, E.; Stoyanova, R. *Solid State Ionics* **1993**, *66*, 143.
(171) Prado, G.; Fournes, L.; Delmas, C. *J. Solid State Chem.* **2001**, *159*, 103.
(172) Prado, G.; Rougier, A.; Fournes, L.; Delmas, C. *J. Electrochem. Soc.* **2000**, *147*, 2880.
(173) Kanno, R.; Shirane, T.; Inaba, Y.; Kawamoto, Y. *J. Power Sources* **1997**, *68*, 145.
(174) Delmas, C.; Menetrier, M.; Croguennec, L.; Levasseur, S.; Peres, J. P.; Pouillerie, C.; Prado, G.; Fournes, L.; Weill, F. *Int. J. Inorg. Mater.* **1999**, *1*, 11.
(175) Pouillerie, C.; Perton, F.; Biensan, P.; Peres, J. P.; Broussely, M.; Delmas, C. *J. Power Sources* **2001**, *96*, 293.
(176) Pouillerie, C.; Croguennec, L.; Delmas, C. *Solid State Ionics* **2000**, *132*, 15.
(177) Nakai, I.; Nakagome, T. *Electrochem. Solid State Lett.* **1998**, *1*, 259.
(178) Brouselly, M. *Lithium Battery Discusssion*, Bordeaux-Arcachon 2001.
(179) Delmas, C.; Capitaine, F. Abstracts of the 8th International Meeting Lithium Batteries; Electrochemical Society: Pennington, NJ, 1996; Vol. 8, abstract 470.
(180) Chen, R.; Whittingham, M. S. *J. Electrochem. Soc.* **1997**, *144*, L64.
(181) Armstrong, A. R.; Bruce, P. G. *Nature* **1996**, *381*, 499.
(182) Capitaine, F.; Gravereau, P.; Delmas, C. *Solid State Ionics* **1996**, *89*, 197.
(183) Chen, R.; Zavalij, P. Y.; Whittingham, M. S. *Mater. Res. Soc. Proc.* **1997**, *453*, 653.
(184) Chen, R.; Zavalij, P.; Whittingham, M. S. *Chem. Mater.* **1996**, *8*, 1275.
(185) Chen, R.; Chirayil, T.; Whittingham, M. S. *Solid State Ionics* **1996**, *86−88*, 1.
(186) Bach, S.; Henry, M.; Baffier, N.; Livage, J. *J. Solid State Chem.* **1990**, *88*, 325.
(187) Bach, S.; Pereiraramos, J. P.; Cachet, C.; Bode, M.; Yu, L. T. *Electrochim. Acta* **1995**, *40*, 785.
(188) Bach, S.; Pereira-Ramos, J. P.; Baffier, N. *J. Solid State Chem.* **1995**, *120*, 70.
(189) Pereira-Ramos, J. P.; Baddour, R.; Bach, S.; Baffier, N. *Solid State Ionics* **1992**, *53−56*, 701.
(190) Stoyanova, R.; Zhecheva, E.; Zarkova, L. *Solid State Ionics* **1994**, *73*, 233.
(191) Doeff, M. M.; Richardson, T. J.; Kepley, L. *J. Electrochem. Soc.* **1996**, *143*, 2507.
(192) Whittingham, M. S. *1996 USDOE BATT Annual Report;* USDOE: Washington, D.C., 1997.
(193) Doeff, M. M.; Peng, M. Y.; Ma, Y.; Visco, S. J.; DeJonghe, L. C. U.S. Patent 5,558,961, 1996.
(194) Doeff, M. M.; Richardson, T. J.; Hwang, K.-T.; Anapolsky, A. *ITE Battery Lett.* **2001**, *2*, B.
(195) Armstrong, A. R.; Huang, H.; Jennings, R. A.; Bruce, P. G. *J. Mater. Chem.* **1998**, *8*, 255.
(196) Chen, R.; Whittingham, M. S. Proceedings of the Annual Automotive Technology Development Customers Coordination Meeting, Dearborn, MI, Oct. 27−30, 1997; USDOE: Washington, DC, 1997; Vol. III, p 301.
(197) Zhang, F.; Ngala, K.; Whittingham, M. S. *Electrochem. Commun.* **2000**, *2*, 445.
(198) Yang, S.; Song, Y.; Ngala, K.; Zavalij, P. Y.; Whittingham, M. S. *J. Power Sources* **2003**, *119*, 239.
(199) Lu, Z.; Dahn, J. R. *Chem. Mater.* **2001**, *13*, 1252.
(200) Lu, Z.; Dahn, J. R. *Chem. Mater.* **2001**, *13*, 2078.
(201) Lu, Z.; Dahn, J. R. *J. Electrochem. Soc.* **2001**, *148*, A237.
(202) Lu, Z.; Dahn, J. R. *Chem. Mater.* **2000**, *12*, 3583.
(203) Eriksson, T. A.; Lee, Y. J.; Hollingsworth, J.; Reimer, J. A.; Cairns, E. J.; Zhang, X.-f.; Doeff, M. M. *Chem. Mater.* **2003**, *15*, 4456.
(204) Dolle, M.; Hollingsworth, J.; Richardson, T. J.; Doeff, M. M. *Solid State Ionics* **2004**, in press.
(205) Shaju, K. M.; SubbaRao, G. V.; Chowdari, B. V. R. *Electrochim. Acta* **2003**, *48*, 2691.
(206) Armstrong, A. R.; Gitzendanner, R.; Robertson, A. D.; Bruce, P. G. *Chem. Commun.* **1998**, 1833.
(207) Numata, K.; Yamanaka, S. *Solid State Ionics* **1999**, *118*, 117.
(208) Fujiwara, M.; Yamada, S.; Kanda, M. Extended Abstracts of 34th Battery Symposium. Nagoya, Japan; The Electrochemical Society of Japan: Tokyo, Japan, 1993; Vol. 34, p 135.
(209) Yoshio, M.; Yamato, K.; Itoh, J.; Noguchi, H.; Okada, M.; Mouri, T. *Electrochem. Soc. Proc.* **1994**, *94−28*, 251.
(210) Nitta, Y.; Okamura, K.; Haraguchi, K.; Kobayashi, S.; Ohta, A. *J. Power Sources* **1995**, *54*, 511.
(211) Caurant, D.; Baffier, N.; Bianchi, V.; Grégoire, G.; Bach, S. *J. Mater. Chem.* **1996**, *6*, 1149.
(212) Rossen, E.; Jones, C. D. W.; Dahn, J. R. *Solid State Ionics* **1992**, *57*, 311.
(213) Spahr, M. E.; Novák, P.; Schnyder, B.; Haas, O.; Nesper, R. *J. Electrochem. Soc.* **1998**, *145*, 1113.
(214) Ohzuku, T.; Makimura, Y. *Chem. Lett.* **2001**, 744.
(215) Ohzuku, T.; Makimura, Y. *Chem. Lett.* **2001**, 642.
(216) Lu, Z.; MacNeil, D. D.; Dahn, J. R. *Electrochem. Solid State Lett.* **2001**, *4*, A200.
(217) Wang, Z.; Sun, Y.; Chen, L.; Huang, X. *J. Electrochem. Soc.* **2004**, *151*, A914.

(218) Tsai, Y. W.; Lee, J. F.; Liu, D. G.; Hwamg, B. J. *J. Mater. Chem.* **2004**, *14*, 958.
(219) Ngala, J. K.; Chernova, N. A.; Ma, M.; Mamak, M.; Zavalij, P. Y.; Whittingham, M. S. *J. Mater. Chem.* **2004**, *14*, 214.
(220) Ngala, J. K.; Chernova, N.; Matienzo, L.; Zavalij, P. Y.; Whittingham, M. S. *Mater. Res. Soc. Symp.* **2003**, *756*, 231.
(221) Hwang, B. J.; Tsai, Y. W.; Chen, C. H.; Santhanam, R. *J. Mater. Chem.* **2003**, *13*, 1962.
(222) Kim, J.-H.; Park, C. W.; Sun, Y.-K. *Solid State Ionics* **2003**, *164*, 43.
(223) Jiang, J.; Dahn, J. R. *Electrochem. Commun.* **2004**, *6*, 39.
(224) Shaju, K. M.; Rao, G. V. S.; Chowdari, B. V. R. *Electrochim. Acta* **2002**, *48*, 145.
(225) Park, S. H.; Yoon, C. S.; Kang, S. G.; Kim, H.-S.; Moon, S.-I.; Sun, Y.-K. *Electrochim. Acta* **2004**, *49*, 557.
(226) Hwang, B. J.; Tsai, Y. W.; Carlier, D.; Ceder, G. *Chem. Mater.* **2003**, *15*, 3676.
(227) Koyama, Y.; Tanaka, I.; Adachi, H.; Makimura, Y.; Ohzuku, T. *J. Power Sources* **2003**, *119*−*121*, 644.
(228) Yoshio, M.; Noguchi, H.; Itoh, J.-i.; Okada, M.; Mouri, T. *J. Power Sources* **2000**, *90*, 176.
(229) Belharouak, I.; Sun, Y.-K.; Liu, J.; Amine, K. *J. Power Sources* **2003**, *123*, 247.
(230) Chen, Y.; Wang, G. X.; Konstantinov, K.; Liu, H. K.; Dou, S. X. *J. Power Sources* **2003**, *119*−*121*, 184.
(231) Yabuuchi, N.; Ohzuku, T. *J. Power Sources* **2003**, *119*−*121*, 171.
(232) Yoon, W.-S.; Grey, C. P.; Balasubramanian, M.; Yang, X.-Q.; Fischer, D. A.; McBreen, J. *Electrochem. Solid State Lett.* **2004**, *7*, A53.
(233) Sun, Y.; Ouyang, C.; Wang, Z.; Huang, X.; Chen, L. *J. Electrochem. Soc.* **2004**, *151*, A504.
(234) Kim, J.-M.; Chung, H.-T. *Electrochim. Acta* **2004**, *49*, 937.
(235) Jouanneau, S.; Eberman, K. W.; Krause, L. J.; Dahn, J. R. *J. Electrochem. Soc.* **2003**, *150*, A1637.
(236) MacNeil, D. D.; Lu, Z.; Dahn, J. R. *J. Electrochem. Soc.* **2002**, *149*, A1332.
(237) Jouanneau, S.; Macneil, D. D.; Lu, Z.; Beattie, S. D.; Murphy, G.; Dahn, J. R. *J. Electrochem. Soc.* **2003**, *150*, A1299.
(238) Reed, J.; Ceder, G.; VanDerVen, A. *Electrochem. Solid State Lett.* **2001**, *4*, A78.
(239) Armstrong, A. R.; Paterson, A. J.; Robertson, A. D.; Bruce, P. G. *Chem. Mater.* **2002**, *14*, 710.
(240) Armstrong, A. R.; Robertson, A. D.; Bruce, P. G. *Electrochim. Acta* **1999**, *45*, 285.
(241) Sharma, P.; Moore, G.; Zhang, F.; Zavalij, P. Y.; Whittingham, M. S. *Electrochem. Solid-State Lett.* **1999**, *2*, 494.
(242) Zhang, F.; Whittingham, M. S. *Electrochem. Solid State Lett.* **2000**, *3*, 309.
(243) Ammundsen, B.; Desilvestro, H.; Paulson, J. M.; Steiner, R.; Pickering, P. J. 10th International Meeting on Lithium Batteries, Como, Italy, May 28−June 2, 2000; Electrochemical Society: Pennington, NJ, 2000.
(244) Storey, C.; Kargina, I.; Grincourt, Y.; Davidson, I. J.; Yoo, Y.; Seung, D. Y. 10th International Meeting on Lithium Batteries, Como, Italy, May 28−June 2, 2000; Electrochemical Society: Pennington, NJ, 2000; Vol. 10, abstract 234.
(245) Paulsen, J. M.; Ammundsen, B.; Desilvestro, H.; Steiner, R.; Hassell, D. *Electrochem. Soc. Abstr.* **2000**, *2002*−*2*, 71.
(246) Whitfield, P. S.; Davidson, I. J.; Kargina, I.; Grincourt, Y.; Ammundsen, B.; Steiner, R.; Suprun, A. *Electrochem. Soc. Abstr.* **2000**, *2000*−*2*, 90.
(247) Grincourt, Y.; Storey, C.; Davidson, I. J. *J. Power Sources* **2001**, *97*−*98*, 711.
(248) Storey, C.; Kargina, I.; Grincourt, Y.; Davidson, I. J.; Yoo, Y. C.; Seung, D. Y. *J. Power Sources* **2001**, *97*−*98*, 541.
(249) Balasubramanian, M.; McBreen, J.; Davidson, I. J.; Whitfield, P. S.; Kargina, I. *J. Electrochem. Soc.* **2002**, *149*, A176.
(250) Ammundsen, B.; Paulsen, J.; Davidson, I.; Liu, R.-S.; Shen, C.-H.; Chen, J.-M.; Jang, L.-Y.; Lee, J.-F. *J. Electrochem. Soc.* **2002**, *149*, A431.
(251) Numata, K.; Sakaki, C.; Yamanaka, S. *Solid State Ionics* **1999**, *117*, 257.
(252) Lu, Z.; MacNeil, D. D.; Dahn, J. R. *Electrochem. Solid State Lett.* **2001**, *4*, A191.
(253) Arachi, Y.; Kobayashi, H.; Emura, S.; Nakata, Y.; Tanaka, M.; Asai, T. *Chem. Lett.* **2003**, *32*, 60.
(254) Venkatraman, S.; Manthiram, A. *Chem. Mater.* **2003**, *15*, 5003.
(255) Sun, Y.-K.; Yoon, C. S.; Lee, Y. S. *Electrochim. Acta* **2003**, *48*, 2589.
(256) Yang, X.-Q.; McBreen, J.; Yoon, W.-S.; Grey, C. P. *Electrochem. Commun.* **2002**, *4*, 649.
(257) Rieck, H.; Hoppe, R. Z. *Anorg. Allg. Chem.* **1972**, *392*, 193.
(258) Makimura, Y.; Ohzuku, T. *J. Power Sources* **2003**, *119*−*121*, 156.
(259) Ariyoshi, K.; Iwakoshi, Y.; Nakayama, N.; Ohzuku, T. *J. Electrochem. Soc.* **2004**, *151*, A296.
(260) Ohzuku, T. Personal Communication, 2004.
(261) Shaju, K. M.; SubbaRao, G. V.; Chowdari, B. V. R. *Electrochim. Acta* **2004**, *49*, 1565.
(262) Kang, S.-H.; Kim, J.; Stoll, M. E.; Abraham, D.; Sun, Y. K.; Amine, K. *J. Power Sources* **2002**, *112*, 41.
(263) Cushing, B. L.; Goodenough, J. B. *Solid State Sci.* **2002**, *4*, 1487.
(264) Reed, J.; Ceder, G. *Electrochem. Solid State Lett.* **2002**, *5*, A145.
(265) Kang, K.; Carlier, D.; Reed, J.; Arroyo, E. M.; Ceder, G.; Croguennec, L.; Delmas, C. *Chem. Mater.* **2003**, *15*, 4503.
(266) Ohzuku, T.; Makimura, Y. *Electrochem. Soc. Abstr.* **2003**, *2003*−*1*, 1079.
(267) Meng, Y. S.; Ceder, G.; Grey, C. P.; Yoon, W.-S.; Shao-Horn, Y. *Electrochem. Solid State Lett.* **2004**, *7*, A155.
(268) Yoon, W.-S.; Iannopollo, S.; Grey, C. P.; Carlier, D.; Gorman, J.; Reed, J.; Ceder, G. *Electrochem. Solid State Lett.* **2004**, *7*, A167.
(269) Ceder, G.; Meng, Y.-S.; Shao-Horn, Y.; Grey, C. P. 12th International Meeting on Lithium Batteries; Electrochemical Society: Pennington, NJ, 2004; Vol. 12, abstract 22.
(270) Kobayashi, H.; Sakaebe, H.; Kageyama, H.; Tatsumi, K.; Arachi, Y.; Kamiyama, T. *J. Mater. Chem.* **2003**, *13*, 590.
(271) Kobayashi, H.; Arachi, Y.; Kageyama, H.; Tatsumi, K. *J. Mater. Chem.* **2004**, *14*, 40.
(272) Liu, Z.; Yu, A.; Lee, J. Y. *J. Power Sources* **1999**, *81*−*82*, 416.
(273) Jouanneau, S.; Dahn, J. R. *Chem. Mater.* **2003**, *15*, 495.
(274) Thomas, M. G. S. R.; David, W. I. F.; Goodenough, J. B. *Mater. Res. Bull.* **1985**, *20*, 1137.
(275) Guilmard, M.; Pouillerie, C.; Croguennec, L.; Delmas, C. *Solid State Ionics* **2003**, *160*, 39.
(276) Ma, M.; Chernova, N. A.; Zavalij, P. Y.; Whittingham, M. S. *J Power Sources* **2004**, in press.
(277) Cushing, B. L.; Goodenough, J. B. *Solid State Sci.* **2002**, *4*, 1487.
(278) Oh, S. W.; Park, S. H.; Park, C.-W.; Sun, Y.-K. *Solid State Ionics* **2004**, *171*, 167.
(279) Li, D.-C.; Muta, T.; Zhang, L.-Q.; Yoshio, M.; Noguchi, H. *J. Power Sources* **2004**, *132*, 150.
(280) Meng, Y. S.; Wu, Y. W.; Hwang, B. J.; Li, Y.; Ceder, G. *J. Electrochem. Soc.* **2004**, *151*, A1134.
(281) Ohzuku, T.; Nakura, K.; Aoki, T. *Electrochim. Acta* **1999**, *45*, 151.
(282) Croguennec, L.; Pouillerie, C.; Delmas, C. *Solid State Ionics* **2000**, *135*, 259.
(283) Yoshizawa, H.; Ohzuku, T. *Denki Kagaku* **2003**, *71*, 1177.
(284) Guilmard, M.; Croguennec, L.; Delmas, C. *Chem. Mater.* **2003**, *15*, 4476.
(285) Guilmard, M.; Croguennec, L.; Delmas, C. *Chem. Mater.* **2003**, *15*, 4484.
(286) Arai, H.; Sakurai, Y. *J. Power Sources* **1999**, *80*−*81*, 401.
(287) Manthiram, A.; Chu, S. *Electrochem. Soc. Abstr.* **2000**, *2000*−*2*, 72.
(288) Chen, R.; Zavalij, P. Y.; Whittingham, M. S.; Greedan, J. E.; Raju, N. P.; Bieringer, M. *J. Mater. Chem.* **1999**, *9*, 93.
(289) Thackeray, M. M.; Johnson, C. S.; Amine, K.; Kim, J. U.S. Patent 6,677,082, 2004.
(290) Thackeray, M. M.; Johnson, C. S.; Amine, K.; Kim, J. U.S. Patent 6,680,143, 2004.
(291) Robertson, A. D.; Bruce, P. G. *Chem. Commun.* **2002**, 2790.
(292) Robertson, A. D.; Bruce, P. G. *Chem. Mater.* **2003**, *15*, 1984.
(293) Armstrong, A. R.; Bruce, P. G. *Electrochem. Solid State Lett.* **2004**, *7*, A1.
(294) Russouw, M. H.; Thackeray, M. M. *Mater. Res. Bull.* **1991**, *26*, 463.
(295) Russouw, M. H.; Liles, D. C.; Thackeray, M. M. *J. Solid State Chem.* **1993**, *104*, 464.
(296) Paik, Y.; Grey, C. P.; Johnson, C. S.; Kim, J.-S.; Thackeray, M. M. *Chem. Mater.* **2002**, *14*, 5106.
(297) Richard, M. N.; Fuller, E. W.; Dahn, J. R. *Solid State Ionics* **1994**, *73*, 81.
(298) Shin, S.-S.; Sun, Y.-K.; Amine, K. *J. Power Sources* **2002**, *112*, 634.
(299) Myung, S.-T.; Komaba, S.; Kumagai, N. *Solid State Ionics* **2004**, *170*, 139.
(300) Zhang, L.; Noguchi, H.; Yoshio, M. *J. Power Sources* **2002**, *110*, 57.
(301) Kim, J.-S.; Johnson, C. S.; Thackeray, M. M. *Electrochem. Commun.* **2002**, *4*, 205.
(302) Kang, S.-H.; Sun, Y. K.; Amine, K. *Electrochem. Solid State Lett.* **2003**, *6*, A183.
(303) Lee, C. W.; Sun, Y.-K.; Prakash, J. *Electrochim. Acta* **2004**, *49*, 4425.
(304) Kanno, R.; Shirane, T.; Kawamoto, Y.; Takeda, Y.; Takano, M.; Ohashi, M.; Yamaguchi, Y. *J. Electrochem. Soc.* **1996**, *143*, 2435.
(305) Kanno, R.; Shirane, T.; Kawamoto, Y. Abstracts of the 8th International Meeting on Lithium Batteries; Electrochemical Society: Pennington, NJ, 1996; Vol. 8, abstract 133.
(306) Whittingham, M. S. U.S. Patent 4,049,887, 1996.
(307) Thompson, A. H.; Whittingham, M. S. *Mater. Res. Bull.* **1977**, *12*, 741.
(308) Jacobson, A. J.; Whittingham, M. S. U.S. Patent 4,143,213, 1978.
(309) Padhi, A. K.; Nanjundaswamy, K. S.; Goodenough, J. B. *J. Electrochem. Soc.* **1997**, *144*, 1188.
(310) Masquelier, C.; Padhi, A. K.; Nanjundaswany, K. S.; Goodenough, J. B. *J. Solid State Chem.* **1998**, *135*, 228.

(311) Morcrette, M.; Wurm, C.; Masquelier, C. *Solid State Sci.* **2002**, *4*, 239.
(312) Masquelier, C.; Padhi, A. K.; Nanjundaswamy, K. S.; Goodenough, J. B. *J. Solid State Chem.* **1998**, *135*, 228.
(313) Chen, J.-M.; Li, Y. J.; Hurng, W.-M.; Whittingham, M. S. (Industrial Technology Research Institute, Chutung, Taiwan) U.S. Patent 5,514,490, 1996.
(314) Li, Y. J.; Whittingham, M. S. *Solid State Ionics* **1993**, *63*, 391.
(315) Yamada, A.; Chung, S. C.; Hinokuma, K. *J. Electrochem. Soc.* **2001**, *148*, A224.
(316) Andersson, A. S.; Kalska, B.; Häggström, L.; Thomas, J. O. *Solid State Ionics* **2000**, *130*, 41.
(317) Andersson, A. S.; Thomas, J. O.; Kalska, B.; Häggström, L. *Electrochem. Solid-State Lett.* **2000**, *3*, 66.
(318) Ravet, N.; Goodenough, J. B.; Besner, S.; Simoneau, M.; Hovington, P.; Armand, M. *Electrochem. Soc. Abstr.* **1999**, *99*−*2*, 127.
(319) Ravet, N.; Besner, S.; Simoneau, M.; Vallée, A.; Armand, M.; Magnan, J.-F. (Hydro-Quebec) European Patent 1049182A2, 2000.
(320) Huang, H.; Yin, S.-C.; Nazar, L. F. *Electrochem. Solid State Lett.* **2001**, *4*, A170.
(321) Masquelier, C.; Wurm, C.; Morcrette, M.; Gaubicher, J. Interantional Meeting on Solid State Ionics, Cairns, Australia, July 9−13, 2001; The International Society of Solid State Ionics: 2001; paper A-IN-06.
(322) Prosini, P. P.; Zane, D.; Pasquali, M. *Electrochim. Acta* **2001**, *46*, 3517.
(323) Yang, S.; Song, Y.; Zavalij, P. Y.; Whittingham, M. S. *Mater. Res. Soc. Proc.* **2002**, *703*, V7.9.
(324) Chung, S.-Y.; Bloking, J. T.; Chiang, Y.-M. *Nat. Mater.* **2002**, *1*, 123.
(325) Herle, P. S.; Ellis, B.; Coombs, N.; Nazar, L. F. *Nat. Mater.* **2004**, *3*, 147.
(326) Croce, F.; Epifanio, A. D.; Hassoun, J.; Deptula, A.; Olczac, T.; Scrosati, B. *Electrochem. Solid State Lett.* **2002**, *5*, A47.
(327) Hu, Y.; Doeff, M. M.; Kostecki, R.; Fiñones, R. *J. Electrochem. Soc.* **2004**, *151*, A1279.
(328) Shiraishi, K.; Dokko, K.; Kanamura, K. 12th International Meeting on Lithium Batteries; Electrochemical Society: Pennington, NJ, 2004; Vol. 12, abstract 297.
(329) Nuspi, G.; Vogler, C.; Eisgruber, M.; Wimmer, L.; Schall, N.; Fietzek, C.; Weydanz, W. 12th International Meeting on Lithium Batteries; Electrochemical Society: Pennington, NJ, 2004; Vol. 12, abstract 293.
(330) García-Martin, O.; Alvarez-Vega, M.; Garcia-Alvarado, F.; Garcia-Jaca, J.; Gallardo-Amores, J. M.; Sanjuán, M. L.; Amador, U. *Chem. Mater.* **2001**, *13*, 1570.
(331) Whittingham, M. S.; Yang, S.; Ngala, K.; Dobley, A.; Zavalij, P. Y. International Meeting on Solid State Ionics, Cairns, Australia, July 9−13, 2001; The International Society of Solid State Ionics: 2001; paper A-KN-06.
(332) Chen, Z.; Dahn, J. R. *J. Electrochem. Soc.* **2002**, *149*, A1184.
(333) Dominko, R.; Gaberscek, M.; Drofenik, J.; Bele, M.; Pejovnik, S. *Electrochem. Solid State Lett.* **2001**, *4*, A187.
(334) Doeff, M. M.; Hu, Y.; McLarnon, F.; Kostecki, R. *Electrochem. Solid State Lett.* **2003**, *6*, A207.
(335) Takahashi, M.; Tobishima, S.; Takei, K.; Sakurai, Y. *J. Power Sources* **2001**, *97*−*98*, 508.
(336) Okada, S.; Sawa, S.; Egashira, M.; Yamaki, J.-i.; Tabuchi, M.; Kageyama, H.; Konishi, T.; Yoshino, A. *J. Power Sources* **2001**, *97*−*98*, 430.
(337) Yamada, A.; Chung, S.-C. *J. Electrochem. Soc.* **2001**, *148*, A960.
(338) Li, G.; Azuma, H.; Tohda, M. *Electrochem. Solid State Lett.* **2002**, *5*, A135.
(339) Delacourt, C.; Poizot, P.; Morcrette, M.; Tarascon, J.-M.; Masquelier, C. *Chem. Mater.* **2004**, *16*, 93.
(340) Song, Y.; Zavalij, P. Y.; Chernova, N. A.; Whittingham, M. S. *J. Electrochem. Soc.*, in press.
(341) Zhou, F.; Cococcionic, M.; Marianetti, C.; Morgan, D.; Chen, M.; Ceder, G. 12th International Meeting on Lithium Batteries; Electrochemical Society: Pennington, NJ, 2004; Vol. 12, abstract 283.
(342) Morgan, D.; Maxisch, T.; Zhou, F.; Cococcioni, M.; Kang, K.; Ceder, G. 12th International Meeting on Lithium Batteries; Electrochemical Society: Pennington, NJ, 2004; Vol. 12, abstract 282.
(343) Osorio-Guillen, J. M.; Holm, B.; Ahuja, R.; Johansson, B. *Solid State Ionics* **2004**, *167*, 221.
(344) Xu, Y.-N.; Chung, S.-Y.; Bloking, J. T.; Chiang, Y.-M.; Ching, W. Y. *Electrochem. Solid State Lett.* **2004**, *7*, A131.
(345) Song, Y.; Yang, S.; Zavalij, P. Y.; Whittingham, M. S. *Mater. Res. Bull.* **2002**, *37*, 1249.
(346) Masquelier, C.; Reale, P.; Wurm, C.; Morcrette, M.; Dupont, L.; Larchera, D. *J. Electrochem. Soc.* **2002**, *149*, A1037.
(347) Hong, Y.-S.; Ryu, K. S.; Park, Y. J.; Kim, M. G.; Leeb, J. M.; Chang, S. H. *J. Mater. Chem.* **2002**, *12*, 1870.
(348) Prosini, P. P.; Cianchi, L.; Spina, G.; Lisi, M.; Scaccia, S.; Carewska, M.; Minarini, C.; Pasquali, M. *J. Electrochem. Soc.* **2001**, *148*, A1125.
(349) Song, Y.; Zavalij, P.; Whittingham, M. S. *Mater. Res. Soc. Proc.* **2003**, *756*, 249.
(350) Song, Y.; Zavalij, P. Y.; Chernova, N. A.; Whittingham, M. S. *Chem. Mater.* **2004**, in press.
(351) Barker, J.; Saidi, M. Y. U.S. Patent 5,871,866, 1999.
(352) Saidi, M. Y.; Barker, J.; Huang, H.; Adamson, G. *Electrochem. Solid State Lett.* **2002**, *5*, A149.
(353) Gaubicher, J.; Goward, G.; Wurm, C.; Masquelier, C.; Nazar, L. F. *Chem. Mater.* **2000**, *12*.
(354) Yin, S. C.; Grondley, H.; Strobel, P.; Nazar, L. F. *J. Am. Chem. Soc.* **2003**, *125*, 326.
(355) Yin, S. C.; Strobel, P.; Anne, M.; Nazar, L. F. *J. Am. Chem. Soc.* **2003**, *125*, 10402.
(356) Huang, H.; Yin, S.-C.; Kerr, T.; Nazar, L. F. *Adv. Mater.* **2002**, *14*, 1525.
(357) Azmi, B. M.; Ishihara, T.; Nishiguchi, H.; Takita, Y. *J. Power Sources* **2003**, *119*−*121*, 273.
(358) Kerr, T. A.; Gaubischer, J.; Nazar, L. F. *Electrochem. Solid State Lett.* **2000**, *3*, 460.
(359) Lim, S. C.; Vaughey, J. T.; Harrison, W. T. A.; Dussak, L. L.; Jacobson, A. J.; Johnson, J. W. *Solid State Ionics* **1996**, *84*, 219.
(360) Zavalij, P. Y.; Whittingham, M. S. *Rigaku J.* **2004**, *21*, 2.
(361) Barker, J.; Saidi, M. Y.; Swoyer, J. L. *J. Electrochem. Soc.* **2003**, *150*, A1394.
(362) Pereira-Ramos, J. P.; Baffier, N.; Pistoia, G. In *Lithium Batteries*; Pistoia, G., Ed.; Elsevier: Amsterdam, 1994; Vol. 5.
(363) Zane, D.; Carewska, M.; Scaccia, S.; Cardellini, F.; Prosini, P. P. *Electrochim. Acta* **2004**, *49*, 4259.
(364) Chirayil, T. A.; Zavalij, P. Y.; Whittingham, M. S. *J. Electrochem. Soc.* **1996**, *143*, L193.

CR020731C